TESTING OF AN AXIAL FLOW MOISTURE SEPARATOR IN A TURBOCHARGER SYSTEM FOR POLYMER ELECTROLYTE MEMBRANE FUEL CELLS

A Thesis
Presented to
The Academic Faculty

By

Daniel George Hays

In Partial Fulfillment
of the Requirements for the Degree
Master of Science in Mechanical Engineering

Georgia Institute of Technology
August, 2005

TESTING OF AN AXIAL FLOW MOISTURE SEPARATOR IN A TURBOCHARGER SYSTEM FOR POLYMER ELECTROLYTE MEMBRANE FUEL CELLS

Approved By:

Sheldon Jeter, Co-Advisor

Said I. Abdel-Khalik, Co-Advisor

Srinivas Garimella

S. Mostafa Ghiaasiaan

Date Approved: 19 May, 2005

Dedicated to

Paul Joseph Hays

and

Mariel Dalmi Friberg

ACKNOWLEDGEMENTS

First I would like to thank my co-advisors, Dr. Sheldon M. Jeter and Dr. Said I. Abdel-Khalik at the Georgia Institute of Technology. I greatly appreciate all the time and work they have put into guiding my research. Without their help and support this investigation would not have been possible.

I would also like to thank Dennis Sadowski for aiding me in my research as needed with finding and creating parts for maintenance and upgrading of my apparatus.

My friends at Georgia Tech also deserve recognition both for helping me learn through teaching me how to run the apparatus and various other equipment necessary for my research and for allowing me diversions when needed. They are Dr. Sam Durbin, J.R. Aspinwall, James McClearen, Dr. Joerg Stromburger, Jeesung Cha, Lyle Fouts, Bart Carter, Dan Hurley, Robert Kramer, and Carl Laniak. I would also like to thank my friends from the University of Portland; Matt Hernandez, Joe Louie, Karen Vail, Jason Quigley, Kyle Jensen, Cotton Anderson, Ryan Givens, Christina Scheuer, Anissa Shoemaker, and Nate Weiss; some of whom visited Atlanta and gave me much needed breaks from school.

Last but certainly not least important, I would like to thank my family who has supported me throughout the entire process from applying to graduate school through defending my thesis. My dad (George Hays), mom (Glenda Hays), and brother (Paul

Hays) have been a great asset during this time as have Will Trimble, Philip Paccassassi, Mariel Friberg, Briana Burgess, Dr. L.J. Tognetti, and Andrea Burgess. Thank you all for your help and support during this time.

TABLE OF CONTENTS

LIST OF TABLES

LIST OF FIGURES

SUMMARY

Proton exchange membrane (PEM) fuel cells, with low operating temperatures and high power density, are a reasonable candidate for use in mobile power generation. One large drawback to their use is that their fuel reformer requires not only fuel but also water, thereby requiring two separate reservoirs to be available. PEM fuel cells exhaust enough water in their oxidant stream to potentially meet the needs of the fuel reformer. If this water could be recovered and routed to the fuel reformer it would markedly increase the portability of PEM fuel cells.

The goal of this research was to test a previously designed axial flow moisture separator. The separator was employed in a test bed which utilized compressed, heated air mixed with steam to simulate the oxidant exhaust conditions of a 25 kW PEM fuel cell. The simulated exhaust was saturated with water. The mixture was expanded through the turbine side of an automotive turbocharger, which dropped the temperature and pressure of the mixture, causing water to condense, making it available for separation. The humid air mixture was passed over an axial flow centrifugal separator and water was removed from the flow.

The separator was tested in a variety of conditions with and without passing chilled water through the separator. The axial separator was tested independently, with a flow straightener preceding it, and with a commercially available centrifugal moisture separator in series following it. It was shown that cooling makes a significant impact on the separation rate while adding a flow straightener does not. Separation efficiencies of 19% on average were experienced without cooling, while efficiencies of 50% were experienced with 3.1 kW of cooling. The separation efficiency of the two moisture separators combined was found to be 31.7% which is 165% that of the axial separator alone under uncooled conditions.

CHAPTER 1
INTRODUCTION

The purpose of this investigation was to test a previously designed axial flow moisture separator in a variety of conditions. The moisture separator was designed for use in conjunction with PEM fuel cells for automotive applications. Water is a byproduct of the energetic reaction of PEM fuel cells; water is also needed by a fuel reformer to turn diesel fuel into gaseous hydrogen. Sufficient water exists in the fuel cell exhaust to completely supply the fuel reformer's needs. If a sufficient amount of the water in the exhaust could be captured and routed to the fuel reformer it would greatly simplify incorporating a PEM fuel cell into an energy system design.

It has been shown in prior research that a turbocharger can be used to recover energy from the oxidant exhaust stream of a PEM fuel cell. This shaft work can then supplement an electric motor in compressing the oxidant stream entering the fuel cell (McTaggert *et al.*, 1998). It has been shown that raising the operating pressure of a PEM fuel cell will increase output voltage (Amphlett *et al.*, 1993). While the turbine in the oxidant exhaust recovers available energy from the oxidant exhaust stream, it also decreases its temperature and pressure, causing liquid water to separate out of the moisture saturated air stream. The moisture separator being tested receives the two phase turbine exhaust and attempts to separate out as much liquid water as possible.

A test apparatus was used that simulates PEM fuel cell exhaust. The temperature, pressure, flow rate, and relative humidity of compressed air were measured as it entered the system. It was then heated to the desired temperature by a finned tube resistance heater. Steam generated by an electric boiler flowed through an orifice plate for flow measurement and was then mixed with the heated air; the temperature and pressure of the mixture were then measured. The amount of dry air entering the system was calculated, while the amount of moisture entering the system with the air was added to the amount of steam entering to give the total mass flow rate of water entering the system. The mixture was expanded by the turbine side of an automotive turbocharger, which reduced the mixture temperature and pressure, causing liquid water to condense out. This two phase flow was passed over an axial flow swirl generating element and water was removed from the system. The amount of water separated over a given time was measured and compared to the calculated amount of moisture in the stream above the amount the stream could hold at saturation. The ratio of water collected to water beyond the saturation point of the stream defined the separation efficiency, and was the main parameter studied in this investigation.

$$\eta_{sep} = \frac{\dot{m}_{sep}}{\dot{m}_{cond}} \tag{1.1}$$

Equation 1.1 presents the method of determining the separation efficiency of an experiment. Here, $\dot{m}_{sep}$ is the measured mass flow rate of water separated while $\dot{m}_{cond}$ is

the calculated mass flow rate of condensed water available for separation and η_{sep} is the separation efficiency.

In this investigation chilled water was run through a copper pipe placed coaxially with the separator housing through the center of the separator itself. The water temperature was measured before the chilled water entered the separator housing and again after leaving the housing. These temperatures, combined with the measured water flow rate, allowed the rate of heat removal to be calculated. The effect of the heat removal rate on the separation efficiency was investigated.

Additional experiments are run with a commercially available centrifugal moisture separator used in series with and placed after the axial flow separator. The preliminary results of this investigation disagreed strongly with previously published results which reported significantly higher separation efficiencies (Aspinwall, 2004) and thus this extra measure was employed to be certain that extra moisture was indeed available in the air stream to be separated, validating the much lower separation efficiencies found in this experiment.

The housing of the axial swirl element was a clear plastic pipe and it was noticed that droplets enter the pipe with a slight swirl in the direction opposite to the direction imparted by the swirl element. The swirl in the opposite direction of the flow was of concern because the moisture separator was designed specifically to present a streamlined shape and minimize pressure drop across the element. If the swirl of the flow needed to

be not only generated but actually reversed, it was believed that this would cause a higher pressure drop across the element and lower the efficiency of the moisture separator. Pressure drop across the swirl element is undesirable due to the fact that it is a large contributor to droplet breakup which reduces separation efficiency since small droplets are much harder to separate than large droplets. The undesired swirl was believed to be generated by the turbine and it was believed that adding a flow straightener between the turbine and the moisture separator might remove the swirl in the incoming flow and result in higher efficiencies by avoiding droplet breakup. A flow straightener was added to the system as described and the moisture separator was again tested with and without cooling. These results are compared to the results found using the axial separator alone to determine if the addition of the flow straightener was worthwhile.

The remaining chapters are organized as follows. Chapter II gives background information on fuel cells in general, the rationale for focusing on PEM fuel cells, and outlines the operating conditions simulated by the apparatus in this experiment. Chapter III is a literature review of previous work on fuel cells in general and on this apparatus specifically including the design of the axial flow swirl element. Chapter IV describes the apparatus itself and the procedure for safely operating the experiment. Chapter V describes how the data was processed and what equations were used. Chapter VI presents the results of this experiment while Chapter VII discusses the results of this investigation and reprocesses data collected in previous research. Chapter VIII gives recommendations for future work that could be performed on this apparatus to meet the

goal of recovering enough water from the exhaust of a PEM fuel cell to supply the fuel reformer.

CHAPTER 2

BACKGROUND AND MOTIVATION

This chapter will provide information concerning fuel cells which will be used to establish the desired operating parameters for the experimental apparatus. Many types of fuel cells will be briefly discussed along with their attributes and detractions. The operating conditions of a Proton Exchange Membrane (PEM) fuel cell, the fuel cell simulated by this apparatus, will be discussed in detail to demonstrate the reasoning for the conditions at which the apparatus was operated. The goal of this research was to test a previously designed moisture separator in a variety of situations which mimic PEM fuel cell exhaust to explore its separation efficiency.

2.1 FUEL CELL PRINCIPLES

Fuel cells are basically composed of two electrodes, an anode and a cathode, separated by an electrolyte. The electrolyte serves as an ion conductor between the two electrodes and the electrodes themselves serve three functions (Hirschenhofer *et al.*, 1998).

1. Electrodes supply a surface site where ionization and de-ionization of fuel and oxidant may occur.
2. Electrodes provide a porous interface between ions in the gaseous streams and the ion conducting electrolyte.

3. Electrodes act as a physical barrier between the gaseous streams and the liquid electrolyte.

Fuel is passed over the anode while an oxidant is passed over the cathode. Electrons are separated at the anode and run through an external circuit, performing work, before returning to the cathode and recombining with hydrogen ions passed from the anode through the electrolyte solution. The hydrogen ions combine with oxygen from the oxidant stream forming water which is then exhausted into the oxidant stream. Figure 2.1 demonstrates this process.

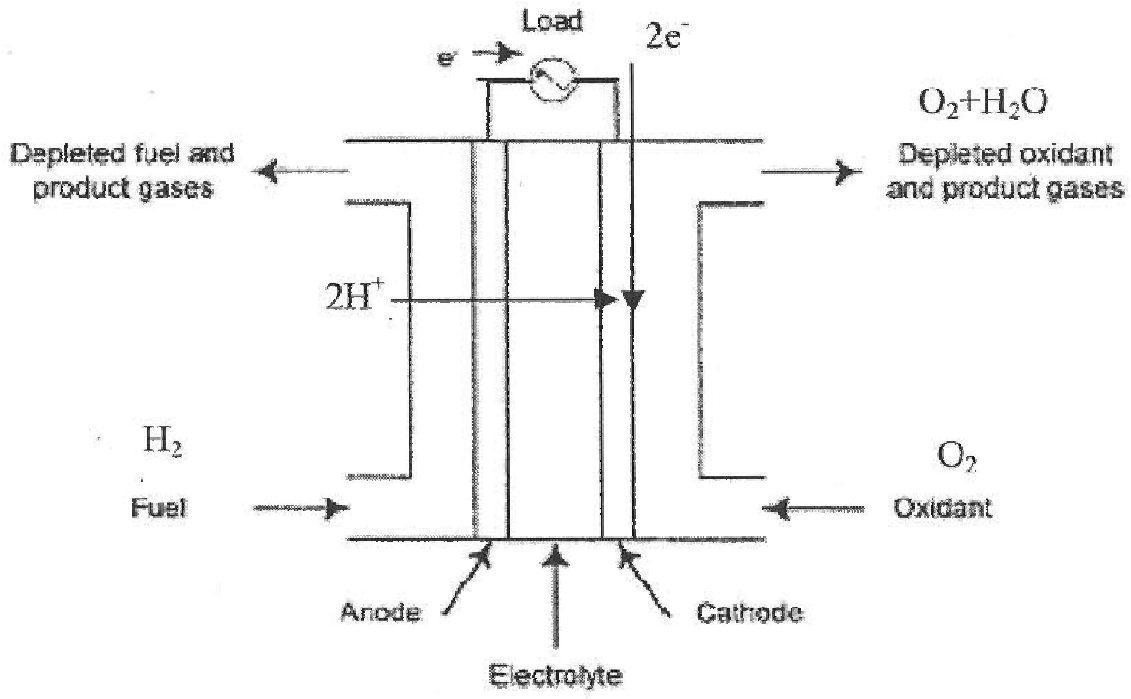

Figure 2.1 – Schematic of Typical PEM Fuel Cell Operation
(Hull, 2002)

Electrical potential is generated when the fuel, usually gaseous hydrogen (H_2), passing over the anode splits into positive ions (H^+) and electrons (e^-). The electrons are

passed by the electrode through an external circuit while the positive ions are conducted through the electrolyte to the cathode. The oxidant, usually oxygen (O_2), passes over the cathode and splits into individual atoms (O^-) which exert a strong negative attraction and draw the positive fuel ions through the electrolyte membrane. When the hydrogen and oxygen ions combine, water is formed and the molecule is exhausted into the oxidant stream.

$$H_2 \rightarrow 2H^+ + 2e^- \quad (2.1)$$

$$O_2 + 4H^+ + 4e^- \rightarrow 2H_2O \quad (2.2)$$

$$2H_2 + O_2 \rightarrow 2H_2O + \text{energy} \quad (2.3)$$

Equations 2.1 and 2.2 represent the chemical reactions at the anode and cathode, respectively, while Equation 2.3 represents the overall reaction of the system (Hirschenhofer *et al.*, 1998).

2.2 TYPES OF FUEL CELLS

Five main types of commercially available fuel cells were reviewed and each type had its own operating parameters. This investigation was primarily interested in portable power generation, as would be applicable to an automobile, and not every type of fuel cell presented here is a good fit for this application. One of the main parameters of concern when choosing a fuel cell is the operating temperature. Many fuel cells operate at temperatures that would make them unsafe or inconvenient for portable power generation.

Solid Oxide Fuel Cells (SOFC) operate around 1000 °C and use a non-porous metal oxide as the electrolyte. Molten Carbonate Fuel Cells (MCFC) operate between 600 and 700 °C and use a molten salt as the electrolyte. Phosphoric Acid Fuel Cells (PAFC) operate between 100 to 220 °C and use concentrated phosphoric acid as the electrolyte. While the high operating temperatures of some fuel cells enable them to reform their own fuel, the high temperatures result in long start-up times and raise safety concerns which make them undesirable for automotive use. These fuel cells are more likely to find use in stationary electricity generation.

Alkaline Fuel Cells (AFC) operate between 65 and 250 °C, with temperatures on the high end of the range being preferred. They use an aqueous potassium hydroxide solution as the electrolyte. AFCs are one of the oldest designs and are relatively inexpensive but have a low power density, measured by the number of Watts per electrode surface area. Due to susceptibility to contamination, the AFC requires extremely pure hydrogen and oxygen supplies, making it expensive. Due to these problems the AFC is unlikely to be developed for automotive use (EG&G, 2002).

The Proton Exchange Membrane (PEM) fuel cell, also known as a Polymer Electrolyte Membrane fuel cell, operates between 70 and 80 °C at 3.1 bar; the electrolyte is a fluorinated sulfonic acid polymer (Hirschenhofer *et al.*, 1998). This fuel cell is the most promising choice for automotive applications; however, it requires adequate hydration to function at peak performance. PEM fuel cells employ a platinum catalyst on the electrodes to promote reactivity between the fuel and oxidant. Power density of these

cells has been increased to between 0.1 and 0.75 W/cm^2, making these fuel cells with their high power density and low operating temperatures particularly attractive for mobile electricity generation.

2.3 PEM FUEL CELLS

As separating moisture from the exhaust of a PEM fuel cell is the focus of this thesis the operating conditions of a 25 kW PEM fuel cell will be discussed here in detail. Of particular interest are the operating temperature, pressure, oxidant concentration, and chemical balance.

2.3.1 PEM Fuel Cell Reactant Pressure

A parametric study was conducted to determine the effects of varying cell temperature, pressure, percentage excess oxidant, and percentage excess fuel on PEM fuel cell performance. The study found that the change in cell voltage from the baseline voltage increases logarithmically with the ratio of increasing pressure to the baseline pressure. Baseline pressure for the study was 1.4 bar (20 psig) and the maximum pressure was 2.4 bar (35 psig), while the baseline voltage was 0.757 V and the maximum voltage was 0.779 V. Figure 2.2 demonstrates these changes (Amphlett *et al.*, 1993).

As the figure shows, fuel cell voltage increases when the reactants are compressed. Pressurizing the air streams to the fuel cell requires power; therefore, if the power used to pressurize the fuel cell is greater than the power gain created, then the pressurization would not be worthwhile. Any energy recovered by the turbine on the

oxidant exhaust and used to compress the incoming oxidant is essentially free to the system. A previous researcher investigated the value of adding a turbocharger to the apparatus being studied (Hull, 2004). In this investigation the data presented here were only used to determine fuel cell exhaust conditions.

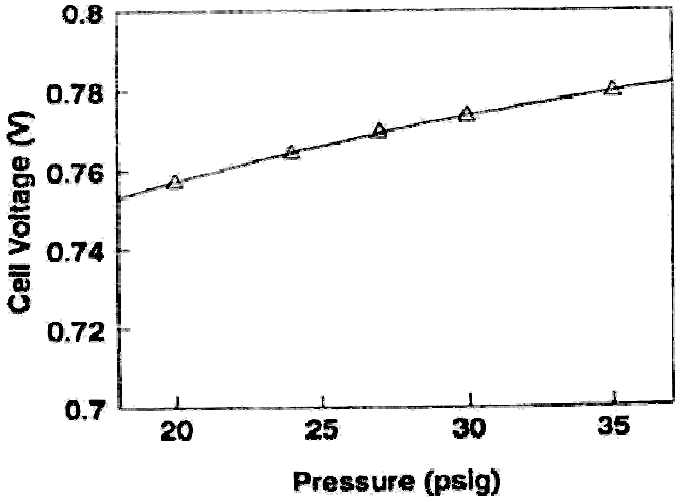

Figure 2.2 – PEM Fuel Cell Voltage as a Function of Pressure
(Amphlett *et al.*, 1993)

Exhaust pressures in the range displayed are acceptable, with pressures on the higher end of the spectrum being preferred as they would generate a higher voltage.

2.3.2 PEM Fuel Cell Temperature

Another important trend was reported in the aforementioned research. Cell voltage was shown to increase linearly with increasing temperature. As temperature rises, the internal resistance of the fuel cell to proton exchange decreases, allowing for higher reaction rates. The upper limit of this voltage gain is determined by the fact that

the electrolyte cannot function at temperatures above 80 °C (Amphlett *et al.*, 1993). Figure 2.3 demonstrates the gains in voltage resulting from increasing cell temperature.

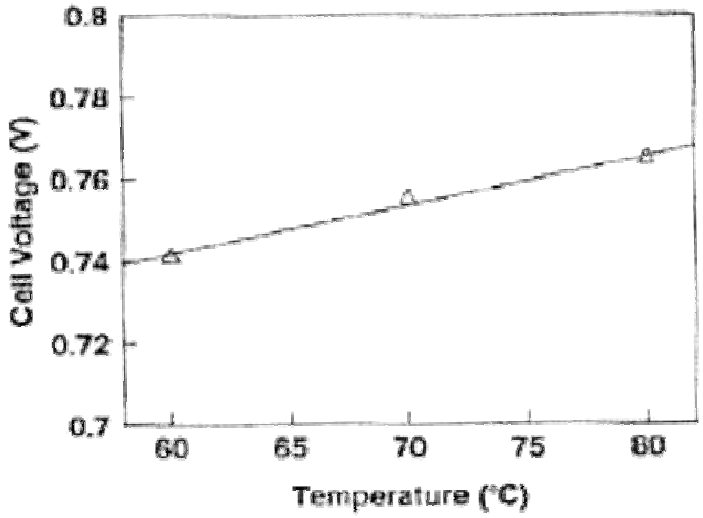

Figure 2.3 – PEM Fuel Cell Voltage as a Function of Temperature
(Amphlett *et al.*, 1993)

Again, this information was used to realistically simulate PEM fuel cell exhaust conditions in this investigation. Temperatures ranging from 60 to 80 °C are realistic temperatures with higher temperatures being preferred.

2.3.3 PEM Fuel Cell Oxidant Concentration

A third result from the previously discussed parametric study shows the effect of oxidant concentration, measured as oxidant mole fraction of the entire oxidant stream, on cell voltage. It was found that increasing the concentration of oxygen supplied to the cathode increases cell voltage as shown in Figure 2.4 (Amphlett *et al.*, 1993).

The upper limit on increasing oxidant available to the fuel cell is set by the condition that the hydration of the fuel cell must be balanced. The electrolyte needs a certain amount of water to operate properly and it is initialized with this amount of water. If all the water generated by the chemical reaction is not carried away from the cell the electrolyte will flood and perform improperly, but if too much water is carried away the electrolyte will dry out, causing it permanent damage. The flow rate and temperature of the oxidant exiting the cell must be balanced such that 100% relative humidity is maintained and the fuel cell neither dries out nor floods.

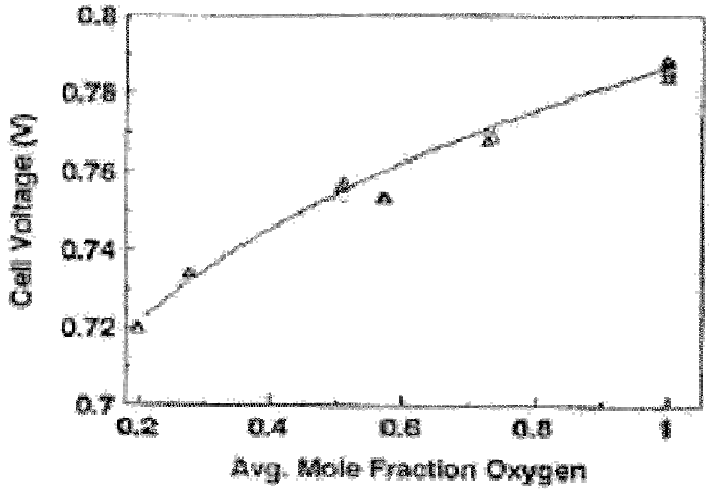

Figure 2.4 – PEM Fuel Cell Voltage as a Function of Oxidant Concentration (Amphlett *et al.*, 1993)

2.3.4 PEM Fuel Cell Fuel Requirements and Cathode Exhaust Condition

This section will discuss the moisture requirements for fuel reformation and the moisture available in fuel cell exhaust. Requirements of a 25 kW fuel cell will be reviewed in all cases.

A PEM fuel cell is being examined and due to its relatively low operating temperatures it requires an external fuel reformer. Usually diesel fuel and water are fed to the reformer, which processes these components and emits carbon dioxide and hydrogen, as shown in Equation 2.4 (Hirschenhofer *et al.*, 1998). Hydrogen is then used by the cell to generate electricity. Diesel fuel is approximated here as $C_{12}H_{26}$.

$$C_{12}H_{26} + 24H_2O \rightarrow 12CO_2 + 37H_2 \qquad (2.4)$$

Using this chemical balance and scaling up the fuel supply rate for a 5 kW fuel cell, a necessary water feed rate can be determined. Table 2.1 presents fuel cell operating requirements for a 5 kW fuel cell, as specified by one manufacturer, and the scaled up requirements for a 25 kW fuel cell (M. Sawyer, personal communication, April 15, 2005).

Table 2.1 - Data on Fuel Cell Operating Conditions

	Given Data 5 kW Fuel Cell	Correlated Data 25 kW Fuel Cell
H_2 Feed Rate (mol/min)	3.1	15.5
H_2 Fuel Utilization	80%	80%
Excess Air	150%	150%
Fuel Cell Operating Pressure (psig)	30	30

From this table it can be seen than 15.5 mol/minute of hydrogen are required by the fuel cell. Scaling Equation 2.4 down by a factor of 2.38 to present it in terms of the correct hydrogen feed rate results in Equation 2.5. The water demand of the fuel reformer is then 10.05 mol/minute as shown in Equation 2.5.

$$0.42\ C_{12}H_{26} + 10.05\ H_2O \rightarrow 5.03\ CO_2 + 15.5\ H_2 \quad (2.5)$$

Now that the water demand of the fuel reformer has been determined the water available in the cathode exhaust stream will be examined to determine what percentage of the available water must be removed to meet the demands of the fuel reformer. Equation 2.2 gave the stoichiometric equation of the oxidant stream using pure oxygen. If the equation is modified to use 150% excess air as specified by the manufacturer, Equation 2.6 results.

$$2.5\ (O_2 + 3.76\ N_2) + 2\ H_2 \rightarrow 2\ H_2O + 1.5\ O_2 + 9.4\ N_2 \quad (2.6)$$

Recalling from the data specified by the manufacturer, only 80% of the hydrogen fuel supplied to the anode will be used and the rest will be exhausted in the fuel stream. Entering the used amount of hydrogen, 12.4 mol/min, into this equation and scaling the rest of the equation to match results in Equation 2.7.

$$15.5\ (O_2 + 3.76\ N_2) + 12.4\ H_2 \rightarrow 12.4\ H_2O + 9.3\ O_2 + 58.28\ N_2 \quad (2.7)$$

The amount of water exiting in the oxidant stream is 12.4 mol/min as demonstrated in the above equation. The amount of water necessary for the fuel reformer was found to be 10.05 mol/min meaning that 81% of the total moisture leaving in the exhaust stream must be recovered in order to make the system self-sufficient in terms of water requirements.

From the information calculated here the humidity ratio of the stream exiting the fuel cell can also be calculated. Equation 2.7 shows 12.4 mol/min of water exit in the oxidant stream accompanied by 9.3 mol/min of oxygen and 58.28 mol/min of nitrogen. In grams, 223 g/min of water and 1930 g/min of air exit. The humidity ratio of this stream is 0.1158 g water/g dry air. These data are presented in Tables 2.2.A and 2.2B.

Table 2.2.A - Summary of Cathode Exhaust Conditions

	mol/min	g/min	%	(g water)/ (g dry air)
Oxygen Flow Rate	9.3	297.6		
Nitrogen Flow Rate	58.28	1632.4		
Total Air Flow Rate		1930.0		
Water Vapor Flow Rate	12.4	223.4		
Relative Humidity			100	
Humidity Ratio				0.1158

Table 2.2.B - Summary of Fuel Reformer Requirements

	g/min	%
Water Flow Rate	181.1	
Percent of Water Available		81

In order to more fully explain how a turbocharger would be incorporated into a fuel cell system, Figure 2.5 presents a schematic of the setup. Oxidant enters the compressor from the atmosphere and flows through the cathode where it becomes saturated with water vapor. This flow then exits the cathode and enters the turbine. The flow is expanded, generating work to help drive the compressor. An electric motor supplements the work generated by the turbine. A moisture separator is placed downstream of the turbine and separates liquid water from the humid air stream.

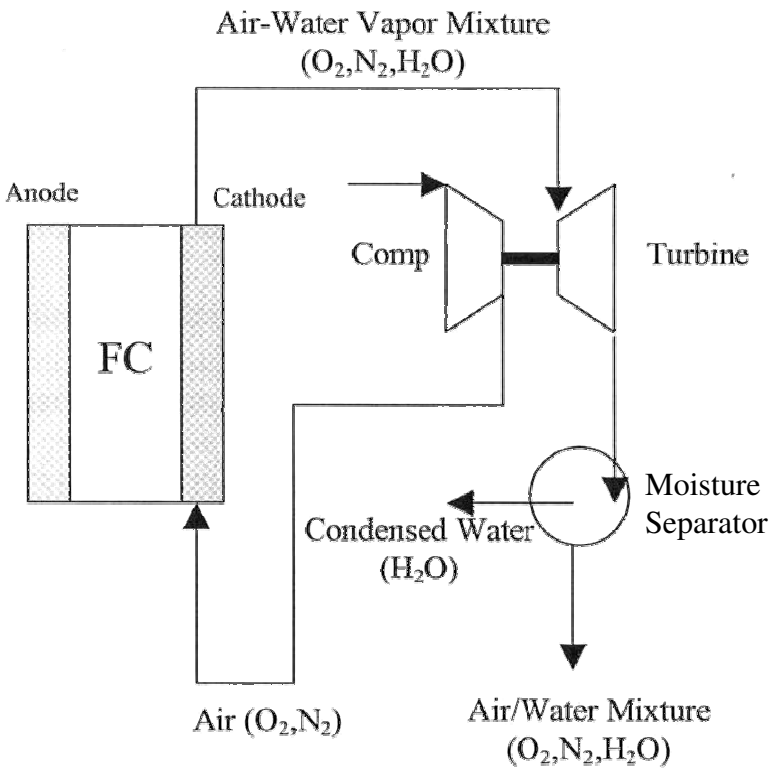

Figure 2.5 – Schematic of Turbocharger Setup (Hull, 2002)

While fuel cell operating conditions are rarely published due to the fact that they are generally regarded as proprietary data, this chapter has presented a realistic set of conditions at the fuel cell's oxidant exhaust stream. The amount of water required to be separated from the oxidant stream was determined to be 81% of the total moisture, or 181 g/min. In summary, this chapter has presented the reasoning for choosing to simulate a PEM fuel cell as well as the conditions of the cell's exhaust.

CHAPTER 3

LITERATURE REVIEW

This chapter provides a summary of literature that was reviewed in preparation for the experimental investigation undertaken in this research. The purpose of reviewing the literature was to gain a greater understanding of fuel cell theory in general and, specifically, the operating conditions desired to be replicated in this research. Some sources discussed fuel cell operating conditions and others detailed previous experimentation on the apparatus being used. Literature discussing centrifugal separators was also reviewed to better understand the moisture separator design currently being utilized in the apparatus.

3.1 FUEL CELL FUNDAMENTALS

Literature which dealt with the fundamentals of fuel cell operation and operating conditions will be reviewed in this section. Literature concerning several aspects of fuel cells was reviewed.

Hirschenhofer *et al.* (1998) discusses many types of fuel cells by concentrating on each fuel cell individually and in detail. The literature reviews PEM fuel cells in addition to other types of fuel cells and addresses operating conditions, applications, advantages, and disadvantages of each type of fuel cell. Fuel cell reactions at the electrodes are analyzed as well as system reactions. Fuel reformers are also discussed.

Amphlett *et al.* (1993) discusses a parametric study performed on one specific PEM fuel cell, Ballard Power Systems' MK IV. In this study, a baseline case was developed and chosen parameters including pressure, temperature, excess pure fuel, excess pure oxidant, and average mole fraction of pure oxidant were varied with respect to the baseline. This study found that increasing either fuel cell temperature, pressure, or the mole fraction pure oxygen in the oxidant stream would independently increase cell voltage.

McTaggert *et al.*, (1998) implemented a turbocharger system in conjunction with a 50 kW PEM fuel cell. The turbine in the system recovered energy from the cathode exhaust and used the energy to compress the incoming oxidant. This system was built to work with the aid of an electric motor. No mention is made in this source of any moisture separation system.

3.2 CENTRIFUGAL SEPARATORS

This section presents literature which was used to design the axial separator being tested in this system.

Nieuwstadt and Dirkzwager (1995) give guidelines for the design of an axial flow moisture separator for use in a system where removal of liquid droplets from a liquid stream is desired. Separation of water from oil is discussed in particular. The design endeavors to create a strong swirling action in the liquid streams while avoiding a

pressure drop which contributes to droplet breakup into smaller, harder to capture, particles.

This source also discusses the motivation for creating an axial flow swirl element. Tangential flow centrifugal separators are fairly commonplace today and are known to create a large pressure drop in the flow, wasting energy. Pressure drop is one of the leading contributors to droplet breakup and therefore in order to have extremely high separation efficiencies a leap in design must be made to a new type of separator. Axial separators hold the promise of a low pressure drop and high separation efficiencies.

3.3 PREVIOUS RESEARCH ON THIS APPARATUS

Two sources were reviewed which were based on work done on the apparatus used for this experiment. They gave an operating procedure for the apparatus as well as general guidelines concerning the conditions at which the apparatus should be run.

Hull (2002) added the turbocharger to the system and concentrated his study on its effects. A power balance was calculated concerning the power gained from the turbine, the power put into the compressor, the power lost to the oil stream, and power lost to the atmosphere. Pressure ratios for the turbine and compressor were calculated. Moisture separation was performed downstream of the turbine using a commercially available moisture separator. No cooling of this separator was performed.

Aspinwall (2004) designed and constructed the moisture separator which was tested in this research and discusses the design parameters at length. Data were collected concerning the performance of the separator at different settling lengths and different air temperatures. All data were taken with the separator assumed to be adiabatic. Separation efficiencies averaging around 90% were reported. Neither settling length nor heated air temperature was found to have an effect on the separation efficiency.

In summary, literature was reviewed that described PEM fuel cells in depth. Operating conditions were gleaned as well as an understanding of centrifugal separators in general. Literature concerning this apparatus was helpful in maintaining safe operating conditions while running the apparatus and was invaluable in achieving steady state conditions.

CHAPTER 4

EXPERIMENTAL APPARATUS

This chapter provides a detailed description of the experimental test setup used for the research. Design requirements, actual design parameters, instrumentation, and procedure for operating the setup will be discussed. This chapter will discuss the system as a whole before reviewing each subsystem individually.

The primary design requirement for the test setup was to accurately simulate hot and moist Proton Exchange Membrane (PEM) fuel cell exhaust. The exhaust was expanded through the turbine side of a turbocharger and the swirl element attempted to separate any condensed liquid water. The major result calculated from the data collected in experiments was the separation efficiency of the moisture separator, defined as the percentage of moisture above the saturation mass of the air that the separator removed from the stream. Experiments were run under many different conditions in order to characterize the performance of the swirl element separator.

Figure 4.1 is a schematic of the system setup in its entirety. Additionally, as individual systems are discussed a detail may be presented. Tables 4.1 and 4.2 list major system components and instruments using both generic and commercial identification.

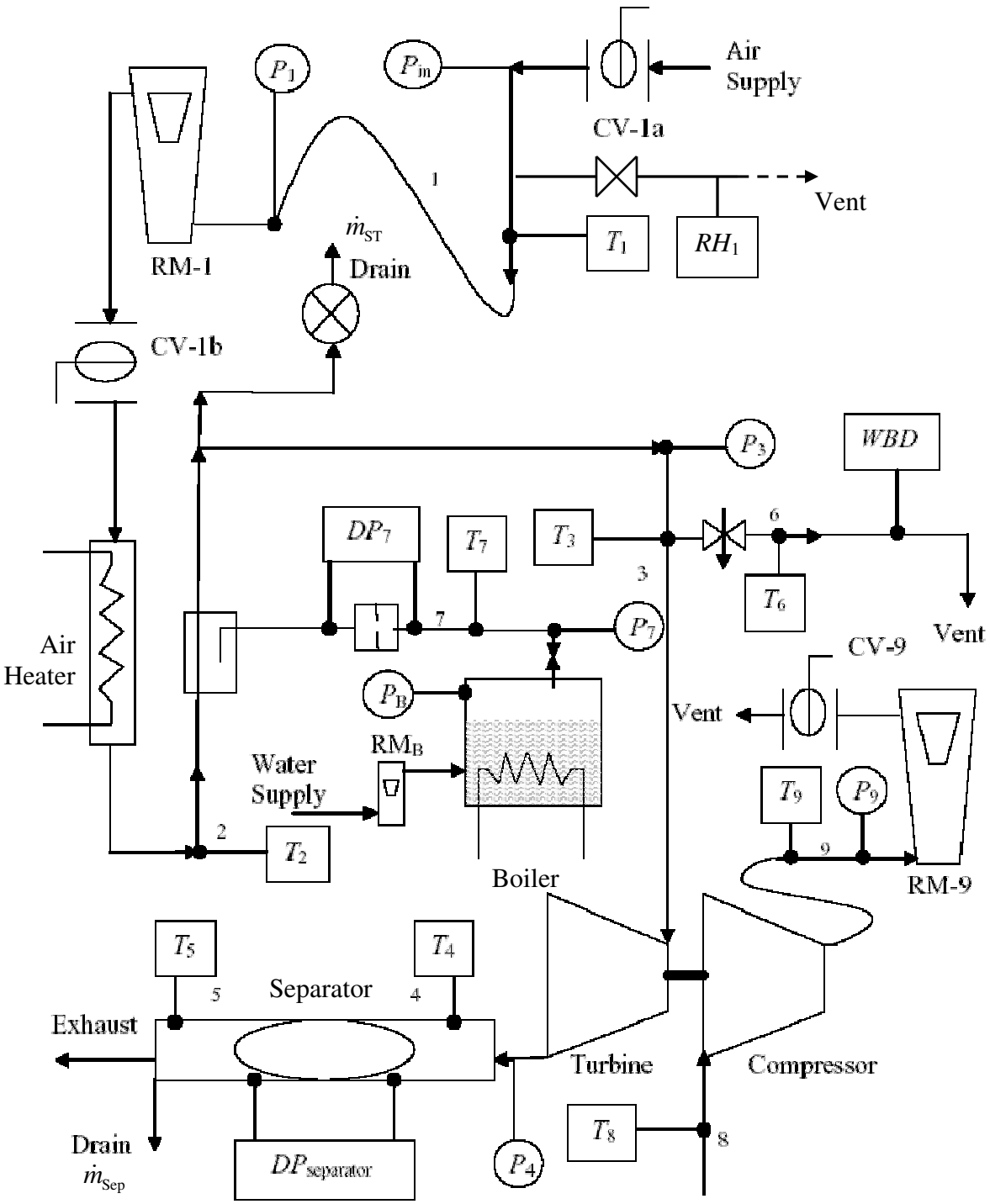

Figure 4.1 - Schematic of Test Setup

To simulate PEM fuel cell exhaust compressed air was heated and then mixed with superheated steam. The compressed air was drawn from the building's supply line and restricted down to 276 kPa gauge pressure (40 psig). The air was then heated by passing it through an electrical resistance heater after which it was mixed with steam generated by an electric boiler. The air and steam mixture was expanded through a turbine where the temperature dropped, allowing water to condense out of the stream and become entrained in the flow. The turbine used was half of an automotive turbocharger while the compressor half of the turbocharger was placed under load to simulate real world conditions. The turbocharger needed a constant stream of oil supplied to it for lubrication; this was provided by a positive displacement oil pump in the oil system. This stream was passed over the axial flow moisture separator and the mass of water separated was measured over a given time period. The moisture separator imparted a strong swirling action to the flow passing over it, causing heavier water droplets to migrate to the outside of the flow, where they then exit the flow through holes in the outside of the swirl element housing. In some experiments cooling water was run through the separator in an attempt to further cool the humid air stream and separate a greater mass of water. Separation efficiency was defined using the temperature of the humid air stream as it entered the separator. As the humid air mixture cooled more moisture condensed and was available for separation. If a significant amount of this additional water could be separated, it was theoretically possible to realize separation efficiencies of over 100%.

To accurately calculate separation efficiency it was necessary to know the working fluid conditions throughout the system. Both the dry air mass flow rate and the

water mass flow rate were measured as were the temperature and pressure at each of fourteen stations in the system. An array of instrumentation was used to capture these data. Temperatures were measured with Type-T thermocouples while most pressures were measured with bourdon tube gauges. A rotameter measured air flow into the system, another measured inlet water flow to the boiler, and a third measured airflow generated by the compressor half of the turbocharger. A differential pressure transducer was used to measure steam flow into the system and a relative humidity sensor measured the moisture introduced into the system with the compressed air. Readings from the thermocouples, pressure transducer, and relative humidity probe were collected by a data acquisition system and recorded by a desktop computer. Pressure measurements and ambient conditions were recorded manually by the researcher. The sources of these measurements and their respective uncertainties will be presented in this chapter.

Table 4.1 - Experimental Apparatus Components

Generic Description	Manufacturer	Model
Air Pressure Regulator	McMaster-Carr	R17-801-RGLA
Water Pressure Regulator	Honeywell	D05
Resistance Heater	Omega	FTS-048475
Flow Orifice	Gerand Engineering	1/4 in. B-5
Steam Trap	Spirax-Sarco	B-1H
Electric Boiler	Electro Steam	LB-20
Turbocharger	Garrett	GT-15
Primary Water Pump	Teel	4P919
Secondary Water Pump	Teel	3P714
Differential Pressure Transducer	Rosemount	1151DP
Turbocharger	Garret	GT-1541V
Cooling Water Pump	Teel	4RK65

In general all system components are schedule 40 brass NPT parts and all sizes listed are nominal pipe sizes unless otherwise specified. All thermocouples are two wire Type T thermocouples, more specifically Omega Type T thermocouples, unless otherwise specified. All elbows are 90° unless otherwise noted.

The remainder of this chapter will be divided into sections describing the main subsystems of the apparatus. As each subsection of the apparatus is discussed, its requirements will be presented. A brief overview of the subsystem will be given followed by a detailed review covering each individual piece of equipment used. Closures will review the requirements of the system and how they were met. Uncertainties of instrumentation will be discussed in Section IV.5, the Uncertainty section.

4.1 PEM FUEL CELL EXHAUST SIMULATION

This section describes the creation of simulated PEM fuel cell exhaust and the passage it follows through the system. Two main components are joined to simulate the exhaust; compressed air and superheated steam. The air system and its heating components will be discussed followed by discussion of the steam generation side of the system. The combined flow will then be traced until it enters the turbine.

Table 4.2 - List of Instrumentation

Measurement	Generic Description	Commercial Description
RM_1	Rotameter	Schutte-Koerting
RM_9	Rotameter	Fischer-Porter 10A3565A
RM_B	Rotameter	Cole-Parmer N044-40
RH_1	Relative Humidity Probe	Vaisalla HMD-40
P_1	Pressure Test Gauge	Omega PGT-30L-100
P_3	Pressure Test Gauge	Omega PGT-30L-60
P_4	Pressure Test Gauge	Marshall-Town 80827
P_7	Pressure Test Gauge	Omega PGT-45B-100
P_9	Pressure Test Gauge	Omega PGT-30L-30
P_{atm}	Barometer	Swift 477
P_b	Pressure Test Gauge	Omega PGT-30L-100
ΔP_5	U-tube Manometer	Dwyer, 0 to 16 inWG, 0.2 inWG
ΔP_7	Differential Pressure Transducer	Rosemount 1151DP
T_1	Type-T Thermocouple	Omega CPSS-18U-12
T_2	Type-T Thermocouple	Omega CPSS-18U-12-DUAL
T_3	Type-T Thermocouple	Omega CPSS-18U-12
T_4	Type-T Thermocouple	Omega CPSS-18U-12-DUAL
T_5	Type-T Thermocouple	Omega CPSS-18U-12
T_6	Type-T Thermocouple	Omega CPSS-18U-12-DUAL
T_7	Type-T Thermocouple	Omega CPSS-18U-12
T_8	Type-T Thermocouple	Omega CPSS-18U-12
T_9	Type-T Thermocouple	Omega CPSS-18U-12
T_{amb}	Mercury In-Glass Thermometer	Fisher, -1 to 51 ºC, 0.1 ºC
T_{fw}	Type-T Thermocouple	Omega CPSS-18U-12
T_{oil}	Type-T Thermocouple	Omega CPSS-18U-12
WBD	Type-T Thermocouple	Omega CPSS-18U-12
m_{sep}	Mass Scale	Ohaus CT6000-S
Δt	Timer	Extech C-510

4.1.1 Dry Air Heating and Delivery

The dry air heating and delivery system was required to meet several criteria. The system needed to deliver a continuous, measured, steady flow of compressed air in a controllable manner. The heater needed to heat the air to a steady desired outlet temperature. Any moisture that entered the system with the air needed to be measured. Figure 4.2 shows a schematic of the heated air delivery subsystem. To minimize heat loss all pipes from the heating element to the mixing chamber are insulated.

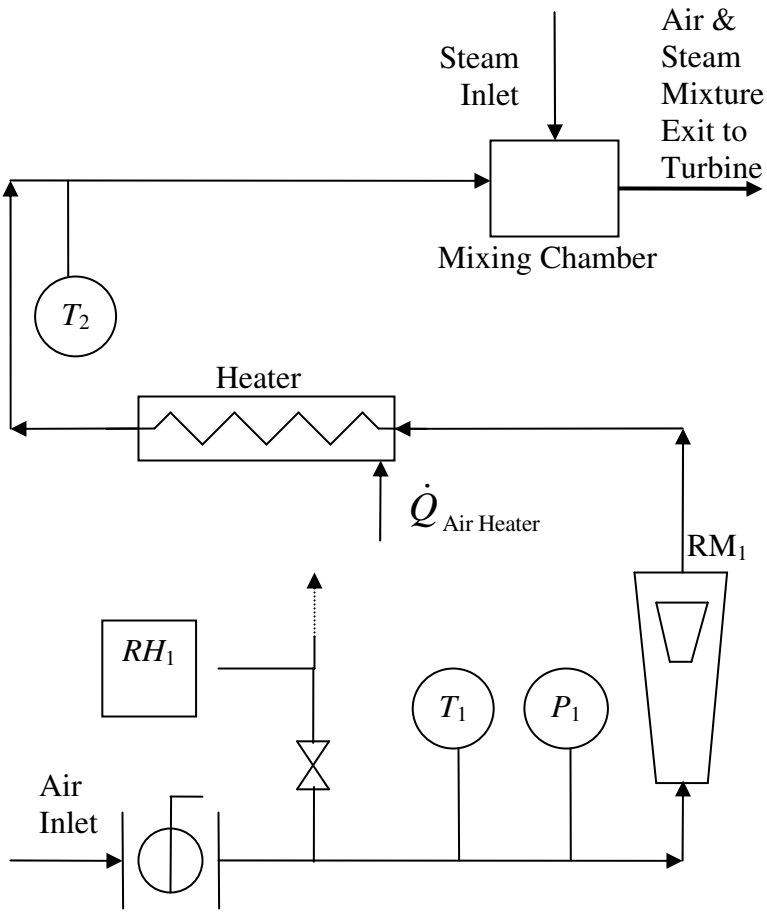

Figure 4.2 – Dry Air Subsystem

Air enters the system through a ball valve; some of the air is diverted and expanded to atmospheric pressure to allow its relative humidity to be measured. The temperature and pressure of the air remaining in the system are then measured. The air flows through a rotameter followed by a internally finned tube resistance heater. The temperature of the air exiting the heater is measured to allow calculation of an energy balance. The heated air is mixed with steam and flows into the turbine.

The source of the compressed air used in the system is the building's air supply line. From here air is branched off through a 3/4 inch copper pipe which connects to a 3/4 inch copper ball valve (CV-1a). This ball valve is set to either open or closed and no fine adjustments are attempted with it. The ball valve connects to a 3/4 inch externally threaded tee. The straight side of the tee is plugged while the branching side of the tee connects to a 3/4 inch to 1 inch reducing bushing which leads to a 1 inch internally threaded tee. A thermocouple (TC-1) is inserted into the divergent side of the tee and a 1 inch pipe nipple leads to a second 1 inch internally threaded tee. A reducing bushing connects to a 1/4 inch needle valve (CV-1b) used to control the airflow passing through one side of the tee. In series with and after the needle valve a CPVC reducing bushing connects to a 1 inch CPVC tee. The straight side of the tee is open to the atmosphere while a relative humidity probe (RH-1) is attached to the other side. As air escapes the system here it flows across the probe which measures its relative humidity.

The outlet of the second 1 inch internally threaded tee attaches to a 1 inch flexible rubber hose. The hose connects to a 1 inch pipe nipple which directs airflow through an

air pressure regulator, more specifically a McMaster-Carr R17-801-RGLA with a range of 0.135 MPa to 1.14 MPa (5-150 psig). The air pressure regulator connects to a 1 inch pipe nipple which connects to a 1 inch internally threaded tee. One side of the tee has two bushings that reduce the pipe size to connect to a 3/8 inch street elbow. The elbow connects to a short length of 3/8 inch pipe followed by a ball valve which connects to a pressure gauge (P_1), more specifically an Omega Engineering 0-60 psi gauge with 0.5 psi subdivisions. The other side of the 1 inch internally threaded tee connects to a 1 inch pipe nipple followed by a rotameter, specifically a McCrometer 10-110 SCFM at standard conditions of 0.322 MPa (32 psig) and 21.1° C (70 °F). At any other temperature and pressure a correction correlation must be used to accurately determine the air flow rate. Using the temperature (T_1), relative humidity (RH_1), pressure (P_1), and rotameter reading (RM_1), the mass of moisture entering the system through the air stream can be calculated.

Air exits the rotameter through a 1 inch pipe nipple which connects to a 1 inch steel ball valve (CV-1b). This ball valve serves as the primary means of exerting fine control over the rate of air flow into the system. A 1 inch pipe nipple attaches to the outlet of the ball valve and to the inlet of a 1 inch to 1 1/4 inch internally threaded elbow. A 1 1/4 inch pipe nipple connects the elbow to a 1 1/4 inch internally threaded tee. One side of the tee is a sealed inlet which allows the wiring leads of the electrical resistance air heater to enter the system. The other side of the tee connects to a 1 1/4 inch pipe nipple and in turn it connects to a 1 1/4 inch union. The union threads into a 1 1/4 inch pipe nipple. The nipple serves as an enclosure for the heating element of an electrical

resistance air heater, more specifically an Omega Engineering model FTS-048475. The union on the inlet to the pipe nipple facilitates access to the heating element should a need arise. The outlet of the heater enclosure connects to a 1 1/4 inch internally threaded tee. One end of the tee is sealed to air and allows heater wiring to exit the enclosure. The other end of the tee directs the heated air into a 1 1/4 inch pipe nipple. The nipple leads to a 1 1/4 inch internally threaded tee. A dual element thermocouple (TC-2) is affixed to one side of the tee and measures the heated air temperature (T_2). The other side of the tee exhausts into a 1 1/4 inch pipe nipple which threads to another 1 1/4 inch internally threaded tee. Steam is passed into one end of this tee and the steam air mixture exits out the other end of the tee. The steam generation system is discussed in the next section and the path of the mixed stream up to the turbine inlet can be found in the section following.

The air heater is a finned tube resistance air heater with a possible heat input range of 0 to 3.45 kW. The leads of the heater attach to an autotransformer, more specifically a Superior Electric model 1256-b, which is used to control the voltage across the leads of the heater, and thus the power input to the air. A wattmeter, more specifically a Weston Portable Standard 0 to 1 kW with 0.01 kW graduations, was used to measure power input to the resistance heater. The resistance heater is also wired in series with a temperature controller capable of PID, PDPI, or PD control. Commercially the controller is identified as an Omega Engineering CN9000A. One set of leads from the thermocouple measuring the heater exit temperature (TC-2) connect to the CN9000A. The controller output signal is passed to a solid-state relay, more specifically an Omega Engineering SSR240DC45 which switches the heater on and off. Using feedback from

the thermocouple measuring heater exit temperatures (TC-2) and proper settings, the controller is capable of very closely regulating the exit air temperature. However, as the controller is only capable of switching power input on and off the wattmeter gives false readings. It is therefore advisable to set the controller to a temperature above the actual desired operating temperature to bypass its function entirely and use the autotransformer to control the power input to the resistance air heater. When air flow rate, air inlet temperature, and power input are steady it is easy to predict and maintain a steady output temperature using only the autotransformer. More about this control issue is detailed in the procedure section of this chapter.

During the course of operation the resistance heater experiences a wide temperature range, capable of generating significant thermal expansion stresses. To prevent failure due to these stresses the heater is constrained only in the radial direction and it is allowed to move freely in the axial direction within the pipe enclosure. Constraint in the radial direction is important to prevent damage caused by vibration.

In review, the requirements of the dry air delivery and heating system are as follows:

1. Measure the mass flow rate of dry air into the system
2. Measure the mass flow rate of any accompanying water into the system
3. Provide a steady, controllable flow of air
4. Provide a steady, controllable exit temperature

As discussed above, the test system is outfitted with instrumentation to allow the determination of the mass of air entering the system and the accompanying mass of water. The combination of temperature, relative humidity, rotameter reading, and pressure allow both masses to be determined through straightforward calculations. The regulator ensures steady air flow at a desired pressure while a ball valve gives control over the air flow rate. The combination of the autotransformer and the resistance heater provides a means to produce and control a steady outlet temperature. The system is able to meet all of the requirements outlined above.

4.1.2 Steam Generation

The steam generation system was required to meet several criteria. Foremost among those criteria was that the system would possess the capability to produce a constant flow of steam into the system at steady state conditions. Consequent to that condition, the steam flow rate would also need to be measured and controlled. To ensure steady state was reached it was necessary to monitor and control the mass flow of water into the boiler. Figure 4.3 is a schematic of the steam generation subsystem. To minimize heat loss and condensation, all pipes leaving the boiler are insulated.

The temperature of liquid water is measured before it flows through a rotameter and into a 20 kW electric boiler. Steam exits the boiler and its temperature and pressure are measured. The steam flows through an orifice plate and the change in pressure across the plate is measured. The steam then enters the mixing chamber where it is mixed with

heated air. The mixture flows through the turbine and is expanded, which will be discussed in a later section.

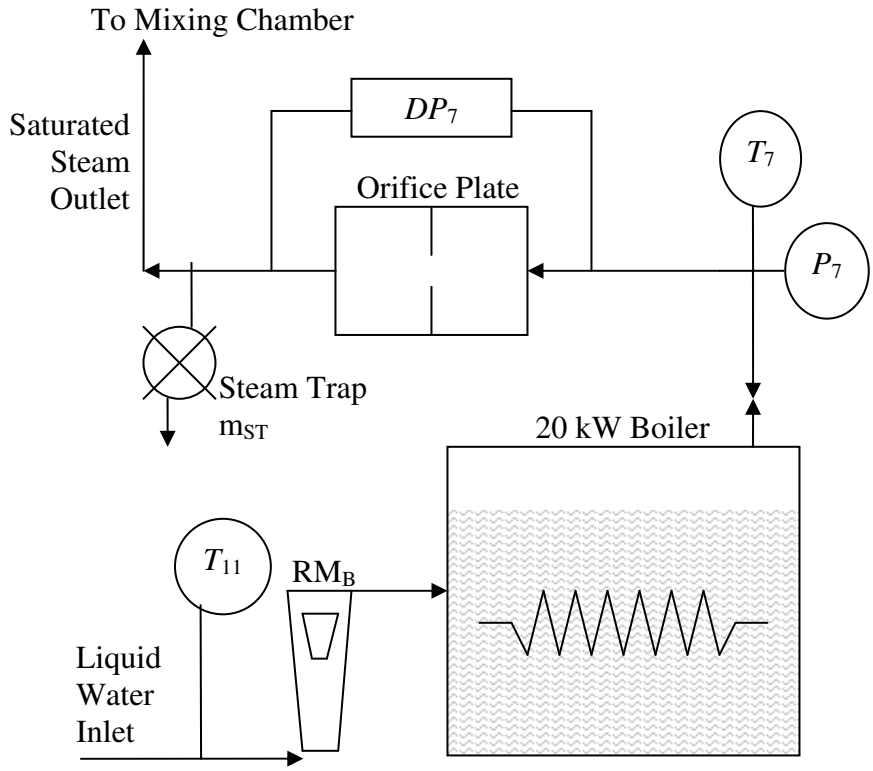

Figure 4.3 - Steam Injection Subsystem

The source of water for this subsystem was the building's cold water supply line. From here water is branched off through a 1/2 inch copper pipe. The pipe connects to a 1/2 inch ball valve which is used to shut off the flow of water when the system is not in use. The valve connects to a pressure regulator, more specifically a Honeywell model D05 via a 1/2 inch pipe nipple. The regulator is used to reduce the water pressure the system is exposed to and to help dampen out any fluctuations that may occur in the building's cold water line. Water then passes through a series of reducing bushings terminating in 3/8 inch OD plastic tubing with a wall thickness of 0.050 inches. The

tubing runs for 10 m at which point it connects to a 3/8 inch externally threaded tee. Here the flow of water diverges into two paths; the first pertains to the water which is constantly fed to the boiler to maintain steady state conditions, while the second water path contains an electronically controlled valve, which feeds water to the boiler only upon startup or under emergency conditions.

The path of water subject to the electronic valve will be described first. This water leaves the externally threaded tee and enters a 3/8 inch internally threaded tee. One side of the tee holds a pressure gauge, more specifically an Ashcroft gauge with a 0 to 200 psi range and 5 psi subdivisions. This gauge measures the inlet pressure of the water but its measurement is used as a visual check and is not incorporated into any calculations. The other side of the tee connects to a series of pipe nipples that attach to the 3/8 inch electrically actuated valve (CV-7h). The valve is controlled by a low level switch in the boiler and is opened only to fill the boiler at startup and under emergency conditions. Attached to the valve is a 3/8 inch pipe nipple connected to a 3/8 inch to 1/4 inch street elbow. This elbow connects to a 1/4 inch pipe union to allow access to the system if necessary. The union connects to a 1/4 inch to 3/8 inch hex nipple which connects to a 3/8 inch internally threaded tee. Here the path of the water again diverges. Some water is fed through the secondary pump, but in case of pump failure some water is fed directly to the boiler through an unmarked pressure regulator to ensure that the boiler will continue to recieve water under emergency conditions.

The secondary pump side will be described first. The water leaves the tee, enters a 3/8 inch pipe nipple and from there enters the impeller housing of the secondary pump. The pump is a Teel model 3P714 and is a rotary vane pump with internal bypass. The outlet side of the pump housing attaches to a 1/2 inch copper pipe nipple which threads into a 1/2 inch stainless steel cross. Here it is met by water which bypassed the secondary pump and by water which is constantly fed to the boiler during operation. All three of these streams meet at this cross and are fed into the boiler together.

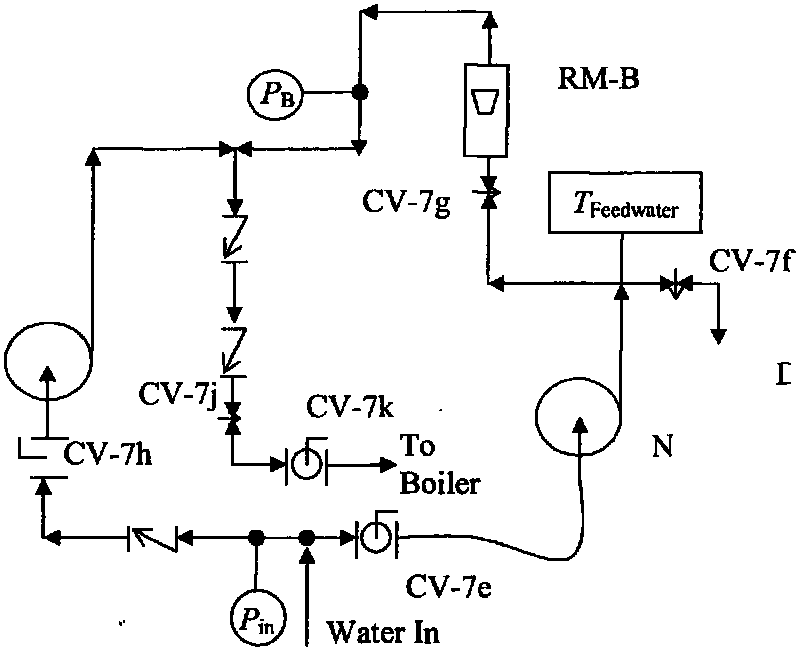

Figure 4.4 - Schematic of Boiler Water Supply (Aspinwall, 2004)

Returning to the tee where water bypassing the secondary pump diverges, the water enters a 3/8 inch pipe nipple from which it enters a short length of 3/8 inch copper tubing bent at a 90° angle. The tubing connects to a 3/8 inch to 1/2 inch reducing hex nipple which threads into an unmarked pressure regulator. The exit of the regulator

connects to a 1/2 inch internally threaded tee. The branching side of the tee connects to a pressure gauge, more specifically a U.S. Gauge 0 to 100 psi gauge with 2 psi increments, through a 1/2 inch street elbow and a 1/2 inch to 3/8 inch reducing bushing. The other side the tee connects to a 1/2 inch pipe nipple whose exit threads into the 1/2 inch stainless steel cross where the three inlet streams converge. The pressure gauge is only used for visual inspection and its measurements are not used in any calculations.

The make-up water side of the stream, which is constantly fed to the boiler, will now be described. The 1/4 inch externally threaded tee connects to 1/4 inch copper tubing which, via a 1/4 inch hex nipple, connects to a 1/4 inch ball valve (CV-7e). This valve could be closed to prevent make-up water from being fed to the boiler, but in practice the valve is always kept open. The valve exits to a 1/4 inch hex nipple which connects to 1 m length of 3/8 inch OD plastic tubing with a wall thickness of 0.050 inches. This tubing connects to a 1/4 inch externally threaded hex nipple followed by a 1/4 inch internally threaded hex nipple followed by a 1/4 inch pipe nipple. The nipple connects to a 1/4 to 1/2 inch reducing bushing which feeds water directly to the primary water supply pump. The pump is a rotary vane pump with internal bypass, more specifically a Teel model 4P919. At startup, once the boiler has reached working pressure steam is allowed into the system followed by the immediate activation of the primary pump. This pump constantly feeds water into the boiler to replace the steam being exhausted.

Water exits the housing of the primary pump and enters a 1/2 inch to 3/8 inch reducing bushing. A 3/8 inch pipe nipple connects this bushing with a 3/8 inch cross. One side of the cross holds a thermocouple which measures the water inlet temperature (T_{11}). The third side of the cross allows water to drain from the system if necessary and the fourth side of the cross feeds water to the rotameter and ultimately to the boiler.

Following the drain side of the cross, the water enters a 3/8 inch 90° elbow followed by a 3/8 inch needle valve (CV-7f). The needle valve can be used to allow water to drain from the system if necessary but is always left closed in practice. The exit side of the valve connects to a 3/8 inch internally threaded hex nipple which threads into a 3/8 inch externally threaded hex nipple that connects to a 1.5 m length of 3/8 inch OD plastic tubing with a wall thickness of 0.050 inches. The exit of this tubing joins the boiler's drainage system.

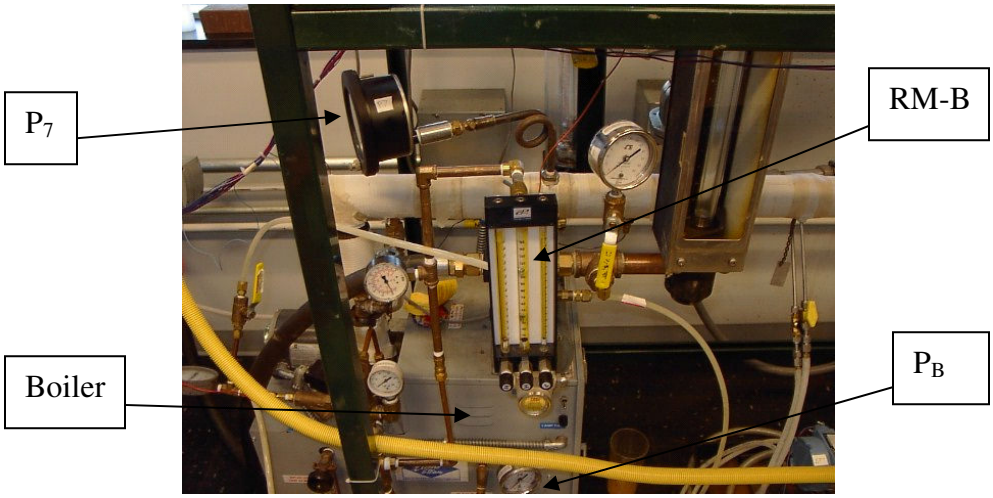

Figure 4.5 - Picture of Steam Boiler and Instrumentation (Aspinwall, 2004)

The side of the cross feeding water to the boiler attaches directly to a 3/8 inch pipe nipple which attaches to a 3/8 inch to 1/4 inch reducing bushing. The bushing feeds water into the boiler inlet rotameter, more specifically a Cole Parmer N044-40 rotameter (RM_B). The rotameter has a built-in needle valve (CV-7g) which allows easy, fine adjustment of the flow of water to the boiler. Water exits the rotameter through a 1/4 inch to 3/8 inch reducing bushing and enters a 3/8 inch steel pipe nipple. The pipe nipple attaches to a 3/8 inch internally threaded elbow which attaches to another 3/8 inch pipe nipple. This nipple threads into a 3/8 inch internally threaded tee. A pressure measurement can be taken off one side of the tee by a pressure gauge, more specifically a Wika 0 to 160 psi gauge with 2 psi graduations. The readings of this pressure gauge are not used in any calculations. The other side of the tee connects to a 3/8 inch pipe nipple which connects to a 3/8 inch internally threaded hex nipple. This nipple threads into a 3/8 inch hex nipple which attaches to a short length of 3/8 inch copper tubing. The tubing connects to a 3/8 inch hex nipple which attaches to a 3/8 inch internally threaded elbow. The elbow attaches to a 3/8 inch copper pipe nipple and it threads onto a 3/8 inch to 1/2 inch reducing bushing. The bushing connects to a 1/2 inch street elbow which connects to the 1/2 inch stainless steel cross where the inlet streams meet.

Now that the three inlets of the cross have been described, the outlet stream will be presented. From the stainless steel cross the water enters a 1/2 inch copper pipe nipple. The nipple feeds the water to a 1/2 inch check valve which passes the water to another 1/2 inch copper pipe nipple followed by a second 1/2 inch check valve. These spring loaded check valves prevent any backflow into the primary and secondary pump

loops. After passing through the second check valve the water enters a 1/2 inch to 3/8 inch reducing bushing followed by a 3/8 inch needle valve followed in turn by another 3/8 inch to 1/2 inch reducing bushing. This needle valve is not used in practice and is always left completely open. A 1/2 inch internally threaded elbow follows the bushing and threads into a 1/2 inch copper pipe nipple. The water enters a 1/2 inch internally threaded ball valve (CV-7j) connected to a 1/2 inch pipe nipple followed by a 1/2 inch to 3/4 inch internally threaded tee. One side of the tee is plugged and the other side of the tee threads directly to the boiler's intake pipe.

The boiler is a 20 kW electric boiler, more specifically an Electro Steam model LB-20. It uses a 220 V three phase electrical power supply to generate superheated steam which exits the boiler through a 1/2 inch steel pipe nipple. The nipple connects to a 1/2 inch internally threaded tee. One side of the tee connects to a 1/2 inch street elbow which connects to an emergency steam release valve. The other branch of the tee connects to a 1/2 inch ball valve (CV-7a). This valve is used to shut the flow of steam on or off and is not used for fine control. The valve connects to a 1/2 inch pipe nipple which connects to a 1/2 inch union. A 1/2 inch 90° elbow threads into the union followed by a 1/2 inch pipe nipple that feeds the steam into a 1/2 inch tee. One side of the tee connects to a pipe nipple that connects to a gate valve (CV-7b) which via a 1/2 inch hex nipple connects to a length of rubber tubing that leads steam out of the window. The gate valve can be used to bleed steam out of the system but has not been used in the course of this experimentation.

The flow that remains in the system exits the tee and enters a 1/2 inch pipe nipple followed by a 1/2 inch to 3/4 inch internally threaded stainless steel reducing coupling. This connects to a 3/4 inch pipe which threads into a 3/4 inch internally threaded stainless steel tee. Through one side of the tee, via a 3/4 inch to 3/8 inch stainless steel reducing bushing and a 3/8 inch 90° pigtail, a bourdon tube pressure gauge (P_7) is attached. More specifically, the gauge is an Omega Engineering 0 to 100 psi gauge with 0.5 psi subdivisions. This gauge measures the pressure of the steam exiting the boiler and is used to fix the state of the steam in calculations and to determine the flow rate through the orifice. Exiting the other side of the tee is a 3/4 inch stainless steel pipe nipple followed by a 3/4 inch stainless steel tee. The branching side of the tee allows a thermocouple to measure the temperature of the stream (T_7). This temperature measurement is useful in fixing the state of the steam and in determining the flow rate through the orifice. The other side of the tee exits into a 3/4 inch stainless steel pipe nipple which attaches to the brass corner tapped flow orifice. More specifically the orifice is a Gerand Engineering model 3/4 inch B-5. Located on either side of the orifice are pressure taps which are connected to a differential pressure transducer, more specifically a Rosemount 1151DP (DP-7).

As the flow exits the orifice it enters a 3/4 inch stainless steel pipe nipple which connects to a vertically aligned 3/4 inch stainless steel tee. The upward facing side of the tee allows steam into the system while the downward facing side of the tee serves as a steam trap to evacuate condensate from the system. The downward facing side attaches to a 3/4 inch to 1/2 inch reducing bushing which threads into a 1/2 inch steel pipe nipple.

The nipple connects to a 1/2 inch female to 3/8 inch male reducing adapter followed by a 3/8 inch internally threaded hex nipple. The nipple connects to 3/8 inch steel needle valve. At system startup this valve is opened fully to allow condensate to quickly evacuate the system. After most condensate has been removed the valve is closed until a steady drip forms. When measurements are being taken the dripped water is collected over a period of time and the mass flow rate of this water which does not proceed into the system is determined.

The upward facing side of the tee connects to a 3/4 inch to 1/2 inch reducing hex nipple which threads onto a ball valve (CV-7d). This valve is used as the primary control valve for the amount of steam injected into the system. The ball valve exits into a 1/2 pipe that, through a series of reducing bushings, directs the steam flow into the injection chamber which is a 1 1/4 inch tee. A 60° full cone steam nozzle, or more specifically a stainless steel full cone spray nozzle with a 3/8 inch connection which will spray 15.14 L/min (4 gpm) at 276 kPa (40 psi), is attached to the end of the copper tube that enters the mixing tee and serves as the injector for the steam into the chamber.

In review, the requirements of the steam generation system are as follows:

1. Provide a constant flow of steam into the system at steady state conditions
2. Provide a measured and controlled steam flow rate
3. Provide a measured and controlled flow of water into the boiler

As discussed above, the boiler is able to provide a constant flow of steam into the system. Using the orifice flow meter with the temperature and pressure data at Station 7 the flow rate of steam can be determined; additionally, by using ball valve CV-7d the flow rate can be controlled. With the combination of the boiler inlet rotameter reading and the boiler inlet temperature measurement the flow rate to the boiler can be determined. The valve built into the rotameter allows the inlet flow to be easily controlled.

4.1.3 Mixed Flow

The mixed flow system delivered the humid air flow to the turbine side of the automotive turbocharger which expanded the flow. The system also measured temperature and pressure of the flow before and after the turbocharger. A wet bulb measurement attempted to determine the amount of moisture in the flow but the measurement was redundant and the results lacked the reliability needed for use in calculations. All pipes in this section were insulated to minimize heat loss.

Air and steam enter the system separately and are mixed at Station 3, the starting point of this subsystem. The temperature and pressure of the mixture are measured before and after the mixture is expanded through a turbine. Exiting the turbine the flow enters the axial flow moisture separator housing, from which it exits through a long hose into the atmosphere. This section will describe the path of the humid airflow from the point of mixing to entering the turbine.

After the mixture leaves the 1 1/4 inch tee which serves as a mixing chamber the mixture flows into a 1 1/4 inch pipe nipple then into a 1 1/4 inch tee. Here the straight path, which would be followed by heavy condensed water droplets, leads to a steam trap, more specifically a Spirax-Sarco model B-1H. The steam trap evacuates any condensed water from the system while preventing steam from exiting the system. In practice the amount of water removed by this trap is quite insubstantial and is not captured for measurement. The other side of the tee changes the flow direction by 90° and routes it into another 1 1/4 inch tee. One end of the tee is fitted with a reducing bushing leading to a 90° 3/8 inch pig tail threaded to a pressure gauge, more specifically an Omega Engineering 0 to 60 psi gauge with 0.5 psi subdivisions, where a pressure measurement (P_3) is made. The flow is then routed through another 90° turn through a tee and into a 1 1/4 inch cross. One branching end of the cross holds a thermocouple (TC-3) where a temperature measurement (T_3) is made. The flow proceeds straight through the cross, into a 1 1/4 inch pipe, and from there it enters the turbocharger.

The other branching side of the cross holds a 1/2 inch needle valve (CV-6) followed by wet and dry bulb thermocouples. This combination is intended to make a wet bulb temperature measurement for determination of the relative humidity of the humid air stream. This measurement has been found to be unreliable in addition to being redundant since the amount of moisture in the stream can accurately be calculated from the inlet air's relative humidity and the orifice flow meter's calculated flow rate. After the flow is throttled through the needle valve it flows through a 1/2 inch elbow. Leaving the elbow the flow is directed through a 1/4 inch tee. One side of the tee is fitted with a

four wire type T thermocouple (TC-6), more specifically an Omega Engineering four wire type T thermocouple. As the flow exits the tee it enters a 1/4 inch cross. The cross is oriented such that one end points up and one end points down while the other two ends remain horizontal. The flow enters the cross and exits to the atmosphere through horizontal ends. The upward facing end holds a thermocouple (TC-WBD) which measures the wet bulb depression of the air stream. The thermocouple is immediately surrounded by a plastic tube, which provides insulation and serves to dampen out fluctuations the thermocouple might experience. The plastic tube is surrounded by a cotton wick which ensures hydration of the thermocouple at all times. The downward face of the cross attaches to a 1/4 inch OD clear plastic tube. The cotton wick runs into the tube and capillary forces bring water up to the thermocouple to ensure hydration. The tube connects to the bottom of a cylindrical water reservoir which is routinely filled with water before any data are taken from the system. This measurement system is illustrated in schematic form by Figure 4.6.

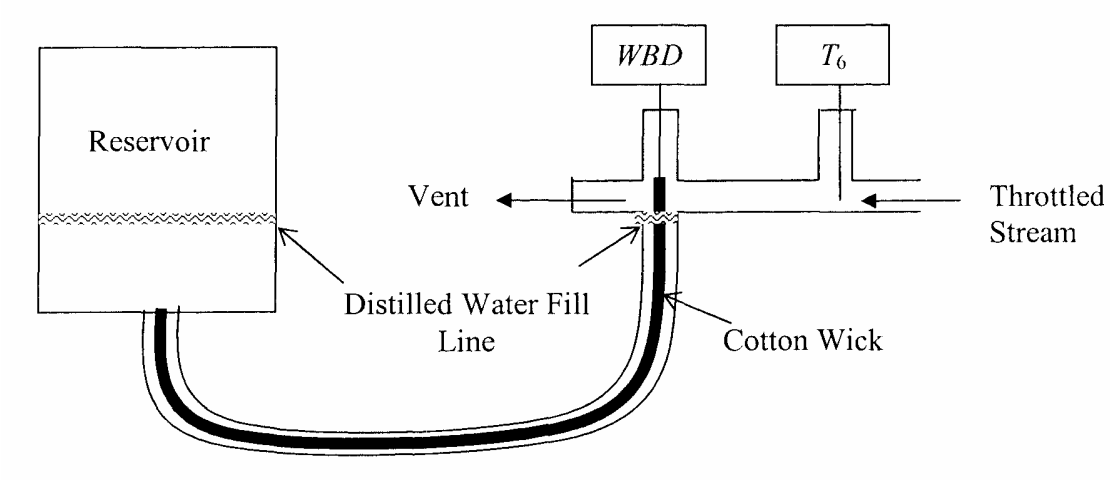

Figure 4.6 - Schematic of Wet-Bulb Measurement Setup (Hull, 2002)

Figure 4.6 shows the wet and dry bulb measurement setup. The thermocouples were set up in a delta temperature configuration to make temperature measurements. The dry bulb thermocouple is a dual element thermocouple and one element is connected in series with the thermocouple used to make the wet bulb depression measurement. The voltage produced by the dry bulb thermocouple was correlated directly to temperature while the voltage read from the wet bulb thermocouple was correlated to temperature using the Sebeck coefficient for a type T thermocouple of 4.3×10^{-5} V/°C corresponding to a constant temperature of 60 °C.

The dry bulb temperature is a straightforward measurement while the wet bulb measurement is delicate. First the pressurized stream must be throttled down to atmospheric pressure without allowing a substantial amount of moist air to escape. Next the wick must be kept properly hydrated. If too little moisture is present on the wick the thermocouple will measure the dry bulb temperature while if too much moisture is present the water temperature will be measured. In practice, the wet bulb depression measurement has a large random variation, 5% of its value, and is usually in disagreement with calculated values. Due to the inherent unreliability of a wet bulb temperature measurement under these experimental conditions, this measurement was disregarded for quantitative results.

In summary, the design requirements for the mixed flow system were to measure the temperature and pressure of the mixed stream and to deliver the humid air stream to the turbocharger. Thermocouples and pressure gauges were used to measure the

temperature and pressure of the stream. The flow exited the mixed flow section to enter the turbine, which is covered in the next section.

4.2 TURBOCHARGER ENERGY RECOVERY SYSTEM

This section describes the part of the experimental setup involving the turbocharger. The turbocharger is composed of a turbine side and a compressor side, along with an oil lubrication system. All three of these parts will be discussed in this section. Figure 4.7 shows a picture of the turbocharger used in this system.

4.2.1 Turbine System

The purpose of the turbine was twofold. The turbine was used to expand the humid air mixture, dropping the temperature and pressure such that liquid water condensed and the mixture became two phase. The flow was then passed to the moisture separator where moisture was removed from the air stream. The turbine was also used to recover energy from the air stream and pass it as shaft power to the compressor system. This section will follow the humid air stream from the point at which it enters the turbine until it enters PVC wye of the moisture separator. None of the pipes in this section of the system are insulated.

The humid air stream enters the turbine, specifically a Garret model GT-1541V, and is expanded. The flow exits through a 1 1/4 inch pipe nipple into a 1 1/4 inch cross. One branching side of the cross is fitted with a pressure gauge, more specifically a Marshall-Town 80827, where the turbine outlet pressure is measured (P_4) and the

opposing side of the cross is fitted with a thermocouple (TC-15). This thermocouple was calibrated but it was added late into experimentation and its measurements were never used in any calculations. It was used to check the temperature drop between the turbine exit and the separator inlet. The humid stream exits the cross, enters a 1 1/4 inch pipe threaded into a 1 1/4 inch PVC female adapter. The adapter is chemically welded to a length of 1 1/4 inch PVC pipe which exits into a reducing bushing that passes the flow into the wye at the beginning of the moisture separator.

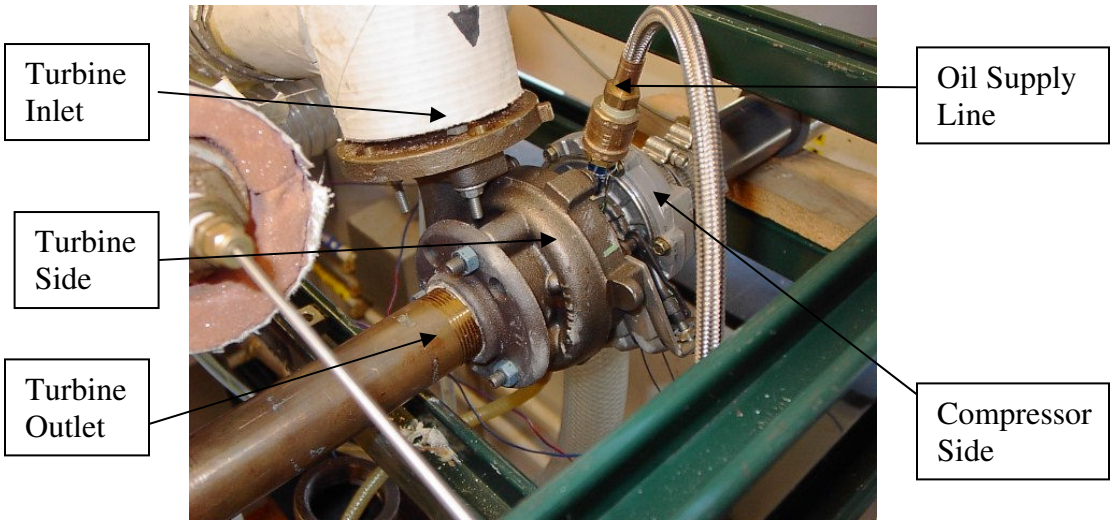

Figure 4.7 - Turbocharger Energy Recovery System (Aspinwall, 2004)

In summary, the design requirements for the turbine system were to expand the humid air stream, dropping the temperature and pressure, and to deliver shaft power to the compressor side of the turbocharger. Both of these requirements were fulfilled. The turbine expanded the humid air stream and liquid water condensed out of the stream. Shaft power was delivered to the compressor, which is discussed in the following section.

4.2.2 Compressor System

The purpose of the compressor was to compress ambient air in a manner such that the turbine was loaded and the compressor's power output could be measured. This allows the power output of the turbine to be calculated. This section will follow ambient air from the point at which it enters the compressor's air filter until it exits again to the atmosphere. None of the pipes in this section of the system were insulated.

Air is drawn into the compressor system through an air filter on its inlet. The purpose of the air filter is to prevent foreign particles from entering the system and damaging the compressor. The filter is connected to a 1 1/2 inch PVC elbow which threads onto a length of 1 1/2 inch PVC pipe. A brass fitting is threaded into the pipe and holds a thermocouple (TC-8). This thermocouple measures the ambient air temperature as it enters the compressor. The exit end of the PVC pipe is connected to the compressor via a 1 1/2 inch flexible pipe coupling. Exiting the compressor, the flow enters a 1 1/2 inch clear flexible plastic hose. A hole is cut into the hose and a thermocouple (TC-9) is inserted into the flow to measure the compressor outlet temperature (T_9). The rubber hose leads into a 1 inch stainless steel pipe which connects to a 1 inch stainless steel tee. The diverging side of the tee is plugged and flow continues through another 1 inch stainless steel pipe and into a second 1 inch stainless steel tee. The branching side of this tee connects to a series of reducing bushings and terminates in a pressure gauge (P_3), more specifically an Omega Engineering 0 to 30 psi gauge with 0.2 psi subdivisions. Air exits the tee and enters a 1 inch stainless steel pipe connected to a 1 inch to 1 1/4 inch reducing bushing.

The bushing connects to a rotameter (RM-9), more specifically a Fischer-Porter 10A3565A. The rotameter measures the airflow generated by the compressor and in conjunction with the temperature and pressure measurements can be used to determine the amount of power provided by the compressor to the working fluid. The rotameter connects to a 1 1/4 inch to 1 inch stainless steel reducing bushing. A 1 inch pipe connects to the bushing and air exits it into a 1 inch stainless steel elbow. The elbow connects to a 1 inch stainless steel pipe which connects to a 1 inch stainless steel ball valve (CV-9). During operation this valve is closed slightly to put back pressure on the compressor. Air exits the valve into a 1 inch stainless steel pipe and from there the air reenters the atmosphere.

As part of a supplementary and redundant measure of the compressor's output power, the rotational speed of the compressor is measured. The shaft of the compressor is marked with a dark dot and an optical sensor which threads into the compressor housing records every time the dot passes its view. Each passing is equal to one rotation of the shaft and a photoelectric sensor, more specifically a Banner D12SN6FPYQ, turns the optical pulses into electrical pulses which are counted by a counter, more specifically a Hewlett Packard 5314A universal counter.

The only design requirement of the compressor system was to compress air and measure the temperature, pressure, and flow rate of the compressed air. Through thermocouples, a pressure gauge, and a rotameter the amount and condition of the compressed air was measured.

4.2.3 Oil Delivery Loop

The purpose of the oil system was to provide a constant oil supply to the turbocharger to feed its forced lubrication journal bearing. The oil must be supplied at a constant, controlled pressure as too much pressure will create oil contamination of the humid air stream. The oil temperature and pressure must be measured to ensure that the oil is able to properly lubricate the turbocharger. The oil system is a closed loop and is outfitted with a positive displacement pump, an oil filter, a thermocouple, and a pressure gauge. The oil reservoir is the only part of the oil system that is insulated.

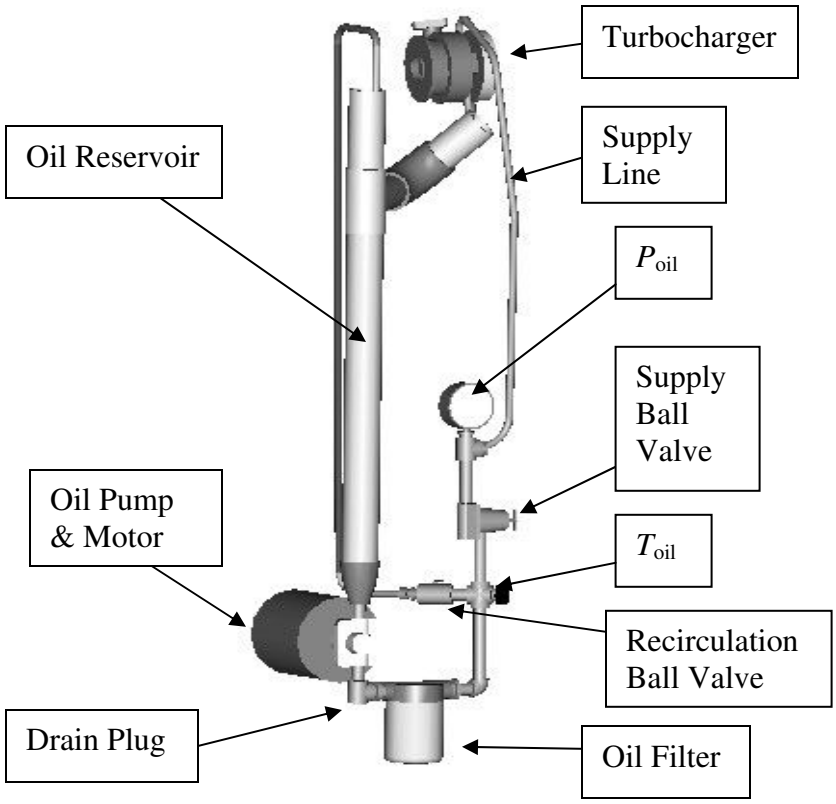

Figure 4.8 - Oil Delivery Subsystem

Figure 4.8 shows a schematic drawing of the oil system. Starting at the oil reservoir, oil is drawn into the pump and consequently forced through the oil filter. A temperature measurement is taken at a cross which splits the oil flow in two directions. One branch of the cross recirculates oil into the reservoir while the remaining side of the cross leads to a pressure measurement followed by the turbocharger. When oil leaves the turbocharger it is directed back into the reservoir. Each side of the tee is controlled by a ball valve and using the ball valves in combination any desired oil pressure to the turbine can be achieved limited only by the pump output.

The oil reservoir is a 2 inch galvanized pipe that is insulated externally to prevent heat loss. Oil leaves the reservoir through a 2 inch to 1/2 inch galvanized reducing coupling and enters a 1/2 inch pipe nipple connected to a 1/2 inch union. Oil leaves the union, enters a 1/2 inch pipe nipple, and enters a positive displacement pump, more specifically a Hypro model 0503C-DE. The reservoir is oriented directly above the pump, allowing the pump to be gravity fed. The pump is capable of supplying 13.2 liters per minute (3.5 gpm) at a pressure of 3.1 bar (30 psig). The pump discharges oil into a 1/2 inch pipe nipple and oil is fed into a 1/2 inch tee with the straight end plugged. The plug is the lowest point in the oil system and can be removed to drain the system. The oil flow turns 90° in the tee and enters a 1/2 inch hex nipple followed by a 1/2 inch stainless steel pipe union. Oil leaves the union to enter a 1/2 inch to 3/4 inch hex nipple.

The hex nipple directs oil into an oil filter, more specifically a Hydac International 0080MA010BN. Flow leaves the oil filter through a 3/4 inch to 1/2 inch

reducing bushing and enters a 1/2 inch street elbow. A short length of 1/2 inch pipe connects the elbow to a 1/2 inch cross. One diverging side of the cross holds a thermocouple (TC-oil or TC-12), while the other two sides of the cross split the oil between a stream directly recirculating into the oil reservoir and a stream lubricating the turbocharger. The second diverging side of the cross connects to a 1/2 inch pipe nipple which connects to a 1/2 inch ball valve. The valve connects to a 1/2 inch hex nipple that threads into 1/2 inch copper tubing which directs oil flow back into the top of the reservoir.

The straight path through the cross directs oil toward the turbocharger. Leaving the cross, oil enters a 1/2 inch pipe that connects to a 1/2 inch stainless steel ball valve. This ball valve was installed into the system where a pressure regulator was formerly located. The pressure regulator was not able to sufficiently decrease oil flow to the turbocharger during startup when oil was being warmed. The ball valve allows total shutoff of oil flow to the turbocharger during this stage while also giving good control of the pressure to the turbocharger during operation. Exiting the ball valve, oil enters a 1/2 inch pipe and flows into a 1/2 inch tee. The straight side of the tee directs oil into a 1/2 inch to 3/8 inch reducing bushing, into a 3/8 inch pipe, followed by a 3/8 inch female hex nipple and terminating in a bourdon tube pressure gauge, more specifically an Ashcroft Duragauge ranging from 0 to 100 psi in 1 psi graduations. The branching side of the 1/2 inch tee connects to a 1/2 to 3/8 inch hex nipple that directs oil into a 3/8 inch braided stainless steel hose. The hose connects to a 3/8 inch pipe nipple threaded into a 3/8 inch coupling. The coupling directs oil into a 3/8 inch to 1/4 inch reducing bushing that

connects to a 1/4 inch aluminum union. The union connects to a 1/4 inch stainless steel hex nipple and the hex nipple threads directly into the turbocharger housing.

Leaving the turbocharger, oil discharges into a 1/4 inch to 1/2 inch hex nipple. Oil enters a short length of 1/2 inch tubing and flows into a 1/2 inch male to 3/8 inch female adapter. This attaches to a 1/4 inch hose nipple which directs the flow into 1/4 inch rubber tubing that dumps oil back into the top of the reservoir.

A strip heater is wrapped around the oil reservoir under a layer of insulation. The heater was used to warm the oil before the pump is turned on. During operation the heater was turned off as lubricating the turbocharger transfers sufficient heat to the oil to maintain its temperature.

The two requirements of the system, supplying a controlled, constant oil stream to the turbocharger and measuring the oil temperature, were accomplished. The pump provides a constant supply of oil to the turbocharger and using the two ball valves in the system the pressure of the stream that reaches the turbocharger can be adjusted to desired operating settings. The oil temperature and pressure are measured and monitoring these readings ensures that sufficient warm oil is available to provide lubrication to the turbocharger.

4.3 AXIAL FLOW MOISTURE SEPARATOR

This section describes the moisture separator which was used to remove condensed water from the humid air stream after the flow ran through the turbine. The moisture separator was designed and built as part of previous research at Georgia Institute of Technology and is therefore not commercially available. The housing of the separator and the separator itself will be described.

4.3.1 Swirl Element Housing

The purpose of the swirl element housing is to force the flow to pass over the swirl element and to permit temperature and pressure measurements of the flow to be taken. After this point the flow exits the system and should be directed away from the researcher or any instrumentation. In this section the mixed flow will be followed from the point at which it enters the housing until it is exhausted into the atmosphere. All fittings in this section are schedule 40 PVC unless otherwise specified. The end assemblies are chemically welded together but, to facilitate potential removal of the swirl element, they are not welded to the clear straight pipe which houses the swirl element. None of this system is insulated.

Figure 4.9 shows a scaled drawing of this system. Flow enters the housing, is passed across a thermocouple and one side of a U-tube manometer. The flow then passes over the swirl element, over the second opening of a U-tube manometer, and is then exhausted out of the system into a hose which directs it safely into the atmosphere.

While the flow is in the straight section of the housing it is exposed to a copper tube through which chilled water is run when cooling is desired.

Humid air and condensed water enter the system through a 1 1/4 inch to 1 1/2 inch reducing bushing and flow into a 1 1/2 inch to 3 inch long turn wye. The side of the wye is drilled and tapped to accommodate a thermocouple which is inserted into the flow and measures the separator inlet temperature (T_4) which is used to calculate the separation efficiency. The top of the wye is ultimately capped while the flow proceeds downwards. Immediately atop the wye is a 3 inch hex bushing with the top hex rounded off such that a 3 inch pipe cap fits onto it. The top of the cap is drilled and tapped for a plastic 1 1/4 inch to 3/4 inch reducing bushing. A 3/4 inch brass pass through bushing allows 1/2 inch copper tubing to enter the enclosure.

The bottom of the wye connects directly to a 76 mm (30 inch) length of 3" clear pipe. The pipe houses the swirl element and is drilled and tapped before and after the swirl element to allow 3/8 inch brass hose nipples which connect a plastic hose to a U-tube manometer, more specifically a Dwyer Instruments 0 to 16 in. H_2O manometer with 0.2 in H_2O. increments. The manometer measures the pressure drop across the swirl element. The swirl element and housing were designed with the ability for the swirl element to be moved within the housing to test different element positions. The pressure taps are therefore located near the ends of the clear plastic pipe.

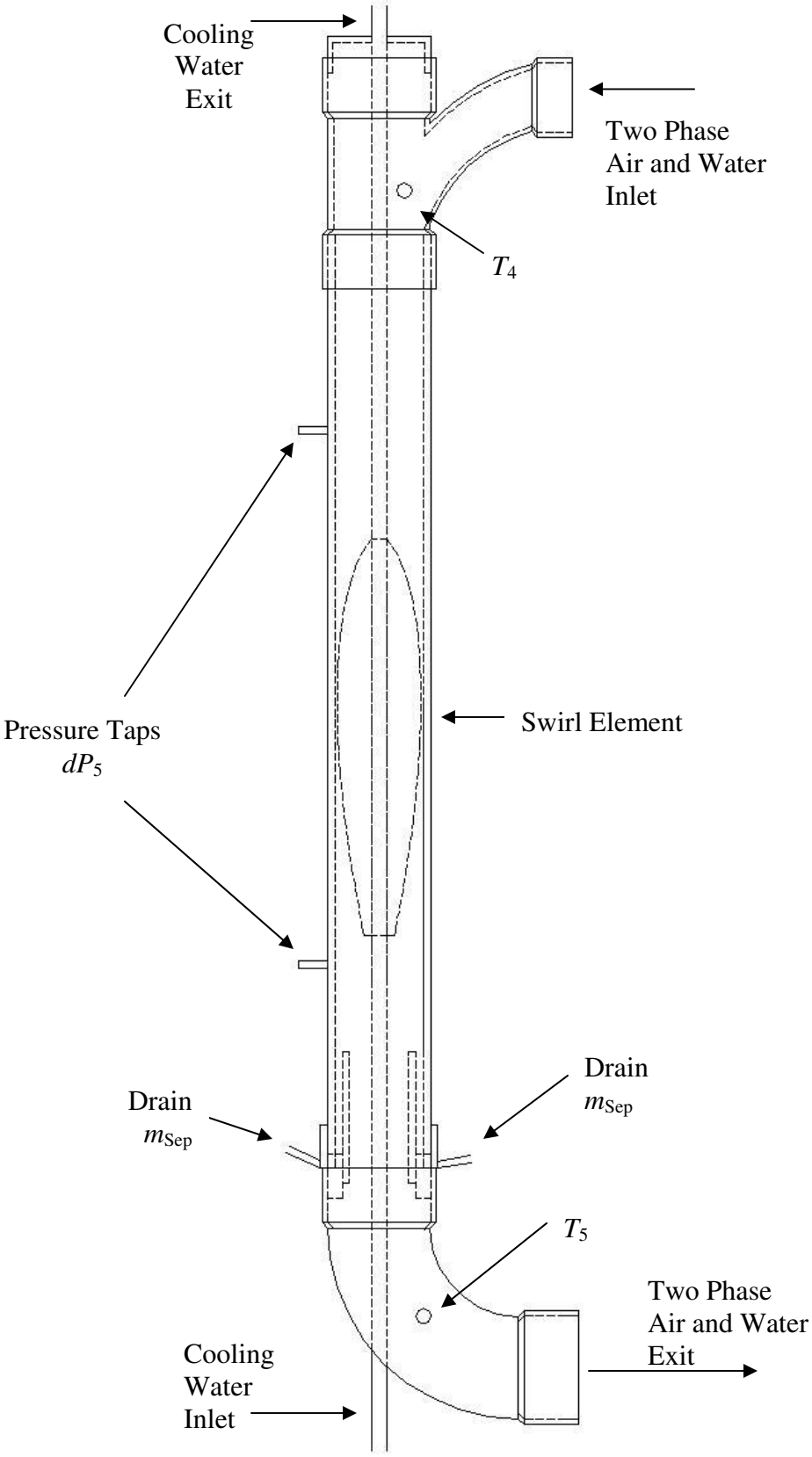

Figure 4.9 - Schematic of Moisture Separator

The saturated air flow leaves the clear pipe and enters a 3 inch external pipe coupling. This coupling is drilled and tapped at two diametrically opposed places and the holes are fitted with 3/8 inch hose nipples. The nipples allow a 3/8 inch plastic hose to be connected to the swirl element housing. The hoses direct separated water (m_{Sep}) into an external container. The inside of the coupling connects to a 3 inch external socket weld bushing with 2 inch internal threads. The internal threads are used to hold a 152.4 mm length of 2 inch CPVC which sticks up into the clear plastic tube. Liquid water flows outside the pipe while the humid air stream continues through it. A flat annulus of CPVC is chemically welded atop the socket weld bushing to prevent water from collecting in the valleys which the manufacturer created in this piece. The annulus fits inside the clear pipe and outside the 2 inch CPVC pipe.

The bushing fits into a 3 inch elbow which directs it into a 3 inch to 1 1/2 inch reducing bushing. The elbow is drilled and tapped to allow a thermocouple (TC-5) to make a final temperature measurement (T_5). The bushing connects to a 1 1/2 inch pipe which, via a 1 1/2 inch to 2 inch flexible rubber adapter, is coupled to a short length of 2 inch CPVC pipe. A 2 inch flexible reinforced plastic hose is hose clamped to the exterior of the pipe and the hose directs the flow out a window safely into the atmosphere.

The requirements of the separator housing are as follows;

1. Force the flow over the swirl element
2. Permit temperature and pressure measurements of the flow

3. Permit liquid water to leave the housing
4. Direct the exhausting flow into the atmosphere safely, away from the researcher and instrumentation

All these objectives are fulfilled in the realization of the separator housing. As the flow is forced through the clear plastic tube it passes over the swirl element. The clear plastic pipe is tapped before and after the swirl element to allow pressure measurements. The wye before and the elbow after the swirl element are tapped to allow temperature measurements. The coupling after the clear pipe is drilled and tapped to allow separated water to be evacuated from the humid air stream.

4.3.2 Swirl Element

The purpose of the swirl element is to impart a strong rotational motion to the humid air stream as it passes over the element and to avoid creating a pressure drop as the flow passes the trailing end of the element. The rotational motion the swirl element imparts forces the heavier water particles to the outside of the flow, allowing them to be separated out from the main body of the flow later. If the swirl element was to create a sudden pressure drop the newly formed water droplets would break up into smaller drops which are harder to separate out of the main flow.

In general, axial swirl elements have streamlined contours that avoid flow separation and fins of some kind around the diameter that direct the flow to produce tangential rotation. Fins may be attached externally or cut into the surface. In this swirl

element, the contour is that of a standardized airfoil and grooves are cut into the surface to create swirl. Figure 4.10.A and Figure 4.10.B show CAD representations of the swirl element.

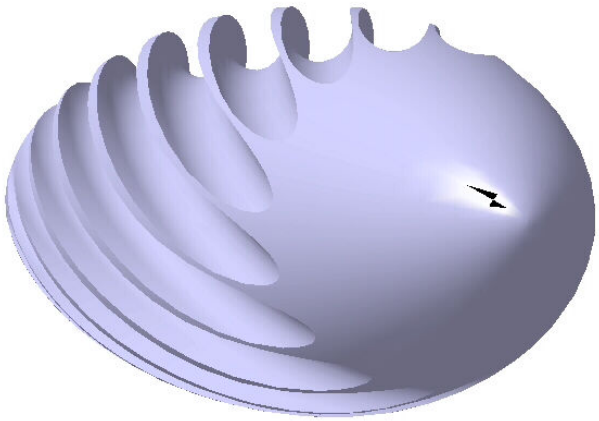

Figure 4.10.A - Axial Flow Swirl Element Model Created in Catia – View 1

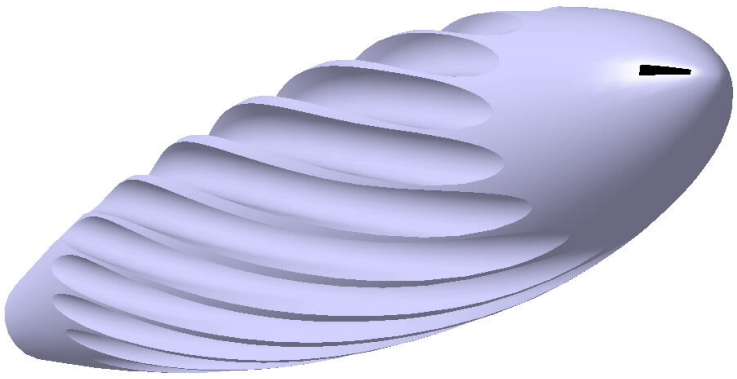

Figure 4.10.B - Axial Flow Swirl Element Model Created in Catia – View 2

The swirl element was designed as part of the research carried out by Aspinwall (2004) and is not commercially available. A brief description of the design of the swirl

element follows. The body of the element was cut out of a billet of 2017 alloy aluminum. The piece is symmetric about its axis and the contour it follows was generated by rotating the top half of a standard 2412 NACA airfoil around its mean chord line. Figure 4.11 presents a 2412 NACA airfoil.

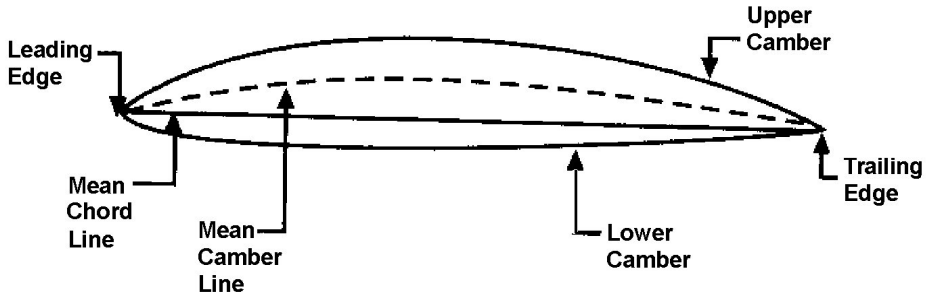

Figure 4.11 - Standard Airfoil Design

This airfoil design is well documented and is often found on light aircraft. It was reasoned that this design's streamlined profile would cause little pressure drop on its rear end and therefore was acceptable (Ladson *et al*., 1996). The airfoil's profile was then scaled such that at its largest diameter it would fit within the 3 inch schedule 40 clear PVC pipe that would be its housing.

Fifteen grooves were cut into the profile at a depth of 17.8 mm (0.700 in.) using a 1/2 inch round tipped mill bit. The grooves wrap around the swirl element at an angle of 20° to the axial direction. The grooves are deepest at the greatest diameter of the element and become shallower toward the front and back. The composite area of the grooves was

calculated to preserve the area of the 2 inch branch of the wye that the flow enters the separator through. This area preservation was intended to help prevent droplet breakup.

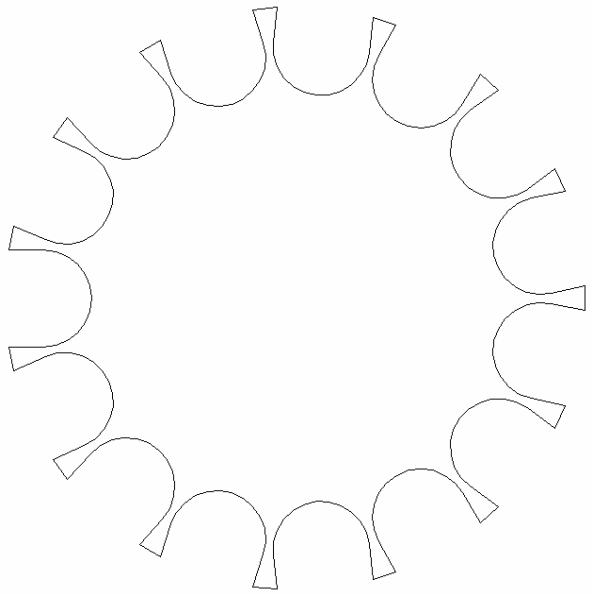

Figure 4.12 - Cross Section of Swirl Element at Largest Diameter

The swirl element and its housing are oriented vertically to take advantage of gravitational effects on the heavier water particles. Air flow proceeds downward within the housing. The swirl element fits slightly loosely within the PVC pipe and is held in place by a press fit onto a 1/2 inch copper tube. The tube runs through the center of the element and serves both to carry cooling water to the element and to hold the element in place. The tube enters the housing through a hole drilled into the bottom elbow and exits through the pass through bushing atop the separator housing which holds the copper tubing in place.

Figure 4.13 displays the actual finished swirl element. Grooves were cut into the surface then the piece was turned on a lathe. The hole through the center of the element was intended to hold a 1/2 inch copper tube through which cooling water flowed. The swirl element was press fit onto the copper tube and the tubing held the element in place. The largest diameter fit snugly within the 3 inch clear PVC pipe that was the main body of the separator housing.

Figure 4.14 shows the swirl element installed in the separator housing. The copper tube which was run through the swirl element is holding it in place. The separation tube is also visible. Water droplets which have swirl imparted to them travel along the inside of the clear pipe wall. The main body of the flow exits this stage of the swirl element housing through the center of the pipe.

Figure 4.13 - Swirl Element

Figure 4.14 - Swirl Element in Separator Housing

In summary, a standard, streamlined airfoil design was followed to avoid creating flow separation, resulting in pressure drop, turbulent and chaotic flow, and ultimately, droplet breakup. Rotational motion was created by passing the flow through grooves cut into the swirl element.

4.4 SYSTEM VARIATIONS

This section describes additional parts of the system. These parts were employed while taking data when noted, but they were neither always employed nor required for the system to operate. The chilled water loop, the commercial separator, and the flow straightener subsystems will be described in this section.

4.4.1 Chilled Water Loop

Water chilled to 6 °C was run through the center of the swirl element and the pipe carrying it was exposed to the air stream before and after entering the swirl element in a counter flow heat exchanger configuration. The purpose of the chilled water was to remove heat from the two phase air and water stream leaving the turbocharger. The mass of water that air can hold is directly related to the temperature of the air. At cooler temperatures a given mass of air will carry a certain mass of water vapor while at a higher temperature the same given mass of air is capable of carrying much more water vapor. Chilling the air therefore made more water available for separation by the moisture separator. Since the separation efficiency is defined using the temperature at which the air enters the separator housing, after which heat removal takes place, it is theoretically possible to achieve separation efficiencies greater than unity. It is essential

that the temperatures before and after water flows through the separator housing are measured and that the flow rate of chilled water is measured and controllable.

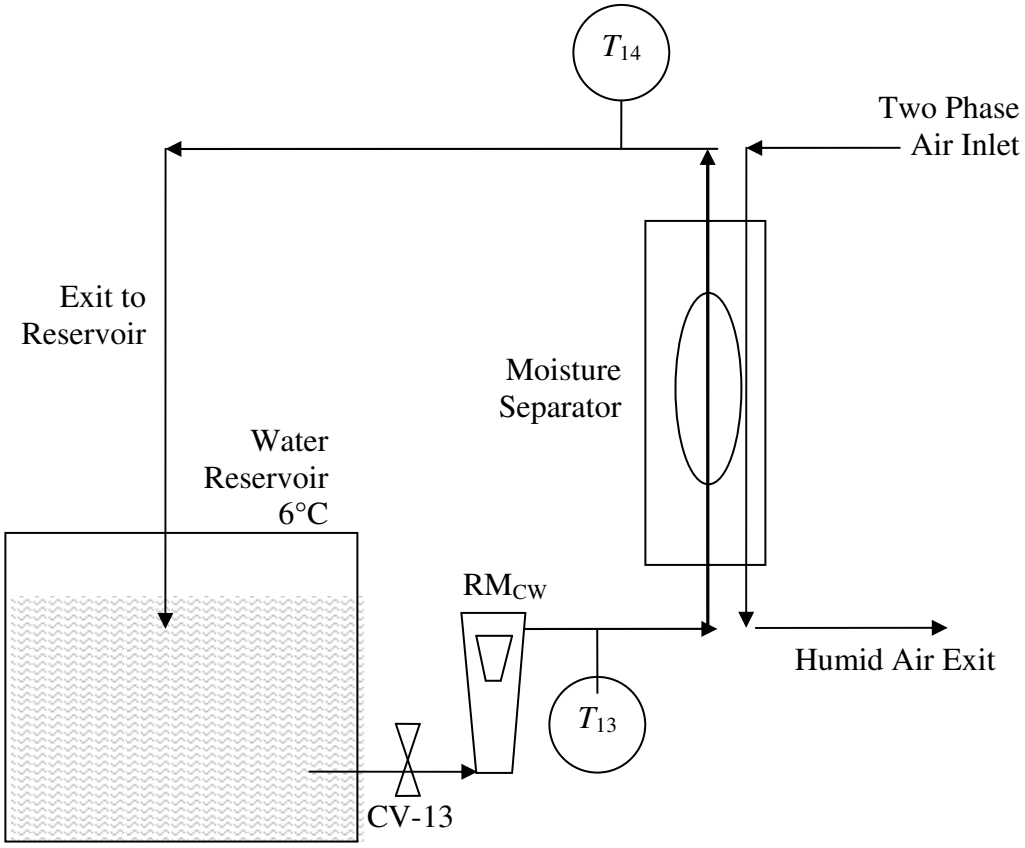

Figure 4.15 – Cooling Water Subsystem

Figure 4.15 shows a schematic representation of the cooling water loop. Cooled water from a 1514 L (400 gallon) reservoir was pumped into the system through a rotameter (RM_{CW}) which recorded the flow in gallons per minute. The rotameter had a valve incorporated into it which allowed the flow rate to be controlled. With the control valve fully open the maximum pump discharge was 11 L/min (3.0 gpm). The system was also run at several different water flow rates between 0 L/min and 11 L/min. After the water flowed through the rotameter the temperature was measured as it entered the

separator housing. Temperature was again measured as the water left the housing. The water was then discharged into the reservoir. Only the reservoir is insulated.

A submersible pump, a Teel 4RK65, was immersed in a reservoir of chilled water. The pump discharged water through a threaded 2 inch outlet into a series of reducing bushings that result in a 3/4 inch hex nipple that threads onto a 5/8 inch flexible plastic hose. The hose is 8 m long and connects to a 3/4 inch to 1/2 inch reducing bushing. The bushing connects to a 1/2 inch CPVC pipe nipple that threads into the rotameter, a King rotameter with a range of 1.89 to 39.74 Lpm (0.5 to 10 gpm) and 0.95 Lpm (0.25 gpm) graduations. Built into the rotameter is a valve (CV-13) which is used to control the flow rate through the system.

Upon exiting the rotameter the flow again enters a 1/2 inch CPVC pipe nipple. The nipple discharges into a 1/2 inch to 3/4 inch reducing bushing which directs flow into a 500 mm length of 5/8 inch flexible plastic hose. Flow exits the hose and enters a 3/4 inch to 1/2 inch reducing bushing that connects to a 1/2 inch to 3/8 inch hex nipple. This nipple threads onto a tee and on the branching side of the tee is a thermocouple which takes a measurement of the chilled water temperature (T_{13}) just before it enters the separator housing. Water flows straight through the tee and enters a 3/8 inch hex nipple. This nipple connects to a copper 3/8 inch female pipe to 1/2 inch socket end tube fitting to which a short length of 1/2 inch copper tubing is soldered. Fit around and clamped on to the trailing end of the pipe is a 150 mm 5/8 inch hose and the other end fits around and is clamped onto a 1.5 m length of 1/2 inch copper tubing which directs water to flow into

the separator housing through a hole in the 3 inch PVC elbow at the exit end of the separator housing. The tubing then enters the swirl element, exits it, and exits the separator housing via a pass through bushing.

A 150 mm length of 5/8 inch hose is slipped over and clamped onto the end of the tubing. The hose discharges water into a short length of 1/2 inch copper tubing with a copper 1/2 inch socket tube to 3/8 inch female pipe fitting on its trailing end. A 3/8 inch tee connects to the fitting and the diverging side of the tee allows a thermocouple (TC-14) to measure the temperature of the cooling water flow exiting the separator housing (T_{14}). Water flows straight through the tee and exits into a 3/8 inch hex nipple. Water flows through the hex nipple and into a 3/8 inch to 1/2 inch reducing bushing followed by a 1/2 inch to 3/4 inch reducing bushing. Water then enters an 8 m length of flexible plastic hose and is discharged into the reservoir.

The requirements of the cooling water loop are as follows;

1. Measure the temperature of the cooling water before and after contact with the humid air flow
2. Measure the mass of cooling water flowing through the separator
3. Control the mass of water flowing through the separator

The temperature is measured before and after exposure to the two phase air stream. The rotameter with a built-in valve provides a means of both of controlling and measuring the flow rate of the chilled water.

4.4.2 Commercial Separator

A commercial centrifugal flow moisture separator was used in series with and placed after the axial flow moisture separator. Its use was intended to verify the low moisture separation efficiencies found in this investigation. If it were able to separate a significant amount of additional water after the flow had already passed through the axial flow moisture separator then it would lend additional confidence to the results found in the investigation, which show unexpectedly poor performance by the axial flow moisture separator.

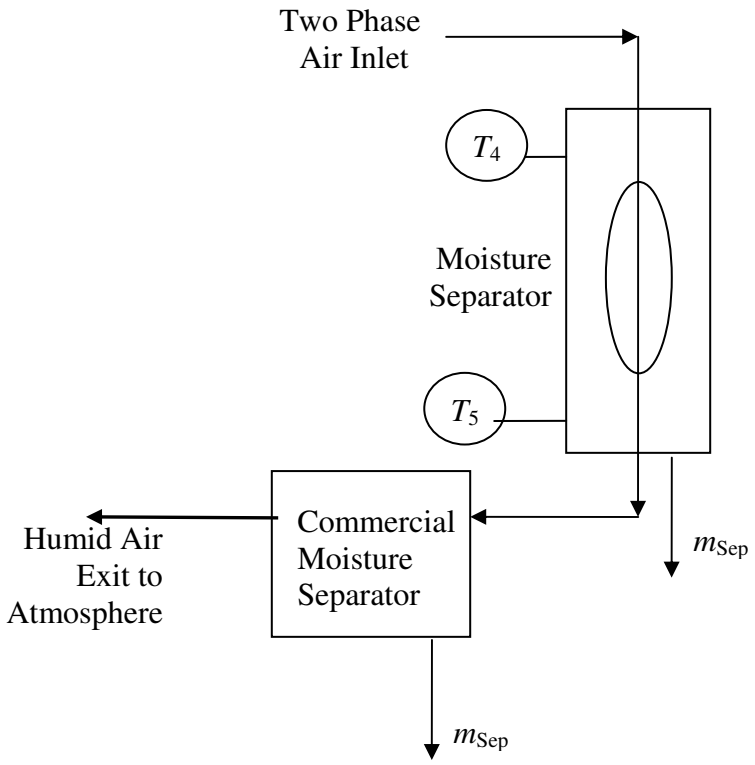

Figure 4.16 – Axial and Commercial Moisture Separator Configuration

The commercial separator was placed as near to the outlet of the axial flow separator as physically possible to prevent heat transfer to the surroundings from lowering the humid air's temperature and influencing the results of the experiments. Humid air left the axial flow moisture separator through a clear flexible steel reinforced hose which was then slipped over and clamped to a 2 inch steel pipe screwed into the inlet of the commercial moisture separator. The commercial moisture separator is a Wright-Austin type 2T centrifugal flow moisture separator. Flow exited the separator and entered a 2 inch steel pipe over which a clear plastic steel reinforced hose was clamped. The hose discharged flow out of a laboratory window. Water separated by this device was directed through a flexible plastic hose into a cup where its mass could be measured.

4.4.3 Flow Straightener

A flow straightener was employed in the system for a series of experiments with cooling with the intention of reducing swirl in the two phase air stream between the turbine outlet and the separator inlet. The idea for the flow straightener was conceived when it was observed that droplets entering the clear pipe which houses the swirl element would enter the pipe with a slight rotation in the direction opposite that of the swirl element. It was hoped that adding a flow straightener upstream of the separator would reduce the pressure drop measured across the swirl element which might, in turn, raise its separation efficiency.

The flow straightener was cut from a grid of white polycarbonate tubes with 3.18 mm (0.125 inch) openings and a 2.54 cm (1 inch) length. A piece was cut to fit tightly inside the 1 1/4 inch PVC pipe which exited into the separator.

4.5 UNCERTAINTY IN INSTRUMENTATION AND MEASUREMENT

This section describes the types of instrumentation used in this experiment and their associated uncertainties. Three types of uncertainties will be reviewed, uncertainty from inaccuracy, uncertainty from imprecision, and overall uncertainty which is a combination of the previous two.

There are two distinct categories of instrumentation used in this experiment, analog and digital. Digital equipment was used to measure relative humidity, temperatures, and change in pressure while analog equipment was employed to measure flow rates and pressures. Data from analog and digital equipment was recorded onto data collection sheets created for this purpose. A sample data collection sheet can be found in Appendix E.

Data from digital instrumentation were recorded by a data acquisition switch unit, an Agilent model 34970A, which sent the signal to a personal computer running Hewlett Packard BenchLink Data Logger software, Version 1.5020801. A personal computer running the Windows XP operating system was used to display, record, and process data. The data card in the data acquisition unit had twenty slots for measuring voltage and 2 slots for measuring current. Fifteen voltage slots were used for thermocouples while one current slot was used for orifice differential pressure measurement and the other was used

for relative humidity measurement. Correction coefficients obtained from instrument calibration were input directly into the data logger software which was then able to display calibrated values. All data collected were averaged over 100 power line cycles to remove random noise and power fluctuations as a cause of inaccuracy in measurement. Table 4.3 lists all the measurements taken in this experiment along with their respective uncertainties.

Table 4.3 – Uncertainties of Instrumentation

Measurement	Units	U_A	U_B	U_C	Source
T_{Atm}	℃	0.05	0.05	0.07	(1, 7)
T_1	℃	0.029	0.25	0.25	(2, 3)
T_2	℃	0.086	0.31	0.3	(2, 3)
T_3	℃	0.036	0.09	0.10	(2, 3)
T_4	℃	0.042	0.07	0.08	(2, 3)
T_5	℃	0.062	0.17	0.18	(2, 3)
T_6	℃	0.58	0.47	0.7	(2, 3)
T_7	℃	0.044	0.5	0.50	(2, 3)
T_8	℃	0.12	0.088	0.15	(2, 3)
T_9	℃	0.089	0.25	0.27	(2, 3)
$\Delta_{Wet\ Bulb}$	Vdc	0.48	N/A	0.48	(2)
$T_{Boiler\ Inlet}$	℃	0.033	0.061	0.07	(2, 3)
T_{Oil}	℃	0.039	0.21	0.21	(2, 3)
T_{13}	℃	0.022	0.050	0.055	(2, 3)
T_{14}	℃	0.025	0.044	0.050	(2, 3)
T_{15}	℃	0.035	0.091	0.098	(2, 3)
P_{Atm}	mmHg	0.5	1.3	1.4	(1)
P_1	Kpa	1.7	3.4	3.8	(1,4)
P_3	Kpa	1.7	2.1	2.7	(1,4)
P_4	mm Hg	0.5	1.1	1.2	(1,4)

Measurement	Units	U_A	U_B	U_C	Source
P_3	Kpa	1.7	2.1	2.7	(1,4)
P_4	mm Hg	0.5	1.1	1.2	(1,4)
ΔP_5	cm H_20	0.3	Negligible	0.3	(1)
P_7	Kpa	1.7	1.7	2.40	(1,4)
ΔP_7	cm H_2O	0.102	0.23	0.25	(2, 3)
P_9	Kpa	6.9	1	7	(1,4)
P_{Oil}	Kpa	3.4	3.4	4.8	(1)
P_{Boiler}	Kpa	1.7	3.4	3.8	(1,4)
ϕ_1	%	0.00049	0.03	0.03	(2, 6)
RM_1	Lpm	1.42	62.3	62.3	(1, 5)
RM_9	Lpm	14.2	62.3	63.9	(1, 5)
RM_B	mL/min	0.5	4.5	4.5	(1, 3)
RM_{CW}	Lpm	0.47	2.31	2.36	(1, 3)
$\dot{W}_{Oil\ Pump}$	Watts	0.50	N/A	0.50	(2)
$\dot{Q}_{Air\ Heater}$	KW	0.005	0.0025	0.006	(1)
$\omega_{Turbine}$	RPM	0.00058	Negligible	0.00058	(1)
m_{Sep}	grams	0.5	0.1	0.5	(1)
m_{ST}	grams	0.5	0.1	0.5	(1)
Δt	H.0M0S	0.01	0.001	0.01	(1)

(1) Determined by Physical Inspection (2) Determined by Inspection of Variation
(3) Calibration Presented in Appendix A (4) Specified by Omega (2005)
(5) Specified by McCrometer (2005) (6) Specified by Vaisala (2005) (7) ANSI Z236.1

All thermocouples were calibrated prior to their use for experimental measurement. Most thermocouples were calibrated six at a time while thermocouples added later were calibrated individually but all were immersed in a constant temperature glycerin bath held in a thermocouple calibrator, a Techne Block Calibrator model DB-35L. A four-wire platinum resistance thermometer (PRT), an Omega model PRP-2, was placed in the bath alongside the thermocouples. The resistance of the PRT was measured by a digital multimeter, a Hewlett Packard 34401A, which was set up for a four wire resistance measurement. The data acquisition system at this time was set to display the measured temperature of the type T thermocouples with a gain of one and an offset of zero. The resistances from the multimeter were converted to temperatures and were recorded along with the temperatures recorded by the thermocouples. Thermocouples were calibrated through a temperature range which was much greater than the range in which they were expected to be operate.

$$T_{corr} = mT_{meas} + b \tag{4.1}$$

Where: T_{corr} is the corrected temperature

T_{meas} is the temperature read by the thermocouple

m is the slope from the regression (gain)

b is the intercept from the regression (offset)

A linear regression was performed using the temperatures measured by the PRT as the independent variable and the temperatures measured by the thermocouples as the

dependant variable. In this way correction coefficients and uncertainty information was obtained for the thermocouples. The gain and offset obtained from this method were then input to the data logger software. Equation 4.1 shows the general form of the regressions. Regression results can be found in Appendix A.1.

Calibration data obtained from a previous phase of this project were used for the boiler feed water rotameter (Aspinwall 2004). The weighing tank method was used, in which water discharged from the rotameter was collected in a tank situated on a scale. The flow rate indicated by the rotameter, the time elapsed, the change in mass on the scale, the temperature of the water and the ambient pressure were all recorded. The change in mass recorded divided by the change in time recorded gives the mass flow rate actually experienced. Water temperature and ambient pressure are used to determine water density. Using the water's density, the volumetric flow rate indicated by the rotameter can be converted into a mass flow rate and compared to the actual mass flow rate as determined by the mass present in the tank. A regression can then be performed which is very similar to the regression performed on the thermocouples. Results of the boiler inlet rotameter calibration can be found in Appendix A.2.

The cooling water rotameter was calibrated by this researcher using the weighing tank method described above. The rotameter was calibrated over a range of flow rates greater than that experienced in experimental conditions. Results of this calibration can be found in Appendix A.5.

The steam orifice flow differential pressure transducer requires a 12 to 45 V DC power supply and provides a 4 to 20 mA output. Calibration data for this instrument were obtained during a previous phase of the project and can be found in Appendix A.3.

The Uncertainty A of the air inlet rotameter was determined to be half of the smallest increment of 2 SCFM by inspection. The Uncertainty B of the air inlet rotameter, as quoted by McCrometer, is 2% of the full scale reading of the rotameter, 110 SCFM. The uncertainties of the compressed air rotameter were determined in the same way.

The Uncertainty A of the pressure gauges was estimated to be 1/2 of their respective smallest graduations by inspection. The Uncertainty B of the pressure gauges made by Omega Engineering was specified to be 0.5% of their full scale.

The humidity probe is a digital instrument and its Uncertainty A was measured as a function of the random variation in its readings. Its Uncertainty B was specified by the manufacturer, Vaisala, to be no more than 3%.

4.5.1 Uncertainty Due to Precision Error

Uncertainty due to precision error, denoted as U_A, is a measure of the random deviation in a measurement. It can be addressed through statistical means as it represents the deviation of repeated measurements from their average. U_A is also commonly addressed through noting half of the smallest graduation of an analog gauge.

The U_A of all measurements which were taken digitally was determined by observation of the system while it operated at steady state. Even while operating at steady state a random variation in readings was displayed. While the system operated at steady state ten successive readings of each measurement were recorded and later analyzed to find the standard deviation from their average. Equation 4.2 was then used to determine U_A.

$$U_A = k_c \frac{\sigma}{\sqrt{n}} \tag{4.2}$$

Table 4.4 - Sample Data Used for Determination of U_A for TC-1

	T_1 Comp. Air Inlet ℃
	21.36129
	21.45795
	21.34635
	21.40514
	21.44400
	21.40016
	21.37226
	21.42108
	21.40813
	21.46792
Average	21.40843
Standard Deviation	0.04066
Number of Points	10
Coverage Factor	2.26216
UA	0.030

The data in Table 4.4 will be analyzed here to demonstrate an example. The number of measurements taken, *n*, was ten in this case. The standard deviation, σ, of the

sample is 0.041 °C. The coverage factor, k_c, determined from a t-distribution with a 95% confidence interval and 9 degrees of freedom is 2.3. The resulting U_A is 0.030 °C.

The U_A for analog instruments such as pressure gauges and rotameters can be addressed, as noted earlier, by inspecting the smallest graduation of the gauge and halving that value.

The U_A of all measurements can be found in Table 4.3.

4.5.2 Uncertainty Due to Possible Bias

The magnitude of uncertainty due to bias is directly related to the quality of the instrument's calibration. In order to minimize this uncertainty, calibrations were performed on all instruments for which calibration equipment was available. Each of these calibrations resulted in a linear regression model. When calibration data are readily available, the standard error of estimate (SEE) can be computed and is the uncertainty due to bias, also known as Uncertainty B or U_B. If a calibration was not performed on an instrument then the U_B was obtained from a calibration provided by the manufacturer. For the U-tube manometer, the oil pressure gauge, and the shaft speed indicator, U_B was deemed to be negligible or much less than U_A. None of these measurements were used in calculating the separation efficiency.

As previously mentioned, the thermocouples, boiler inlet rotameter, cooling water rotameter, and differential pressure transducer were all calibrated by this researcher or previous researchers in this laboratory. For these instruments the SEE was determined

from the calibration data and the U_B was determined as the product of the SEE and the coverage factor based on the number of data points taken in the calibration and the regression model used.

Uncertainty due to possible bias for pressure gauges, relative humidity meter, air inlet rotameter and compressed air rotameter was determined from the manufacturer's stated total uncertainty.

Combined uncertainty, U_C, is a combination of U_A and U_B as shown in Equation 4.3. Table 4.3 presents the U_A, U_B, and U_C for all instrumentation used to take measurements on the system.

$$U_A^2 + U_B^2 = U_C^2 \tag{4.3}$$

In summary, this section reviewed the types of instrumentation present in the apparatus and discussed the uncertainty present in each. The methods of calibration used were discussed and the resulting uncertainties presented.

4.6 PROCEDURE FOR OPERATION OF APPARATUS

This section chronologically details the steps followed to safely operate the test facility and collect repeatable data on the performance of the moisture separator. Additionally, safety precautions are discussed that will ensure the safety of the operator and the apparatus. The experimental apparatus is complicated in many aspects and, with a 20 kW boiler being present, may quickly become dangerous if proper precautions are

not followed. Consistently following the prescribed procedure will ensure data that are repeatable and accurately represents the performance of the device being tested.

Many of the procedural steps are intended to provide safety, both to the operator and to the apparatus. To protect the operator, hearing protection should always be worn while compressed air is being allowed into the system. The compressor side of the turbocharger compresses air which is then expanded back into the atmosphere through valve CV-9. This expansion is extremely loud and could result in hearing damage if protection is not worn.

To protect the apparatus, time must be allowed to warm the oil before it is run through the turbocharger and the oil should not be run to the turbocharger during oil warm up. The strip heater should be set at 70%. After the strip heater has warmed the oil, the pump should recirculate the oil with the ball valve to the turbocharger closed. When the direct oil valve is closed, the bypass valve should be fully open to ensure that the oil pump never works against dead head. The oil pump is a positive displacement pump and working against dead head will damage it and/or the system. After the oil is warmed to approximately 60 °C, the turbocharger should be supplied with no more than 97 kPa (14 psi) of oil pressure to prevent oil from leaking past the turbocharger's seals and contaminating the air and moisture stream. Oil contamination can add mass to the separated water container, resulting in false high readings. The oil also often becomes emulsified and clogs up the passages through which the air and water mixture flows. Though the turbocharger manufacturer recommends 207 kPa (30 psi) be supplied to the

turbocharger, it has been experimentally determined that leakage occurs at pressures over 97 kPa (14 psi). Oil should always be run to the turbocharger at 97 kPa (14 psi) when compressed air is being allowed into the system, causing the turbocharger to run. Failure to run oil to the turbocharger will destroy its bearings.

Any time the resistance heater is in operation it is necessary for air to be run through the system. The heater should never be operated without air running over it, to do so could overheat the heater and cause damage to the system. After heater shutdown, the air should be run over it for several minutes until the heated air temperature is below 30° C.

Any time the boiler is releasing steam into the system the compressed air must also be run to prevent steam from flowing backward and reaching the air heater, possibly condensing on electrical components and causing damage. At start up the air must be run before the boiler is opened to the system and after boiler shut down the air should be run for several minutes to eliminate moisture from the system.

To ensure reliable and repeatable results, the apparatus must be run at steady state. Following the prescribed procedure helps ensure that the apparatus is run the same way every time and thus the results will be consistent. Data were recorded by the data acquisition software from system startup through shutdown and these data were stored on the computer hard drive to enable the researcher to revisit the data to discover trends. Graphical displays of recorded data showing units of measurement and time on the axes

were used as the main source of verification to ensure steady state operation. Steady state operation of the apparatus was defined as having none of the recorded data varying by more than one unit over a six minute period with the exception of the wet bulb temperature, which was not used in calculations and tended to be subject to unpredictable and uncontrollable fluctuations.

At steady state incoming air and water supplies could be unbalanced by demands for air or water elsewhere in the building. Fluctuations in air flow rate and pressure caused by demands on the compressed air line elsewhere in the building could cause disruptions in the operation of the system. In order to minimize fluctuations a pressure regulator was used to maintain the system air pressure at 276 kPa (40 psi), which is well below building air pressure. The system was also run after working hours to decrease the chance that other demands would be placed on the building air supply.

Water was constantly supplied to the boiler to maintain steady state, but disruptions in the building water line carry with them the potential to create surges and/or reductions in flow. Fluctuations in the boiler's water level create fluctuations in steam production and make it impossible to maintain the system at an absolute steady state. To avoid this problem a pressure regulator was employed on the water supply line feeding water to the boiler, which restricted the water down to 3 bar (30 psig) from the building pressure of 4.1 bar (45 psig). The boiler is equipped with a gauge glass and a quick check of steady state can be performed by noting the water level compared to the water level last time the boiler was checked. The water level was quickly checked between

runs to ensure steady state boiler operation. If necessary, the boiler inlet rotameter was slightly adjusted to supply more or less water as individual cases demanded.

Once the system was operating at steady state, data were recorded. Data were recorded from the data acquisition software and from various pressure gauges and manometers located on the experiment onto printed data sheets to ensure the same, correct data were collected every time. Collecting data in a set order also eased data processing as a spreadsheet was used to automatically format the data for processing with EES, helping to eliminate the possibility of mistyped data.

An important aspect of operation which was carried out differently in this research than in previous work was the operation of the air heater. The air heater is controlled by two mechanisms which can be redundant if used incorrectly. Worse than redundancy, the combination or incorrect use of these instruments can result in steady state operation being impossible to achieve. An Omega CN9000 PID controller directly controls the air heater while an autotransformer controls the power the CN9000 is able to send the air heater. The Omega CN9000 is capable of keeping the air at a desired heater exit temperature, but only by actuating a relay to switch power on and off. This method of controlling temperature causes the wattmeter readings used to check the air flow rate to be incorrect. The autotransformer however, once set, feeds a constant stream of power to the heater, which is easily monitored using the wattmeter. For correct operation of these devices the Omega CN9000 should be used as an emergency shut-off and set to heat the air to a temperature higher than the desired temperature. The Variac should then

be adjusted to supply only enough power to the heater to heat the air to the desired temperature. The desired Variac setting will be based on both air flow rate and air inlet temperature and Attachment D.1 can be used as a quick guide to selecting the proper Variac setting. By using this procedure, the PID controller will remain always on, and the wattmeter will read correct values.

Listed here are the steps followed for each experimental test run. Often ten to thirty experiments were performed during any one session, with the system parameters being somehow changed after the completion of the each group of five experiments. For locations of any valves or other parts of the apparatus referenced here please see Figure 4.2.

1. If the experiment was to be made with cooling water, the chiller power source was initialized several hours before the run was to be made. The chiller was set to cool the water to 5°C, the minimum operating temperature for the chiller.
2. All empty containers intended to be used for water collection were weighed with their lids and the weights recorded.
3. The strip heater which surrounds the oil reservoir was switched on and the autotransformer controlling it was set to no more than 70%.
4. The DC power supplies for the orifice flow meter, the humidity probe, and both components of the tachometer were switched on.
5. The data acquisition system was initialized and the computer program reading it was loaded.

6. The oil bypass valve was set to the fully open position.
7. The direct oil valve was closed for the duration of oil warm up.
8. The oil delivery pump was energized by plugging it into the wattmeter and turning on the wattmeter.
9. The valve allowing water to the boiler was opened.
10. The main power switch for the boiler was turned on and the boiler was energized. At initialization the boiler automatically fills to a predetermined level, marked on the watch glass.
11. The temperature of the oil was monitored. Once the temperature of the oil reached 65 °C, the direct oil valve was fully opened and the oil bypass valve was partially closed with the combination of valves being manipulated in order to ensure no more than 97 KPa (14 psig) to the turbocharger.
12. Once the oil reached 70 °C, the oil strip heater was unplugged.
13. When the boiler neared 483 KPa (70 psig) the building compressed air inlet ball valve (CV-1a) was fully opened.
14. Once the boiler reached 552 KPa (80 psig) the primary boiler ball valve (CV-7a) was set to the fully open position.
15. A cup was placed underneath the boiler steam trap needle (CV-7c) and it was fully opened to allow condensed steam to exit the system. Once it was determined that the steam condensed between runs had exited the system the needle valve was closed until a steady drip was formed.
16. The primary boiler pump was plugged in and the boiler rotameter valve opened and adjusted. Most tests were run at a rotameter reading of 115.

17. The valve to the compressed air humidity sensor, CV-1a, was fully closed, and then slowly opened until air could be felt escaping the system through the valve.
18. If necessary, the secondary air inlet ball valve was manipulated to achieve a desired flow rate, as represented by the air inlet rotameter. Usually it was left fully open.
19. The main power switch for the air heater was switched on and the power to the air heater was switched on. The reset button was pressed and held for a few seconds. The autotransformer was set to supply a rate of power that would maintain the incoming air stream at a predetermined temperature. The transformer setting which will generate a chosen temperature is airflow dependant. Most tests were run at 0.590 kW and an air inlet rotameter reading of 7.0 which correlates to an air temperature at Station 2 of 70°C.
20. The boiler secondary ball valve (CV-7d) was fine-adjusted to allow steam into the system. Most tests were run at an orifice flow meter reading of 27 in. H_2O. The flow allowed into the system by the ball valve must be controlled in tandem with the rotameter ball valve which allows water into the boiler in such a way that the boiler remains at steady state. The boiler watch glass should be monitored in order to verify the water level is being maintained at a steady state.
21. The wet bulb throttling valve (CV-6) was closed then opened until a slight flow and definite heat could be felt in the air exiting the valve. The wet bulb reservoir was then slightly overfilled and the extra water allowed to drain. This overfilling ensured that the reservoir was filled to the top and the wet bulb wick would not dry out.

22. If the run was to be made with cooling water, the sump pump was submerged in the cooling water reservoir and the pump was plugged in. Sometimes the pump needed to be shaken to release air pockets and be primed. The cooling water rotameter valve was adjusted such that the desired flow rate was achieved.
23. The system was allowed to run until all measurements reached steady state values. The system was considered to be at steady state when temperatures changed no more than 1°C in a 6 minute period.
24. A container was placed underneath the boiler condensation steam drip and the start time recorded.
25. A container was placed under the separation tubes of the moisture separator and a stopwatch was started. If the conventional separator was being run in series with the experimental separator a container was also placed under it to capture any separated water.
26. Measurements were recorded from the Agilent BenchLink Data Logger program, pressure gauges, rotameters, and manometers. Digital data were cut and pasted to an Excel file for later interpretation. For a sample data collection sheet and a complete listing of the measurements collected please reference Appendix E.
27. When data recording was completed, the stopwatch was stopped and the separation container removed. 310 seconds were used to record data.
28. The separation container(s) was (were) weighed.
29. Both the container weight(s) and duration time were recorded on the data sheet.
30. The boiler water level was checked to ensure steady state.
31. If more runs were desired Steps 25 through 30 were repeated.

32. A minimum of 5 runs were made at any one setting before variables were changed.
33. If desired, the air temperature or cooling water flow rate could be changed between runs. Time must then be allowed for the system to reach a new steady state.
34. The container under the boiler steam drip valve was removed and the weight and end time noted.
35. Once the desired number of data points were collected system shutdown began. If cooling water was used the sump pump was unplugged and removed from the cooling water reservoir.
36. The boiler was switched off and its main power switch was also switched off.
37. The primary boiler pump was switched off and the rotameter closed.
38. The air heater was switched off and its main power switch was also switched off.
39. Once the boiler pressure reached 207 KPa (30 psig) the primary boiler ball valve was fully closed.
40. Once the air temperature at Station 2 reached 30 °C the air inlet ball valve (CV-1a) was fully shut.
41. The oil bypass valve was set to fully open and the direct oil valve was fully shut.
42. The oil supply pump was unplugged and the pump wattmeter switched off.
43. The Agilent BenchLink Data Logger computer program was stopped and all data saved to the computer hard drive.

44. All power supplies; including the chiller, orifice flow meter, the humidity probe, both components of the tachometer, and the data acquisition system; were switched off.

Three types of experiments were conducted. Experiments were conducted using only the moisture separator with or without chilled water flow through the separator. The uncooled experiments simulated experiments run by a previous researcher on the experimental setup. A commercially available moisture separator was added to the exit of the moisture separator in series to determine if extra moisture was available for separation. A flow straightener was added to the flow upstream of the moisture separator and downstream from the turbine; tests were again run with and without chilled water.

In summary, the procedure listed above was followed to ensure that the experiment was safely operated and that reliable data were collected at steady state conditions. A sample data collection sheet is shown in Appendix E. After data collection was complete, the sheets were taped into a laboratory notebook for record keeping.

CHAPTER 5

DATA PROCESSING

This chapter describes how data collected during the test runs was processed. The goal of this research was to characterize the performance of an axial flow moisture separator with and without cooling. Separation efficiency, defined as the mass flow rate of water separated per mass flow rate of water above the saturation mass flow rate of the air stream when it entered the separator, was the most important parameter, and was calculated based on conditions at the system inlet and exit. Secondary calculations were used to verify initial calculations to ensure accuracy of calculated air and steam flow rates. The system was run with a few variations, a flow straightener was added and an additional moisture separator was added in series with the separator being tested. The calculations required to process the data from these test runs will be explained.

This chapter will follow the system by first examining each of the two streams entering, air and steam, then examining their mixture. The stream then is expanded through a turbine and at this point, as the flow exits the turbine and enters the separator, the properties of the flow will again be examined. The calculations involved in determining the separation efficiency will then be detailed. Additional calculations are performed by the EES program listed in Appendix C such as calculating turbocharger power and efficiency, but these calculations are not important to the separation efficiency determination, and will thus not be presented here.

5.1 AIR FLOW RATE, STATIONS 1 AND 2

Compressed air was routed from the building's supply into the experiment. Temperature, pressure, and relative humidity were measured just before the air flowed through a rotameter at Station 1. The rotameter reading required a correction to be performed if the flow was not at the specified temperature and pressure conditions corresponding to its graduations. Equation 5.1 gives the correlation between measured conditions and the conditions for which it is graduated.

$$\dot{m}_{air} = \mathrm{RM}_{air}\left(\frac{P_1 \cdot T_{std}}{T_1 \cdot P_{std}}\right)^{\frac{1}{2}} \tag{5.1}$$

Where: $\dot{m}_{air}$ is the mass flow rate of air at Station 1

P_1 is the measured pressure at Station 1

T_1 is the measured temperature at Station 1

P_{std}, 322 Kpa atm, is the specified pressure corresponding to the graduations

T_{std}, 294.44 K, is the specified temperature corresponding to the graduations

This correction follows a simple model and is a straightforward calculation, but to ensure accuracy a check was made. After Station 1 the air is heated by flowing through a finned tube resistance heater. The power supplied to the heater is measured and at Station 2, as the air exits the heater, air temperature is again measured. Using these two temperatures and the power input to the heater a mass flow rate can be calculated as shown in Equation 5.2.

$$\dot{m}_{\text{air}} = \frac{\dot{Q}_{\text{heater}}}{C_{\text{P}}\left(T_2 - T_1\right)} \tag{5.2}$$

The mass flow rate calculated in this manner was shown to be in good agreement with the flow rate measured by the rotameter. Over 141 data points the flow rate measured with the rotameter was on average 88.7% of the flow rate calculated using power input with a standard deviation of only 1%. The discrepancy between measured and calculated airflow rates can be explained by heat being lost to the atmosphere. The ends of the heater are uninsulated and though the body of the heater is insulated, some heat losses will still occur. Since the readings are steady a correction factor may be employed as shown in Equation 5.3.

$$\dot{m}_{\text{air}} = \frac{0.887\dot{Q}_{\text{heater}}}{C_{\text{P}}\left(T_2 - T_1\right)} \tag{5.3}$$

This is the version of the equation employed in the EES program used for calculations and gives very good agreement between measured and calculated airflow. While this agreement is reassuring, it is not an independent confirmation and ideally an improved calibration of the rotameter is called for.

The moisture content of the air entering the system was also measured. Air was throttled across a valve and a relative humidity probe was used to measure the moisture content of the air as it exited to atmospheric pressure. Atmospheric pressure, compressed air temperature, and relative humidity were all measured and using these parameters EES

was used to calculate the humidity ratio (w_1) of the compressed air. The humidity ratio is then used to calculate the mass of dry air and the mass of water vapor entering the system. Equation 5.4 is used to determine dry air mass flow rate ($\dot{m}_{da}$) and Equation 5.5 shows how the mass flow rate of water vapor ($\dot{m}_{wv}$) is calculated.

$$\dot{m}_{\text{da}} = \frac{\dot{m}_{\text{air}}}{\left(w_1 + 1\right)} \tag{5.4}$$

$$\dot{m}_{\text{wv}} = \frac{\dot{m}_{\text{air}}}{\left(\frac{1}{w_1} + 1\right)} \tag{5.5}$$

These equations are derived from the basic definition of humidity ratio, Equation 5.6, and the mass balance of air and water vapor flowing through the rotameter at Station 1, shown in Equation 5.7.

$$w_1 = \frac{\dot{m}_{\text{wv}}}{\dot{m}_{\text{da}}} \tag{5.6}$$

$$\dot{m}_{\text{air}} = \dot{m}_{\text{wv}} + \dot{m}_{\text{da}} \tag{5.7}$$

Using the equations presented above the mass flow rate of dry air and the mass flow rate of water vapor entering the system with the air can both be calculated.

5.2 STEAM MASS FLOW RATE, STATION 7

Steam was generated by a 20 kW boiler and as it entered the system at Station 7, measurements were made to enable calculation of the mass flow rate of steam entering the system. Pressure and temperature of the steam were measured just prior to the steam flowing through an orifice plate. The change in steam pressure across the orifice was measured and using a series of calculations the mass flow rate of the steam through the orifice was extracted.

It should be noted before further discussion that in some cases, the measured temperature and pressure at Station 7 incorrectly identify the state of the steam as compressed liquid water instead of as saturated vapor. The boiler being used does not have a superheater and outputs saturated steam. In order to prevent EES from determining that liquid water was being passed through the orifice a simple routine was programmed. The density of the water is checked based on temperature and pressure measurements. If the water is steam the density should be around 3 kg/m^3, but if the water is compressed liquid water the density is around 900 kg/m^3. Therefore the density is calculated and if the density is greater than 100 kg/m^3 EES calculates the temperature of the steam based on the measured pressure and the quality being set equal to one. Arbitrarily, one degree Celsius is added to this temperature to ensure superheated properties are used. If the density passes the check, then the measured temperature is used. This calculated temperature is then used in calculations and to look up properties of the steam at Station 7. This calculated temperature is passed to other parts of the EES

program which perform checks on the calculated orifice flow rate and will be discussed later.

The general equation used to calculate the volumetric flow rate of steam ($\dot{V}_{steam}$) through the orifice is presented in Equation 5.8. Equations 5.8 – 5.14 are from ASME (2001).

$$\dot{V}_{steam} = C \cdot Y \cdot F_A \cdot A_o \left(\frac{2\Delta P_7}{\rho_7 (1-\beta^4)} \right)^{1/2} \tag{5.8}$$

Some of the variables used here are directly calculated based on physical constants of the orifice and some of the variables are included in an iterative routine to determine the volumetric flow rate. Two values based on measurements made during test runs are the pressure drop across the orifice, ΔP_7, and the density of steam at Station 7 based on measured temperature and pressure data, ρ_7. Two values that are physical constants for the orifice plate setup being used are the area of the orifice opening, A_o, and the ratio of the orifice diameter (d_t) to the pipe's inner diameter (D), β. F_A is a calculated value equal to the thermal expansion factor of the orifice as described in Equation 5.9.

$$F_A = 1 + \left(\frac{2}{1-\beta^4} \right) \left(\alpha_{PE} - \beta^4 \alpha_P \right) \left(T_7 - T_{atm} \right) \tag{5.9}$$

Here α_P is the thermal expansion coefficient of the stainless steel pipe while α_{PE} is the thermal expansion coefficient of the brass orifice. T_{atm} is the atmospheric temperature and T_7 is the calculated temperature at Station 7.

Y is a calculated value equal to the expansion value of the orifice based on upstream pressure. Equation 5.10 is used to determine its value.

$$Y = 1 - \left(0.41 + 0.35\beta^4\right)\left(\frac{\Delta P_7}{27.73 \cdot k \cdot P_{7,abs}}\right) \tag{5.10}$$

Here, $P_{7,abs}$ is the pressure measured at Station 7. k is the ratio of specific heats of the steam flowing through the orifice and is determined based on the measured pressure and calculated temperature.

The next variable, C, the discharge coefficient, is determined by iteration. C, λ, and K_{SB} are all linked in the iterations and their equations will be listed below before the reason for the iterations is discussed. λ and K_{SB} are dimensionless numbers.

$$C = K_{SB}(1 - \beta^4)^{1/2} \tag{5.11}$$

$$K_{SB} = \left[0.5991 + \frac{0.0044}{D} + \left(0.3155 + \frac{0.0175}{D}\right)\left(\beta^4 + 2\beta^{16}\right)\right] +$$

$$\left[\frac{0.00052}{D}-0.000192+\left(0.01648-\frac{0.00116}{D}\right)\left(\beta^4+4\beta^{16}\right)\right]\lambda \tag{5.12}$$

$$\lambda=\frac{1000}{\sqrt{\mathrm{Re_D}}} \tag{5.13}$$

$$\mathrm{Re_D}=\frac{V*D}{v} \tag{5.14}$$

It can be seen that the start of the iteration is in calculating the Reynolds Number; however in order to calculate the Reynolds Number the flow rate must be known and this is the very thing that is being determined. The value of C, once obtained, is inserted into Equation 5.8 and the volumetric flow rate is found. This iteration is performed by EES using a starting guess and convergence is usually met in approximately three iterations. Convergence is defined as the percent difference between the volumetric flow rate of the current iteration and the result of the previous iteration being less than 0.001. Note that V is the velocity of fluid through the orifice and v is the kinematic viscosity of the steam.

Once convergence is obtained the volumetric flow rate is converted into a mass flow rate of steam, $\dot{m}_{st}$, into the system as shown in Equation 5.15.

$$\dot{m}_{\mathrm{st}}=K_{\mathrm{Cal}}\cdot\rho_7\cdot V_{\mathrm{steam}} \tag{5.15}$$

K_{Cal} is a correction factor applied to the mass flow rate which is the slope of the orifice flow meter calibration (Hull, 2002). From this mass flow rate the mass flow lost to the system through the steam trap is subtracted. The remaining mass flow of steam is added to the flow rate of water vapor entering with the air stream to determine the total mass flow rate of water entering the apparatus. The mass flow rate as determined by the orifice flow meter is the flow rate used by EES to determine the amount of water entering the system. The other two checks are visually compared by the researcher but are not used in calculation by EES.

Two checks on the orifice flow rate are performed and will be reviewed here. The first check that will be reviewed is the boiler inlet rotameter flow rate. The rotameter reading is converted, using a linear calibration, into a volumetric flow rate and multiplied by density to get a mass flow rate. This flow rate is compared to the orifice flow rate and is routinely within a few percent of the steam mass flow rate found using orifice calculations. At data point 156 for example, the steam flow rate calculated by the steam orifice flow meter was 0.00639 kg/s while the flow rate of the boiler inlet rotameter was 0.0068 kg/s, a difference of only 6%.

The second method used to check the flow rate of steam leaving the boiler is an energy balance. The power input to the boiler is known and the states of the fluid entering and leaving the boiler are known, allowing enthalpy to be calculated. Equations 5.16 and 5.17 can then be used to calculate the mass flow rate of steam leaving the boiler

under steady state conditions. $V_{3\phi}$ is the three phase voltage and $i_{3\phi}$ is the three phase current supplied to the boiler.

$$\dot{m}_{\text{steam,b}} = \frac{\dot{Q}_{\text{boiler}}}{h_7 - h_{fw}} \tag{5.16}$$

$$\dot{Q}_{\text{boiler}} = \sqrt{3} \cdot V_{3\phi} \cdot i_{3\phi} \tag{5.17}$$

This check also compared favorably with the flow rate calculated using the steam orifice flow meter. At data point 156 the steam mass flow rate calculated using the orifice flow meter was 0.00639 kg/s while the mass flow rate calculated using the power balance was 0.006482 kg/s, a difference of approximately 1%.

5.3 MIXED STREAM PROPERTIES, STATION 3

At this point in the system the flow rates of dry air, water vapor, and steam entering the system have all been determined. At Station 3 the air and steam streams are mixed and the resulting temperature and pressure measured. After this station the flow enters the turbine and is expanded. The humidity ratio of the stream, w_3, can be calculated using Equation 5.18.

$$w_3 = \frac{\dot{m}_{\text{vap}} + \dot{m}_{\text{st}}}{\dot{m}_{\text{da}}} \tag{5.18}$$

After the flow has passed through the turbine the temperature and pressure drop and are again measured at Station 4 as the flow enters the moisture separator. These properties are used to determine the humidity ratio of air saturated with water at this state, w_4. A check is performed to ensure that the air is indeed saturated with moisture by examining the relative humidity at 4 based on the temperature and pressure at Station 4 and the humidity ratio at Station 3. If the resultant relative humidity is greater than one then the air indeed holds more moisture than necessary for saturation and there is moisture available for removal. The mass of condensate available for removal, $\dot{m}_{\text{cond}}$, is determined using Equation 5.19.

$$\dot{m}_{\text{cond}} = \dot{m}_{\text{da}} \left(w_3 - w_4 \right) \tag{5.19}$$

The separation efficiency, η_{sep}, is defined as the mass of moisture actually separated from the stream, $\dot{m}_{\text{sep}}$, divided by the mass of moisture available for separation as shown in Equation 5.20.

$$\eta_{\text{sep}} = \frac{\dot{m}_{\text{sep}}}{\dot{m}_{\text{cond}}} \tag{5.20}$$

The separation efficiency was the most important piece of data calculated in this analysis. As shown above, this measurement is based on the amount of air and water entering the system. All air entering the system passes through the air inlet rotameter and carries a small amount of moisture with it. The majority of water entering the system is

heater by the boiler and passes through the orifice flow meter. It is then crucial that these two flow meter measurements and their necessary assisting measurements are accurate.

5.4 COOLING WATER FLOW, STATIONS 13 AND 14

In some test runs, cooling water was delivered to the moisture separator. The temperature of the water was measured before entering and after leaving the separator housing. Atmospheric pressure and the measured temperatures were used to determine the enthalpy of the water entering and leaving the separator. The heat transfer rate from the moist air flow was then calculated using Equation 5.21.

$$\dot{Q}_{13\to14} = \dot{m}_{\text{cw}} C_p (T_{14} - T_{13}) \tag{5.21}$$

Here, $\dot{m}_{\text{cw}}$ is the mass flow rate of cooling water supplied based on the cooling water rotameter reading and its calibration. $Q_{13\to14}$ is the amount of heat removed from the moist air stream.

5.5 SYSTEM VARIATIONS

Two variations were employed in the system. A flow straightener was added in the belief that it would improve separation efficiency. Data processing was unchanged in this case and proceeded as outlined above.

A commercial moisture separator was added in series with and after the axial flow moisture separator. Water was collected from the axial flow moisture separator and the

commercial separator over the same time period and the masses were simply added and used in Equation 5.20 to determine combined efficiency.

In summary, several calculations and checks were performed in order to ensure the accuracy of the calculated conditions entering the moisture separator. Separation efficiency was defined as the ratio of the mass of water actually separated to the mass of water above saturation in the stream.

CHAPTER 6

EXPERIMENTAL RESULTS

This chapter will describe the results found in this investigation. Three types of experiments were run; experiments with the axial separator alone, experiments with a flow straightener just upstream of the axial separator, and experiments with the commercial separator in series with the axial separator. Some experiments with the axial separator alone and with the flow straightener employed cooling water to explore the effect on the separation efficiency.

In total, 175 parametric experiments were conducted in this investigation. Only 82 experiments will be presented and discussed here, as many early experiments were either conducted improperly or at unsteady conditions. It was possible for the system to run and appear to be at steady state from monitoring digital measurements. However unless the boiler water level and inlet rotameter are closely monitored, the system will not be at steady state and power cycling of the boiler or other problems may occur. The system is capable of settling at near steady state conditions with slightly different states which produce slightly different results. If the system is run on two different days and allowed to come to steady state, operating at the same conditions, different results may be obtained, with the average of tightly grouped separation efficiencies varying by as much as 5% between days. In order to avoid this, efforts were made to collect all data for any one of the three conditions discussed here in one day. Unfortunately, during the

progression of any one day the air supply would dwindle, having an impact on the amount of water it was possible to separate in a given test run.

The experiments were set up as shown in Table 6.1. It was endeavored to conduct at least 5 experiments at any one operating point.

Table 6.1 – Experimental Design

Experimental Design		
Type of Experiment	Cooling Water Flow Rate	Number of Experiments Conducted
1	0 Lpm	5
1	1.89 Lpm	5
1	2.84 Lpm	5
1	3.88 Lpm	5
1	7.57 Lpm	5
1	11.36 Lpm	5
2	0 Lpm	15
2	1.89 Lpm	7
2	2.84 Lpm	5
2	3.88 Lpm	5
2	7.57 Lpm	5
2	11.36 Lpm	5
3	0 Lpm	10

Types of Trials	
1	Axial Separator
2	Axial Separator with Flow Straightener
3	Axial Separator with Commercial Separator

Tables 6.2, 6.3, and 6.4 present the Uncertainty B information of measurements that affected the separation efficiency in the units that were input to EES. It can be seen that by far the leading single contributor to uncertainty in measurements is the air inlet rotameter, RM_1. The manufacturer, McCrometer, specifies that the rotameter is good to within 2% of the full scale value, 110 CFM in this case (McCrometer, 2005). With

special calibration the accuracy may be halved to 1%. The pressure gauges from Omega are specified to be accurate to within 0.5% of their full scale values. The relative humidity sensor by Vaisala is specified to be accurate within 3% RH. The U_B of the thermometer was 0.5% of the full scale of 52 °C as specified by ANSI Z236.1. Other U_B values were determined by inspection or calibration as indicated. No uncertainty was attributed to T_7 due to the fact that the calculated temperature was used at this data point. All U_B calculations were performed on data point 156 taken at 2.84 Lpm (0.75 gpm) of cooling water on March 8, 2005 which is a representative experiment.

Table 6.2 – Determination of U_B of Mass Flow Separated by Axial Separator

Measurement x_i	Units	Value	U_{x_i}	$\frac{\partial \dot{m}_{Sep}}{\partial x_i}$	$U_i^2 = \left(U_{xi} \frac{\partial \dot{m}_{Sep}}{\partial x_i} \right)^2$	Percent of Uncertainty (%)	Basis	Source
m_{Sep}	g	180	0.1	0.2	0.0004	100	Resolution	(1)
Δt	s	310.28	0.001	-0.1	0.00000001	0	Resolution	(1)
			Sum of U_i^2		0.0004			
			Expanded Uncertainty B (g/min) =		0.02			

(1) Determined by Physical Inspection

Table 6.3 – Determination of U_B of Mass Flow Separated by Steam Trap

Measurement x_i	Units	Value	U_{x_i}	$\frac{\partial \dot{m}_{ST}}{\partial x_i}$	$U_i^2 = \left(U_{xi} \frac{\partial \dot{m}_{ST}}{\partial x_i} \right)^2$	Percent of Uncertainty (%)	Basis	Source
m_{ST}	g	467	0.1	0.01	0.000001	100	Resolution	(1)
Δt	s	5049.00	0.001	-0.001	0.000000000001	0	Resolution	(1)
			Sum of U_i^2		0.0000014			
			Expanded Uncertainty B (g/min) =		0.001			

(1) Determined by Physical Inspection

Table 6.4 – Determination of U_B of Separation Efficiency

Measurement x_i	Units	Value	U_{x_i}	$\frac{\partial \eta_{Sep}}{\partial x_i}$	$U_i^2 = \left(U_{xi}\frac{\partial \eta_{Sep}}{\partial x_i}\right)^2$	Percent of Uncertainty (%)	Basis	Source
T_{Atm}	℃	23.4	0.26	0.0002	0.0000000015	0.00	Resolution	(7)
T_1	℃	20.88	0.25	-0.0037	0.00000085	0.03	Calibration	(4)
T_4	℃	56.06	0.07	0.09	0.00004	1.49	Calibration	(4)
T_7	℃	158.86	0.5	0.00	0.00	0.00	Calibration	(4)
ϕ_1	*100%	0.06	0.03	-0.2	0.00005	1.98	Manufacturer Specified	(5)
P_{Atm}	mmHg	738.0	1.3	-0.002	0.000009	0.33	Resolution	(1)
P_1	psi	42.0	0.3	0.01	0.00002	0.67	Manufacturer Specified	(2)
P_4	in. H_2O	31.0	1.1	-0.005	0.00002	0.90	Resolution	(1)
P_7	psi	77.25	0.5	-0.01	0.000029	1.06	Manufacturer Specified	(2)
ΔP_7	in. H_2O	26.13	0.09	-0.04	0.00001	0.45	Calibration	(4)
RM_1	CFM	70.0	2.2	0.02	0.003	93.08	Manufacturer Specified	(3)
$\dot{m}_{Sep}$	g/min	34.03	0.02	0.01	0.0000001	0.00	Calculated	(6)
$\dot{m}_{ST}$	g/min	5.550	0.001	0.005	0.00	0.00	Calculated	(6)
				Sum of U_i^2	0.003			
				Expanded Uncertainty B =	0.05			

(1) Determined by Physical Inspection (2) Specified by Omega (2005) (3) Specified by McCrometer (2005) (4) Calibration Presented in Appendix A (5) Specified by Vaisala (2005) (6) Presented in Table 6.2 or 6.3 (7) ANSI Z236.1

These two tables present the calculated uncertainty of the mass separation flow rates. The values found in these tables were then used in Table 6.4 to determine the overall uncertainty of the separation efficiency. As shown in the table the expanded U_B is $\pm 5\%$ of the calculated value.

It does seem reasonable that the uncertainty of the measurement of airflow into the system would create the greatest uncertainty present in the system. When the two phase air and water mixture is exiting the system approximately 77% of the water is saturating the air, and only the remaining condensed water is available for separation. A

difference in air flow rate would cause a difference in the amount of condensed moisture available for separation and could have a great effect on the performance of the system.

As detailed in Table 6.4, the U_B of the separation efficiency was found to be $\pm 5\%$. The U_A for the data with the axial separator run alone correlating heat removal to separation efficiency was found to be 2.8% based on the error propagation analysis of the quadratic regression line fit to the data. U_C based on these two values was calculated to be 6%.

6.1 AXIAL SEPARATOR

The experiment was run with and without cooling with the axial separator being the only means of removing moisture from the expanded, humid air stream. It was endeavored to match the state of the humid airflow entering the turbine to the PEM fuel cell operating conditions described in Chapter II, but unfortunately there was not enough air available under steady state conditions from the supply to match these conditions. The best method of controlling the humidity ratio is to increase the amount of dry air in the mixture but in this investigation the airflow rates achieved in earlier investigations were unattainable as described in Section 7.4. The mixture temperature at Station 3 was maintained near 80°C, the highest temperature likely to be sustainable by a PEM fuel cell, and the pressure was 25 psi. These values are very close to the 70-80 °C operating temperature and 20-35 psi pressure recommended for operation of a PEM fuel cell as shown in Chapter II (Amphlett *et al.*, 1993). The humidity ratio however was 0.147, which is almost 25% higher than the goal of 0.125. A lower level of steam production would allow less steam to be generated, reducing the humidity ratio. The steam generator

currently in use however allows only full power operation and has no variable power settings.

Figure 6.1 – Swirl Element in Separator Housing Showing Oil Streaks

Figure 6.1 shows the swirl element in its housing after an early run where oil contamination was present. In the figure emulsified oil has coated the inside of the clear pipe wall in a helical pattern, showing that the swirl element had imparted a strong swirling motion to the flow. It can also be noticed that what start as several individual streams, each leaving a separate vane, soon join into one trail. It is unknown why this occurs or what the effect of this merging is.

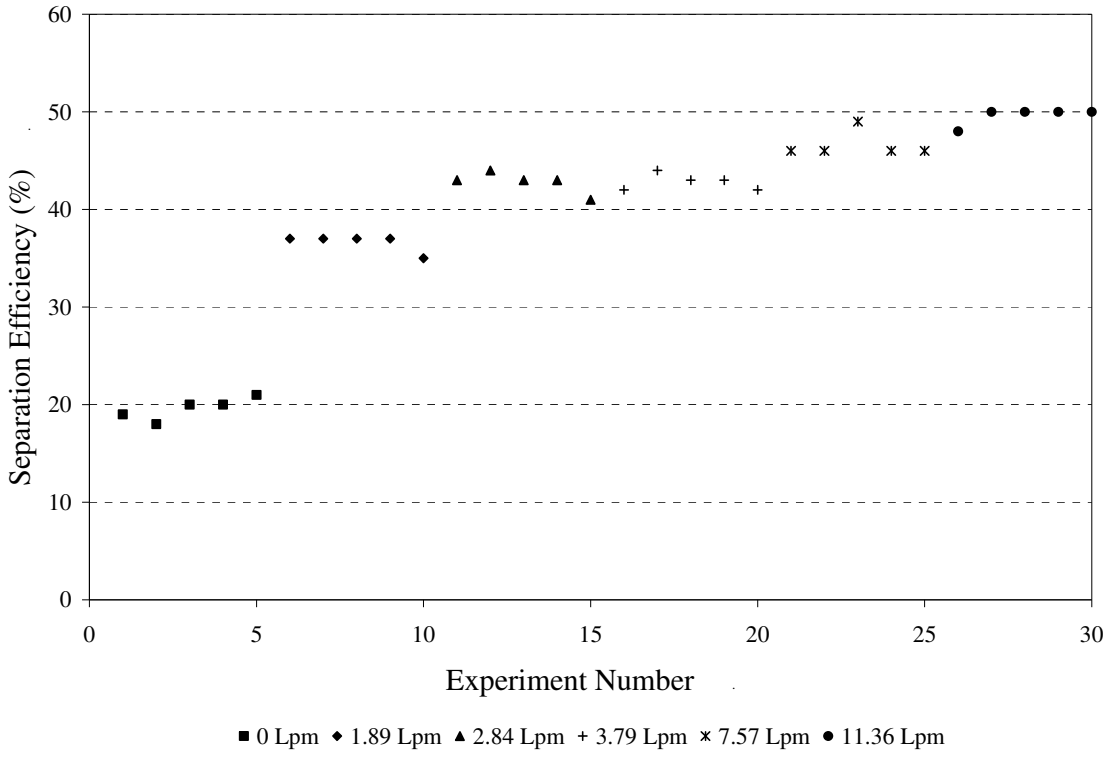

Figure 6.2 - Axial Separator Efficiencies

The performance of the moisture separator is shown in Figure 6.2. Here separation efficiency is plotted against the experiment number to show the progression of separation efficiencies as the flow of cooling water was increased. The data can also be

seen to be consistent, as each group of data corresponding to a given flow rate show minimal variation.

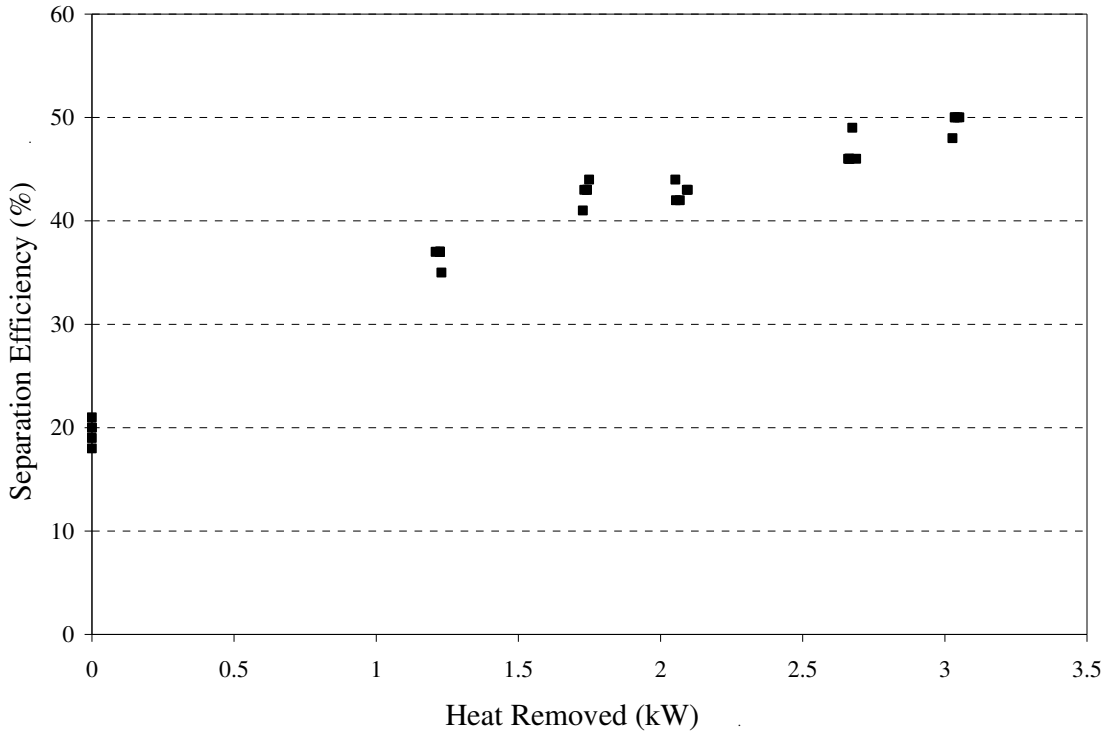

Figure 6.3 - Axial Separator Efficiencies as a Result of Cooling

Another way of plotting this data is seen in Figure 6.3. This figure shows a correlation between the heat removed from the humid air stream and the separation efficiency experienced. While higher separation efficiencies are experienced at higher heat removal rates, it can be seen that increasing the heat removal results in only marginally higher separation efficiencies at the top end of the scale.

Table 6.5 – Axial Separator Averages

Cooling Water Flow Rate (Nominal)	Heat Removed	Separation Efficiency	Mass Separated Average	Mass Flow Possible	Mass Flow Separated	Mass Flow Possible Standard Deviation	Mass Flow Separated Standard Deviation	Uncertainty A
Lpm	kW	%	g	g/min	g/min	g/min	g/min	g/min
0	0	19.6	74.6	73.89	14.40	2.64	0.48	0.81
1.89	1.2224	36.6	150	79.37	28.98	1.02	0.24	0.81
2.84	1.7382	42.8	175.4	79.33	33.81	1.03	0.34	0.81
3.79	2.0726	42.8	184.6	83.06	35.69	1.16	0.32	0.81
7.57	2.6702	46.6	206.4	85.60	39.90	2.04	0.10	0.81
11.36	3.0388	49.6	218.2	85.18	42.18	1.39	0.17	0.81

The data points seem slightly scattered but when the data presented in Table 6.5 is considered it can be seen than the amount of water collected is extremely steady, with a standard deviation of only a fraction of a gram per minute in all cases. However the standard deviation of the mass flow possible to be collected is much greater, over 1 gram per minute in all cases and over 2 grams per minute in two cases. The fluctuation of the mass of water available for separation is also greater than the Uncertainty A. The variation in separation efficiencies is due mainly to the variation in calculated water available for separation, not to the amount of water being collected.

Figure 6.4.A presents the axial separator data with its associated uncertainty. All data points fall within the bounds of both the error limit on the data and the error limits of the regression model. No magnification of the coverage factor is used on this plot to better show the error limits. The R^2 value of this fit is 0.9827 and the alpha risk is only a negligible 2.14×10^{-9}. The high R^2 value shows that the line is a good fit to the data and the low alpha risk, much lower than the commonly accepted 5% threshold, shows that the regression model is not being force-fit to random variation in the data. The error bands on the data and the regression model are somewhat unusual in that the error limits of the regression model are broader than those of the data. This is explained by the fact that the

U_B is much larger than the U_A and thus dominates the combined uncertainty. Figure 6.4.B presents the same data with the same error bands as Figure 6.4.A, but in addition the bounds of U_A are plotted with U_B neglected

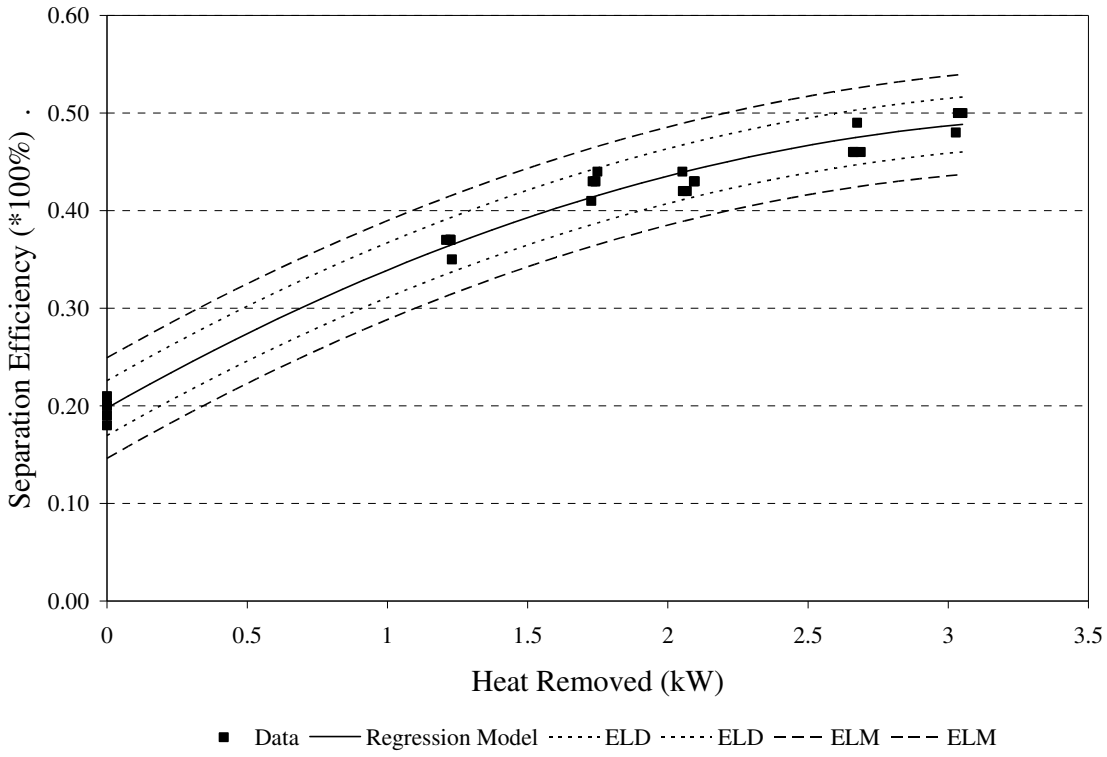

Figure 6.4.A – Axial Separator Data with Uncertainty

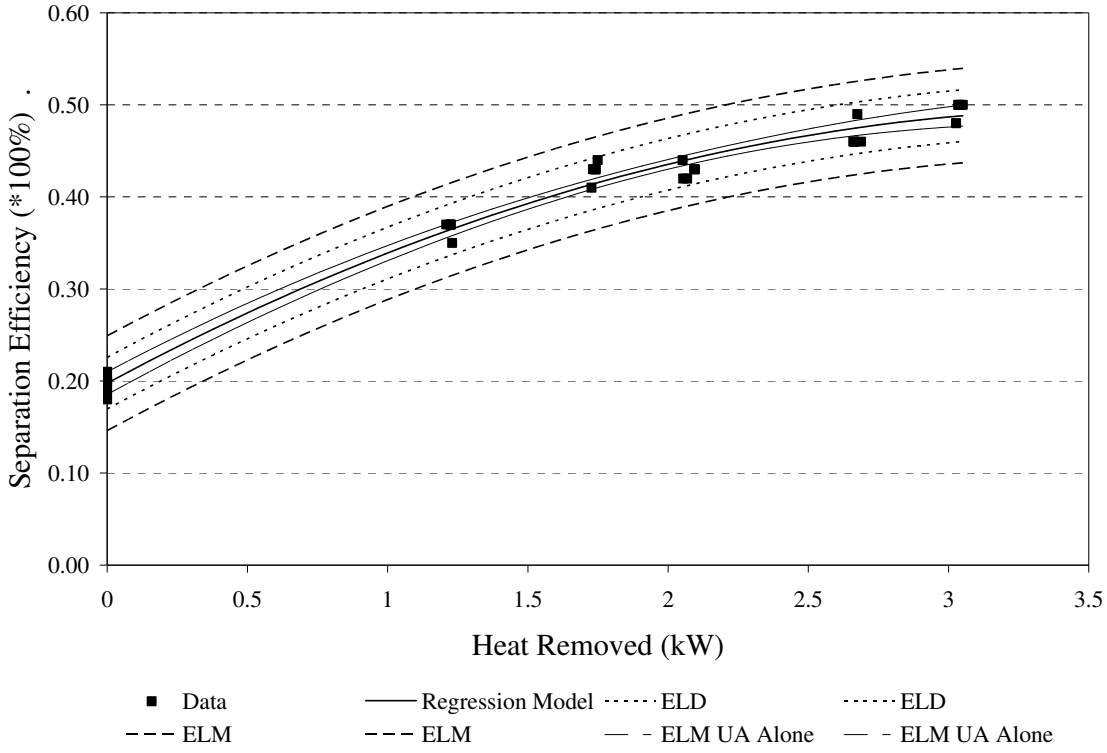

Figure 6.4.B – Axial Separator Data with Uncertainty and Uncertainty A Bands

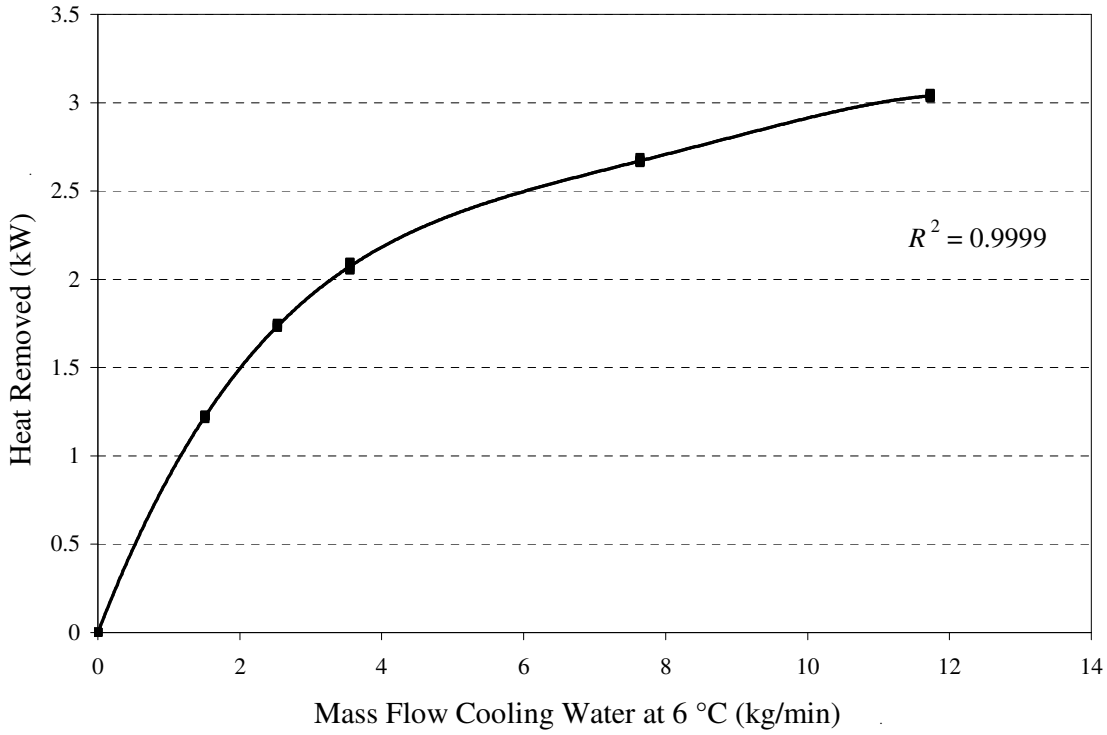

Figure 6.5 - Axial Separator Heat Removed

Figure 6.5 presents the same data plotted as cooling water flow rate against heat removed from the air water stream. This chart is valid with water entering Station 13 at 6°C. A leveling off effect can again be seen as higher cooling water flow rates remove only slightly additional amounts of heat. A quartic trend line is fit through the data with the R^2 value shown. A quartic value was used because both quadratic and cubic correlations showed an improper slope at the end, eventually decreasing as the mass flow of cooling water increased. The alpha risk of this fit is 3.75×10^{-12}, making the line a very good fit.

6.2 AXIAL SEPARATOR AND FLOW STRAIGHTENER

A flow straightener was added to the system upstream of the moisture separator and downstream of the turbine. The reasoning for adding the straightener was that the moisture droplets entering the clear separator housing could be seen to swirl in the direction opposite the swirl imparted by the moisture separator. It was believed that adding a flow straightener would decrease or eliminate this swirl and possibly increase the efficiency of the moisture separator. Visually a difference was seen, as droplets entered the housing in a much straighter fashion, but this is hard to present here as the particles must be observed over time to see their direction of flow and this is difficult to capture with a still frame camera.

The results of the experiments with the flow straightener are presented in Figure 6.6. Again, cooling was employed and there was a positive correlation between more cooling water being supplied and higher separation efficiencies.

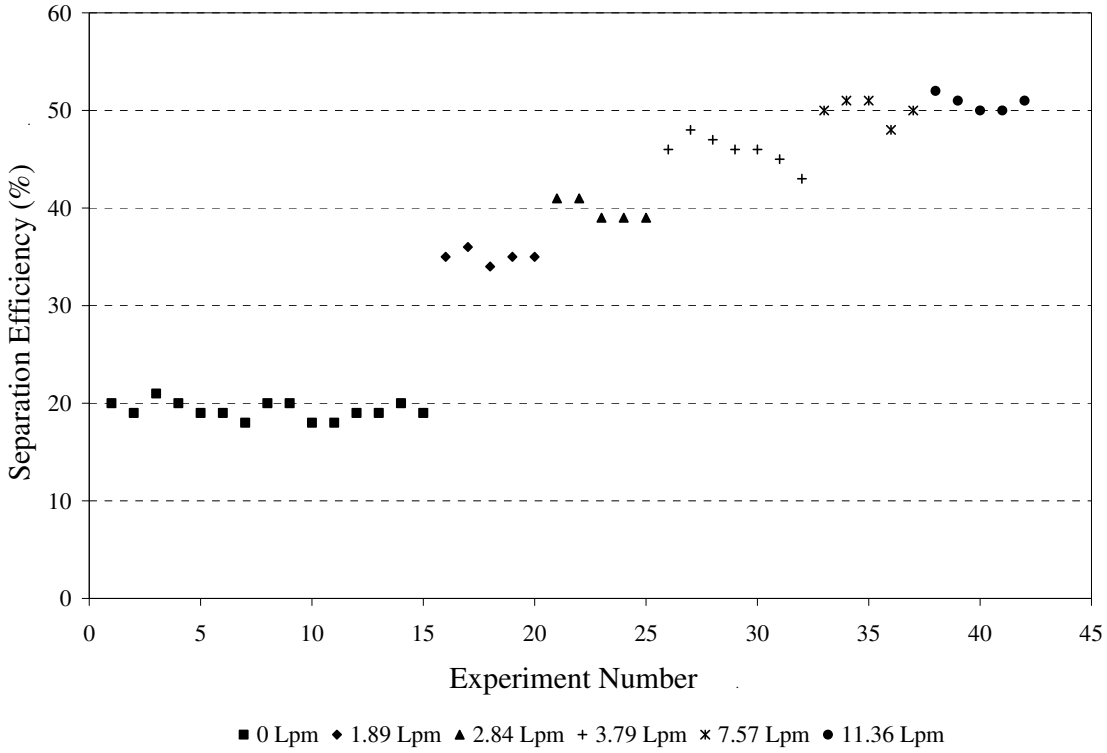

Figure 6.6 - Flow Straightener Separation Efficiencies

Figure 6.7 shows the correlation between heat removed from the air and moisture stream and separation efficiency. As more heat is removed from the stream more moisture is able to be separated. With no cooling, efficiencies average 19.2% while with 3.11 kW removed from the stream, separation efficiencies average 50.8%, which is over 260% of the uncooled efficiency.

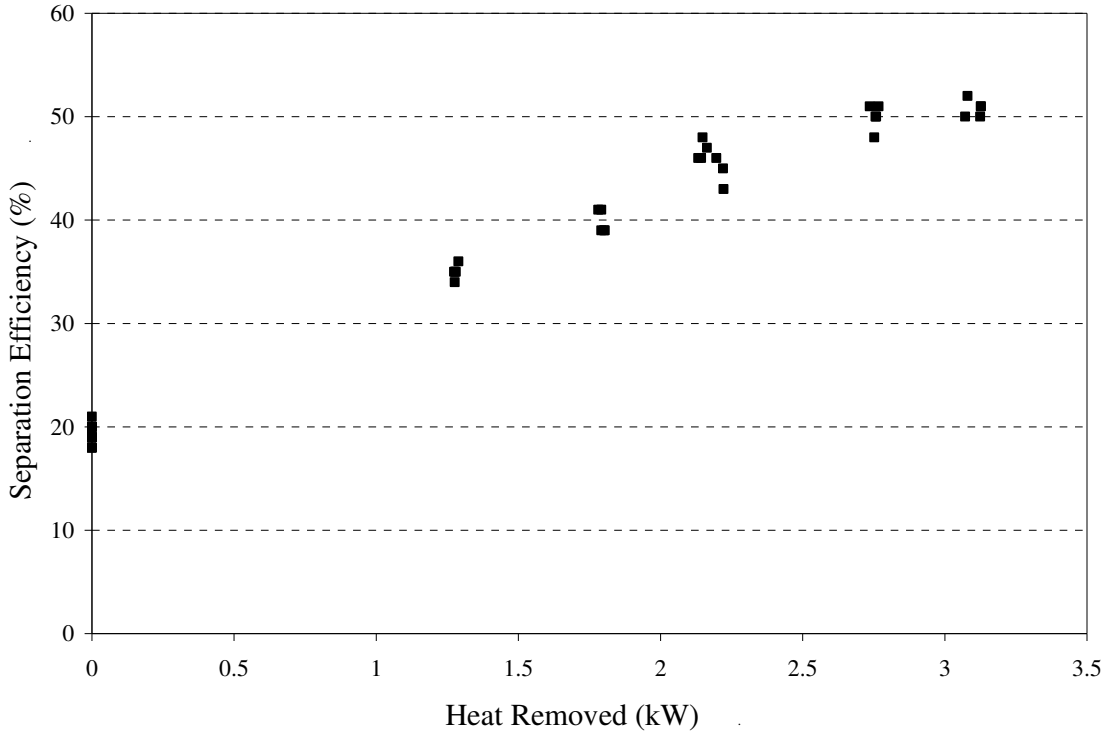

Figure 6.7 - Flow Straightener Efficiencies as a Result of Cooling

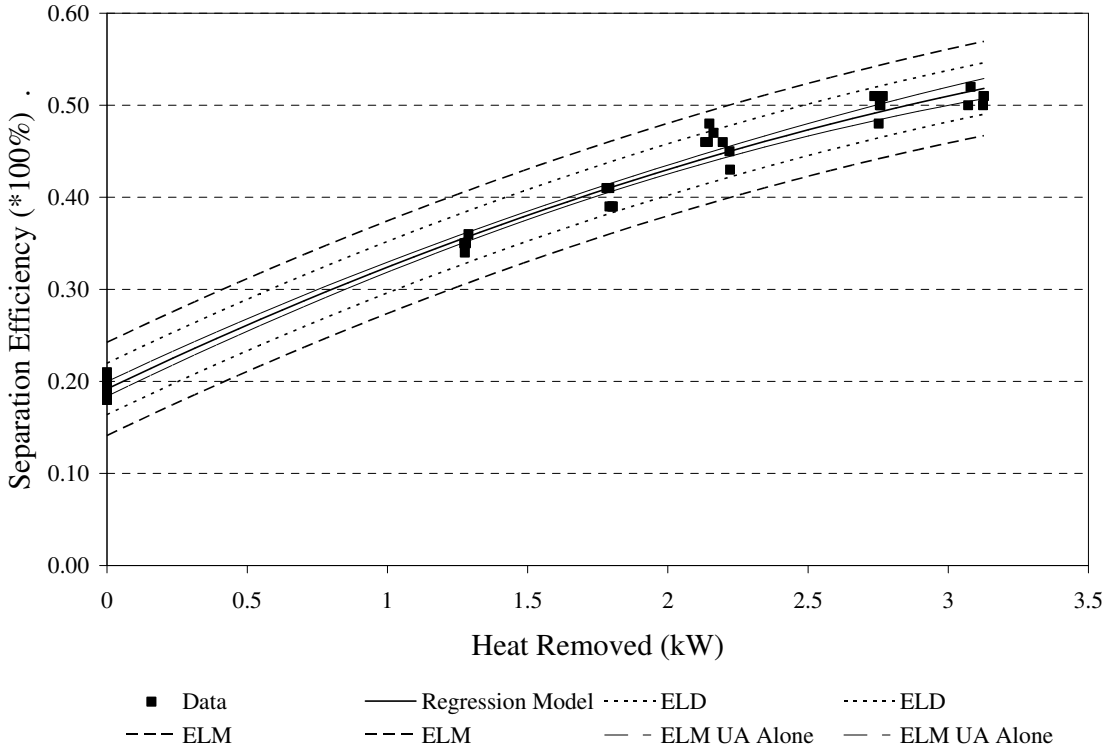

Figure 6.8 – Flow Straightener Data with Uncertainty

Figure 6.8 presents the flow straightener data with error bands. One point is seen to lie outside the error limits on the data but the remaining data is within the bars and all of the data lies very close to or within the error limits on the regression model. No magnification of the coverage factor was used on this plot to better show the error limits. The R^2 value of this fit is 0.9894 and the alpha risk is 7.07×10^{-7}. Again the regression model's error limits have been plotted with and without the influence of U_B.

Table 6.6 – Flow Straightener Averages

Cooling Water Flow Rate (Nominal) Lpm	Heat Removed kW	Separation Efficiency %	Mass Separated Average g	Mass Flow Possible g/min	Mass Flow Separated g/min	Mass Flow Possible Standard Deviation g/min	Mass Flow Separated Standard Deviation g/min	Uncertainty A g/min
0	0.00	19.27	84.40	83.15	15.99	4.49	0.84	1.65
1.89	1.28	35.00	158.00	87.59	30.50	0.79	0.79	1.65
2.84	1.79	39.80	182.00	88.58	35.18	1.87	0.14	1.65
3.79	2.18	45.86	206.00	87.84	40.09	0.70	1.14	1.65
7.57	2.75	50.00	224.40	86.92	43.41	0.74	0.74	1.65
11.36	3.11	50.80	235.00	88.92	45.23	0.58	0.75	1.65

As shown in Table 6.6, the standard deviations of the mass flow possibly separated and the mass flow actually separated are approximately the same. Neither value is routinely larger than the other. For most cooling water flow rates both values are less than the Uncertainty A.

6.2 AXIAL AND CENTRIFUGAL SEPARATORS IN SERIES

Due to the fact that the separation efficiencies experienced here were substantially lower than those found in previous investigations a centrifugal moisture separator was added in series with and after the axial separator to prove that little moisture was being separated and there was additional moisture available to be separated. This experiment was conducted for a total of ten data points with no cooling and the results of the mass

separated by the axial separator were plotted with the results of the combined axial and commercial separators.

The axial separator alone averaged 20.1% efficiency while the axial and commercial separators combined to separate 31.7% of the moisture available. This demonstrates that additional moisture was in the air stream available for separation and the calculated efficiencies are correct.

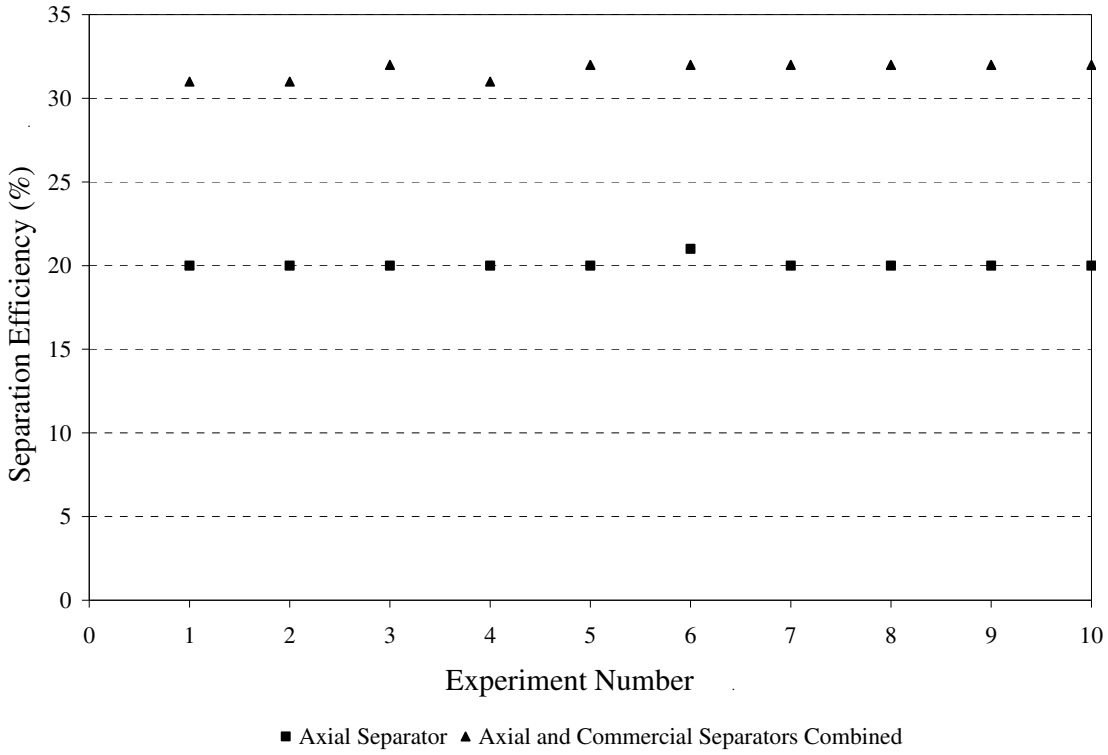

Figure 6.9 - Axial and Commercial Separators Separation Efficiencies

In summary, a positive correlation was shown between separation efficiency and the amount of cooling provided in both the case of the axial separator run alone and with

the flow straightener. Efficiencies without cooling in both cases averaged around 19.5%. Efficiencies with the maximum amount of cooling supplied averaged 50%. The commercial separator was able to separate moisture in addition to that separated by the axial swirl element. Experimental data collected during this research may be found in Appendix F.

CHAPTER 7

DISCUSSION

The results presented in the previous chapter will be interpreted and their implications discussed in this chapter. The data from different types of experiments will be compared and the difference examined to measure the significance of the difference. In addition, results from previous research will be reinterpreted with the reprogrammed EES code and examined.

Table 7.1 summarizes the results presented in the previous chapter.

Table 7.1 – Summary of Results

Cooling	Cooling	Axial		Flow Straightener		Axial and Commercial	
		Separation Efficiency	Mass Flow Separated	Separation Efficiency	Mass Flow Separated	Separation Efficiency	Mass Flow Separated
Lpm	kW	%	g/min	%	g/min	%	g/min
0.00	0.0	19.6	14.4	19.3	16.0	31.7	23.3
1.89	1.3	36.6	29.0	35.0	30.5		
2.84	1.8	42.8	33.8	39.8	35.2		
3.79	2.1	42.8	35.7	45.9	40.1		
7.57	2.7	46.6	39.9	50.0	43.4		
11.36	3.1	49.6	42.2	50.8	45.2		

In general, separation efficiencies increased as the amount of cooling was increased. The commercial separator was able to separate out an additional 50% of the amount of moisture separated by the axial flow separator alone. Separation efficiencies calculated from data collected with and without the flow straightener were very similar.

7.1 COMPARISON OF COOLED FLOW WITH UNCOOLED FLOW

Cooling the flow had a significant impact on separation efficiency in both the case of the separator alone and when the flow straightener was employed. Uncooled efficiencies averaged around 19% while efficiencies with 3 kW of cooling were 50% on average. There is a significant difference between cooled and uncooled experiments in the complexity of the system. With cooling comes a need to input energy both to cool and to pump water. It is possible that the amount of energy used may overtake the usefulness of the added separation efficiency. Therefore the benefits and costs of adding cooling must be examined and weighed carefully before implementation of a design with cooling.

In addition it was seen that a slight amount of cooling created a large change in separation efficiencies. For the axial separator operating alone, at 0 Lpm the average separation efficiency was 19.6%. At 1.7 kW of cooling the average efficiency jumped to 42.8% while after almost doubling that amount of cooling to 3 kW the average separation efficiency only raised to 49.6%. Substantial gains were seen with cooling up to 1.7 kW and diminishing returns were seen with additional rates of cooling.

7.2 USEFULNESS OF FLOW STRAIGHTENER

As demonstrated in Figure 7.1, the separation efficiencies of the axial separator operating alone and the efficiencies of the separator operating with the flow straightener were not significantly different. The data between the types of experiments is closely

grouped and the averages across the range of cooling rates are very close. There is no significant added benefit to employing a flow straightener in the system.

Figure 7.1 shows the plain axial separator data and the flow straightener with the axial separator data. The error bands which are plotted are based on the axial separator data. It can be seen that very few flow straightener data points fall outside of the error limits of the axial separator data and no data points fall outside the error limits of the regression model. In addition, a quadratic trendline is plotted for the flow straightener data and it lies well within the error limits of the axial separator data.

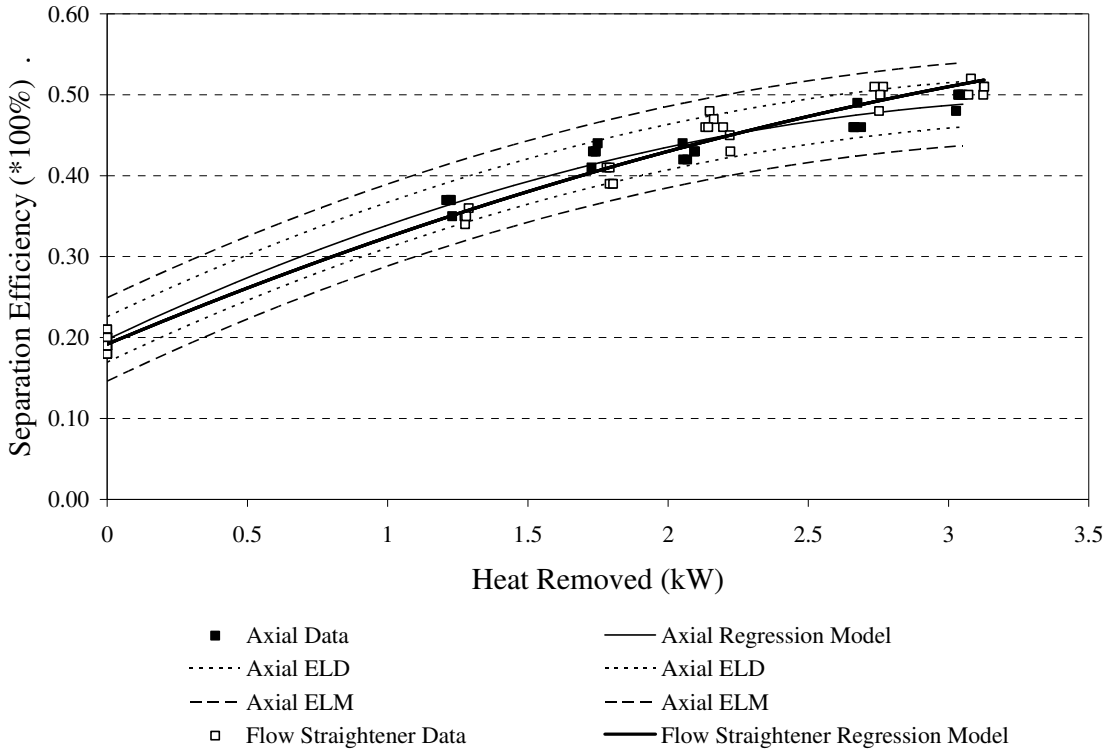

Figure 7.1 - Axial Separator and Flow Straightener Efficiencies Together with Error Bands from Axial Separator Experiments

It can conclusively be said that there was no significant difference in separation efficiencies created by the use of the flow straightener and no further testing needs to be done.

7.3 SEPARATORS IN SERIES

When the separators were placed in series a significant additional amount of moisture was separated. This concept is interesting and merits further investigation. The currently tested axial separator could possibly be scaled down and used in stages of imparting swirl and separation. If several swirl elements were placed in a row with a pipe running axially through all of them cooling could be imparted to the flow. As the flow cooled it would be swirled and moisture removed followed by further cooling and moisture removal. This could link several separators in a row and the gains may be substantial. As this design is currently in the prototype stage and the current swirl element was specially machined from billet aluminum, it was not feasible to create several swirl elements for testing. Nevertheless, some form of series combination of separators should be considered.

7.4 DISCUSSION OF PREVIOUS RESULTS

The average separation efficiency found in the research done in Aspinwall (2004) was found to be approximately 90% without the use of cooling water. Unfortunately, the EES code used in that investigation did not use absolute pressure for the evaluation of properties at Station 7, the orifice flow meter. This error resulted in the calculation of an erroneous water flow rate. In addition, the check to be sure the temperature and pressure

at Station 7 place the steam in the superheat region was not present, but this is of minor consequence. Correctly using absolute pressure in the flow calculation formulae creates a large change in the separation efficiencies found by that research when the data is re-processed. This change is demonstrated in Figures 7.2 and 7.3.

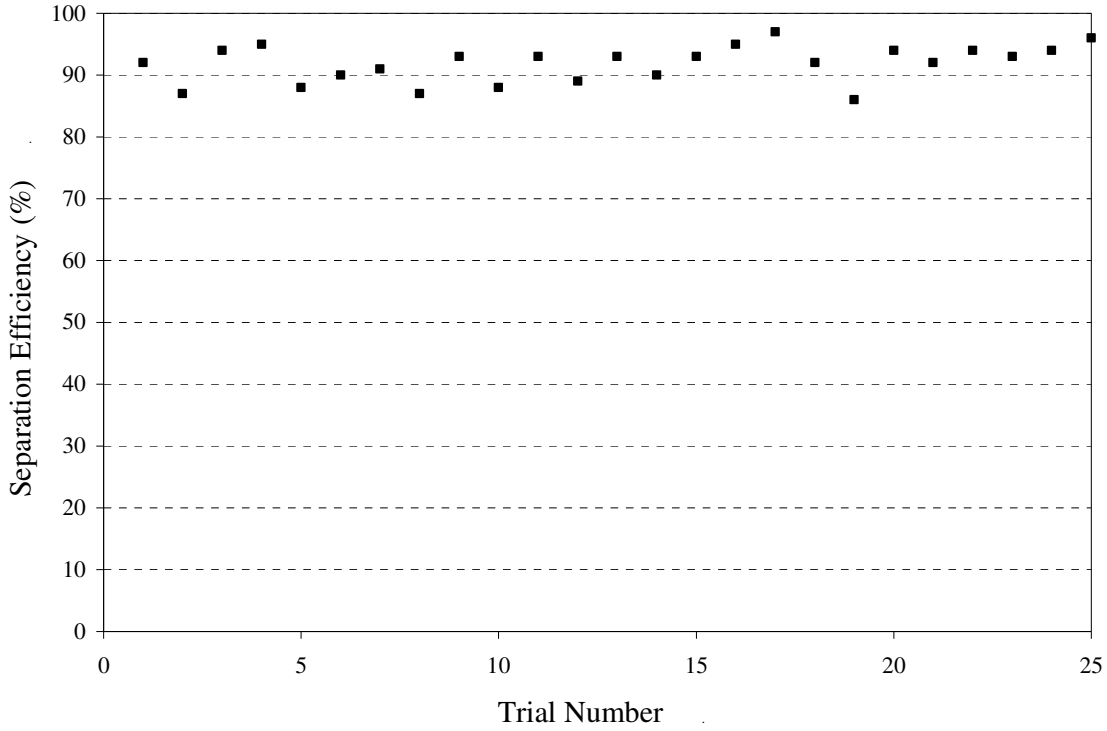

Figure 7.2 - Aspinwall (2004) Efficiencies as Presented

Figure 7.2 presents the data from the Aspinwall paper as reported in that source. Two variables were manipulated during the Aspinwall research, settling length and heated air temperature. The erroneous Figure 7.2 supports the conclusions of the paper that there was no significant difference between settling lengths or heated air temperature. Figure 7.3 shows the same data in the same order reprocessed with the fixed EES code.

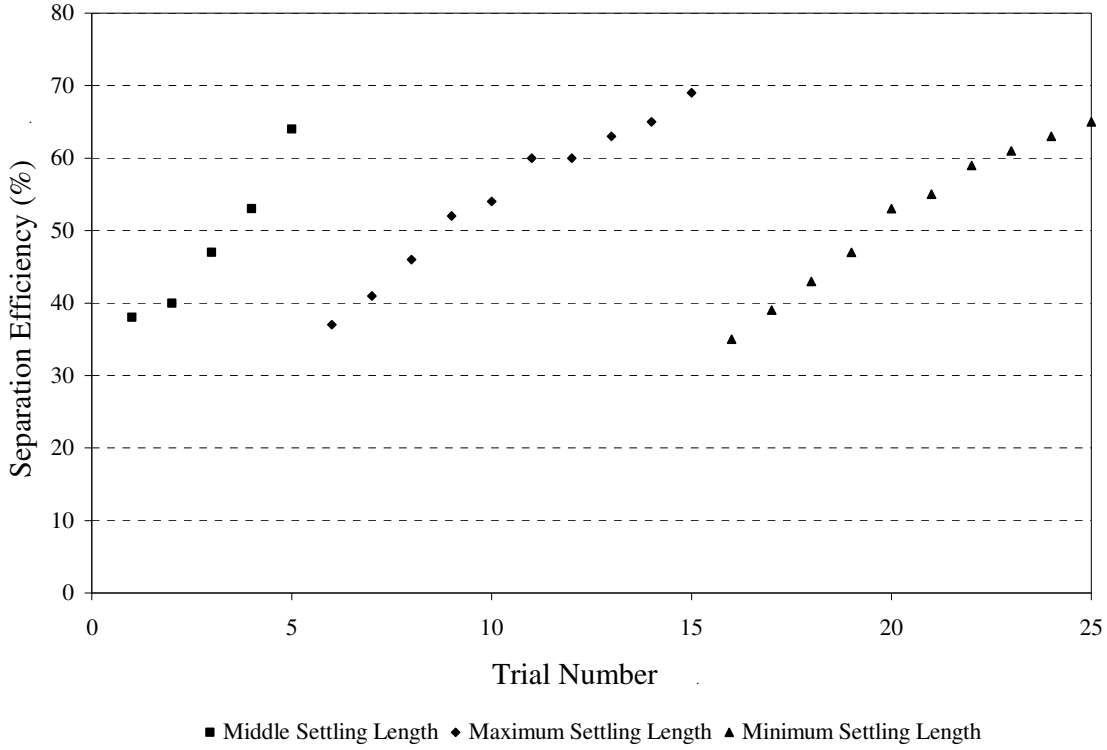

Figure 7.3 - Aspinwall (2004) Data Reprocessed

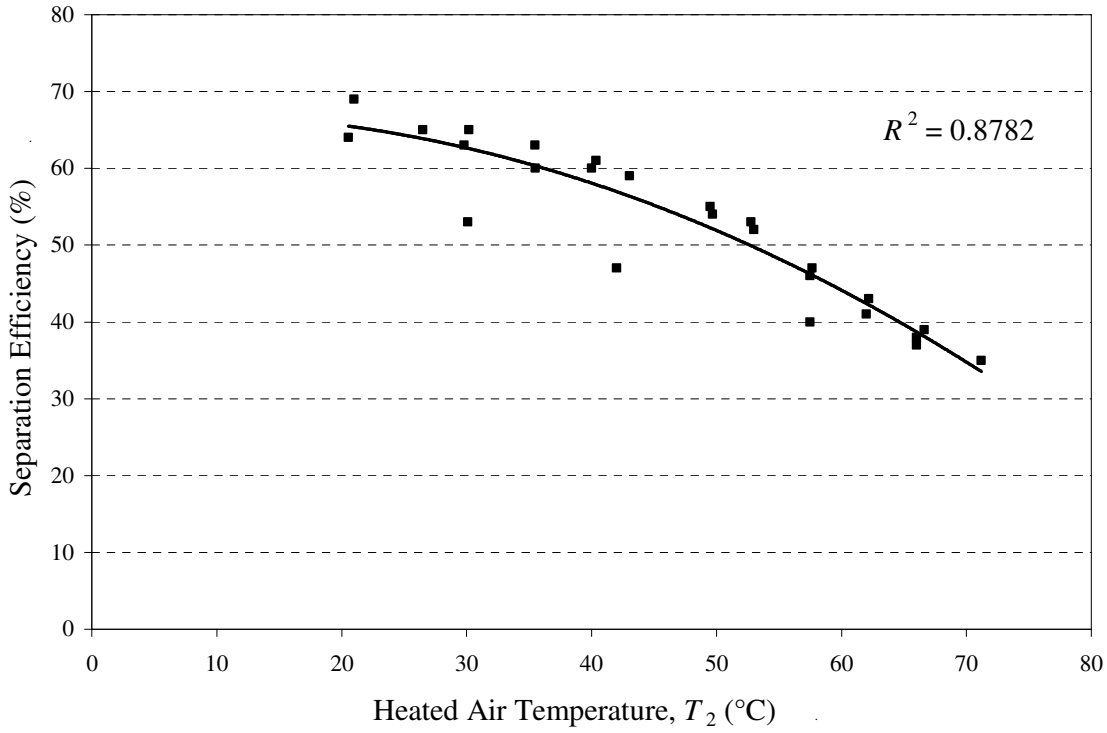

Figure 7.4.A - Aspinwall (2004) Data Reprocessed and Showing T_2

It can be seen that there is a large difference in these two graphs. Each lower left to upper right progression in Figure 7.3 is a set of experiments at one settling length with varying heated air temperature. Three settling lengths were tried and as can be seen, there is no substantial difference between them. The lines progress upward diagonally as the heated air temperature was lowered. The strong effect of the heated air temperature is shown clearly in Figure 7.4.A.

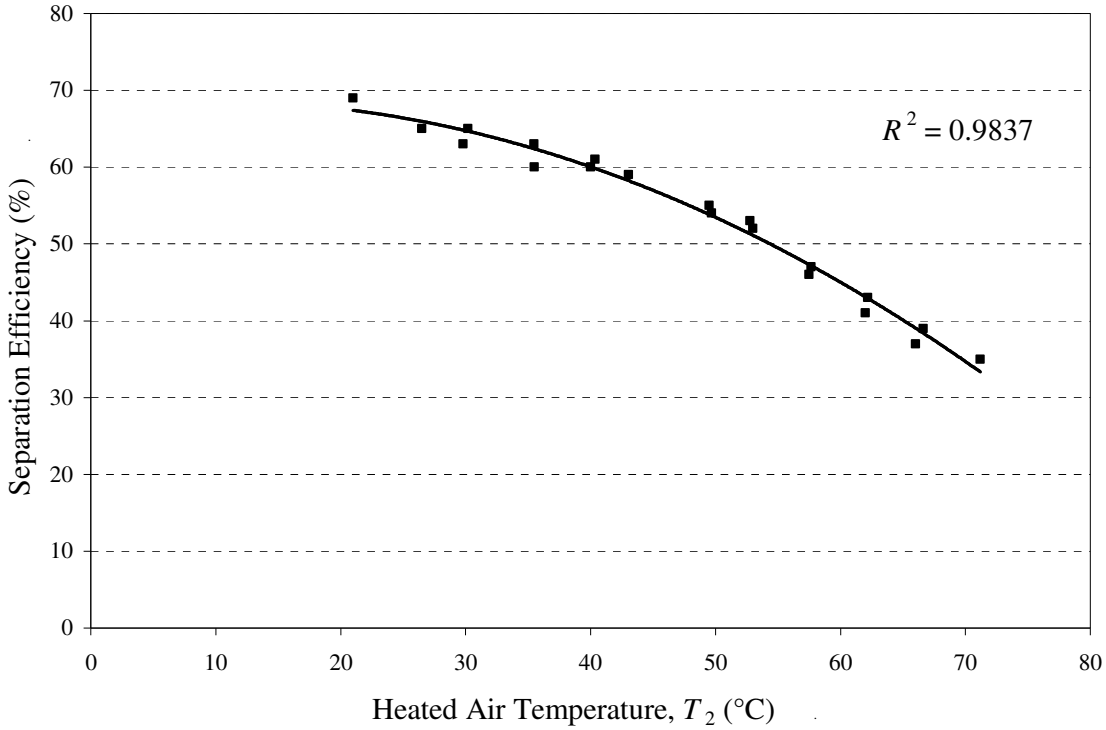

Figure 7.4.B - Aspinwall (2004) Data Reprocessed and Showing T_2 Excluding Midrange Settling Length

Upon reviewing Figure 7.4 there is definitely a change in separation efficiency due to the change in heated air temperature. This directly contradicts one of the basic findings of the Aspinwall paper. Interestingly, if Figure 7.4 is replotted omitting the midrange data Figure 7.4.B results, with a much closer cluster of data. It is not

understood why the long and short settling lengths would match trends so well while the midrange data did not fit in. The effect of heated air temperature on the separation efficiencies should be studied if the separator research is continued.

However, even upon reprocessing the separation efficiencies of Aspinwall at air temperatures similar to those experienced in this investigation the separation efficiencies of Aspinwall are much higher. The data shows efficiencies of approximately 37% at temperatures where this research found efficiencies of only 19%. It is believed that this discrepancy is due to the fact that the experiment was run with an airflow inlet rotameter reading of 80 cfm while in this investigation the rotameter would not read above 70 for any sustained period of time. It is unknown whether hardware was changed within the building's system to cause this change in air flow rates. It is possible that the duty cycle of the compressor has been changed which has reduced the possible steady-state flow rate.

Testing was done to see what air flow rates could be sustained by the building's air supply. When compressed air is first let into the system the airflow can be made to read 110 CFM, the maximum reading on the air inlet rotameter, at approximately 60 psi by adjusting the air flow regulator but higher flow rates do not occur at the 40 psi operating condition that the apparatus is normally run at. The building's compressed air system consists of a positive displacement compressor which discharges into a storage tank. From the tank, lines are run to laboratories in the building. A test was run to measure the maximum airflow rate the compressor could sustain. The air was opened

and the regulator setting was varied to determine the possible flow rates of air. The regulator was then set to supply air at 45 psi. Within 11 minutes of introducing air to the system the inlet air pressure dropped to 40 psi and no amount adjustment of the regulator would raise either this pressure or the flow rate of incoming air. It is believed that after 11 minutes the air supply in the storage tank had run out and the compressor was directly feeding compressed air to the system. Under these steady state conditions airflow rates around 70 cfm and 40 psi are the maximum that can be sustained.

7.5 COOLING NECESSARY FOR DESIRED WATER FLOW

It was shown in Chapter II that the water supply necessary to make a PEM fuel cell self-sufficient was 10.05 mol/min. This equates to 183 g/min. While there are approximately 390 g/min of water carried in the air flow at Station 4, typically 300 g/min (77%) are water vapor saturating the air flow and only 90 g/min (23%) are available for separation. Even at 100% separation efficiency this figure is only half of that needed to make the PEM fuel cell self-sufficient. This finding prompted the development of the cooled separator tested in the current research.

If the data taken using the axial flow separator is manipulated to give the relation shown in Figure 7.5 the heat transfer rate could be extrapolated at which the mass flow rate needed by the PEM is created. At 9.6 kW of cooling the desired mass flow rate is achieved. It should be cautioned that this is a large extrapolation as experimentally determined data ends at 3 kW of cooling and further analysis with higher levels of cooling may prove this estimate to be invalid. The main thrust of this discussion is that

current testing has not shown any means for the PEM fuel cell to become self-sustaining with respect to water requirements.

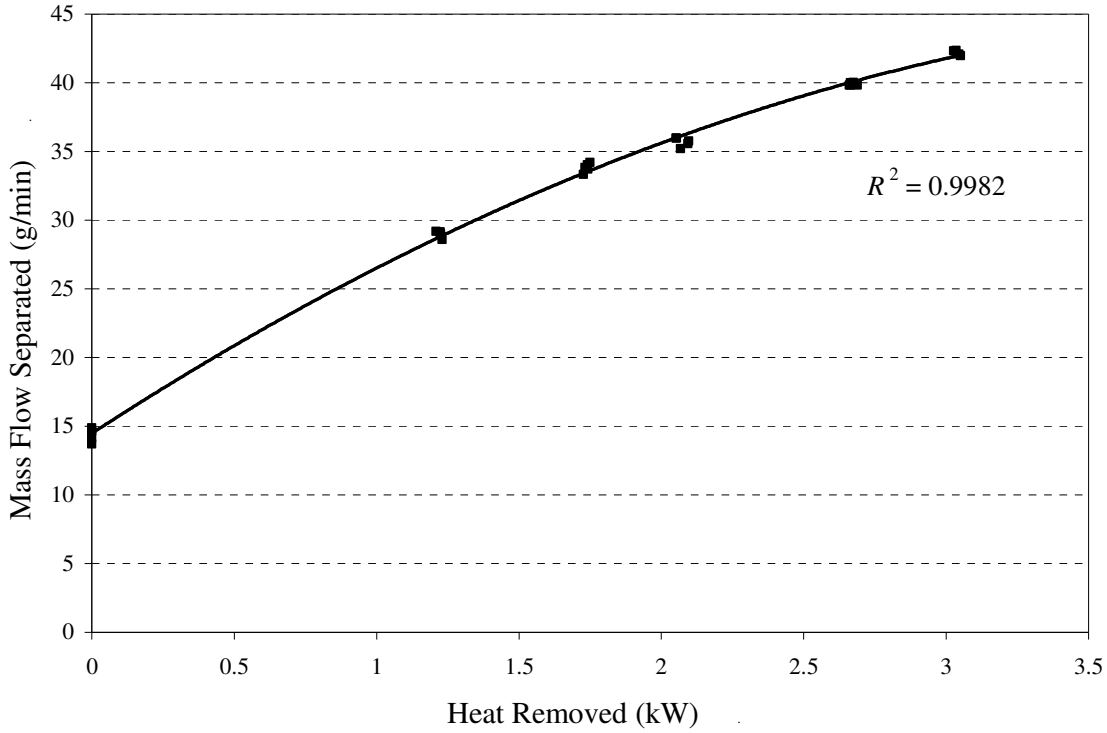

Figure 7.5 - Axial Separator Mass Flow Separated

It is hypothesized that the reason that more water mass is not collected is that uncaptured water is in very fine droplets. The chilled slide method was used to determine the average droplet size, which was one of the parameters of the swirl element design (Aspinwall, 2004). The chilled slide method uses a chilled glass microscope slide coated with a non-wetting surface covering which may be wax, oil, or any non-wetting surface treatment. The slide was held momentarily in the path of an open valve located after the turbine in the system. Droplets settled on the slide and the slide was quickly withdrawn, placed under a microscope, and photographed. The chilling of the slide was intended to

prevent evaporation of parts of or whole droplets in the short time between droplet collection and the photographic capturing of their presence. The non-wetting surface covering was intended to prevent small droplets from coalescing into larger droplets and to give a more accurate size representation of the droplets which are collected. The non-wetting surface prevented droplets from spreading out on the surface and appearing larger than they would be in air where they would have a somewhat spherical form. Extremely small droplets would have a tendency to evaporate very quickly and using the chilled slide method they may not be detected at all since they could evaporate before any photographs are taken. The average droplet size was found to be approximately 0.01 mm in diameter (0.0005 in.). A smaller than expected droplet size is a possible explanation as to why so little water mass was collected during experimental tests.

If the separator research is continued and refined, it would be critical to improve the measurement of droplet sizes. An improvement of the chilled slide method the minimize evaporation of small droplets should be possible. Ideally, some in line optical method, such as interference observation, should be implemented.

In summary, the flow straightener was unable to offer any greater separation rates than the axial flow moisture separator operating alone. Previous data does show a close link between separation efficiency and heated air temperature. The separators in series were able to offer additional moisture separation capabilities, confirming that there was extra water in the stream that the axial flow moisture separator was not separating.

Calculations show the current amounts of water being separated are inadequate to hydrate a PEM fuel cell.

CHAPTER 8

RECOMMENDATIONS

This chapter makes recommendations for future work based on the results of this investigation. The project goal was to improve the chilled axial separator but most effort was expended trying to duplicate previous results. There are three reasons that previous data could not be successfully verified. The air flow rate into the system experienced in this investigation was lower than that in previous investigations. Unknowingly, absolute pressure was incorrectly used to calculate flow rates of steam entering the system in previous investigations. The air heater was also possibly operated in an unsteady manner in previous investigations, which has an unknown effect on the results.

It was hoped that this separator would be able to provide a stream of water capable of meeting the needs of the fuel reformer thereby requiring no water to be added to the system. The amount of cooling provided to the system was inadequate to create the amount of moisture separation required for reforming a typical hydrocarbon fuel.

The first group of recommendations consist of instrumentation and apparatus upgrades. The Uncertainty B of the separation efficiency measurement was shown to be heavily reliant on the uncertainty generated by the air inlet rotameter. The manufacturer specifies that this uncertainty can be halved by special calibration. The rotameter should be either sent to the manufacturer for calibration or calibrated at Georgia Tech using a

more reliable instrument such as a laminar flow element. This would significantly decrease the uncertainty in the results.

The addition of a variable power control for the boiler would make a large difference in the range of testing able to be accomplished with the apparatus. Currently the air-water mixture is oversaturated at Station 3, before entering the water. Due to the fact that no more air flow can be obtained at steady state, the logical choice then to lower the humidity ratio would be to decrease the amount of steam entering the system. Currently the boiler is a 20 kW electric steam generator capable of operation only at full power. If a variable power boiler was introduced to the system it would allow testing to more closely mimic a wider range of PEM fuel cell conditions. With a variable power boiler the orifice flow meter calibration could be greatly improved. The calibration has been done with the best equipment available but essentially it is a two point calibration, through one point at the origin and one point at the operating level of the boiler. The improvement in calibration may affect the correction factor used in calibrations.

Currently it is believed that the reason more water mass is not separated is due to the fact that the water which is not being separated is in the form of very small droplets. The truth of this should be investigated through further investigation of the droplet size present in the system.

If a heat exchanger were added that could condense more of, or almost all of, the water present in the air stream it would greatly help in raising separation efficiencies. At

atmospheric temperature and pressure air is saturated with 40 g/min of water, much less than the 300 g/min which saturate the air flow at 55 °C, the temperature at which the humid air stream leaves the turbine. If the humid air stream could be cooled to 20 °C a separator of nearly 100% efficiency would be needed to recover enough water from the air stream to supply the diesel fuel reformer for a PEM fuel cell. There is no need for cooling water. If the humid airflow was passed through an automotive type heat exchanger and a fan was blown over the heat exchanger a pressure drop would be added but the amount of cooling provided might be sufficient to separate the necessary amount of water.

The second class of recommendations consists of test parameters which should be explored. One only partially explored avenue is to try varying the temperature air is heated to at Station 2 before being mixed with steam. Preliminary results are available for this testing from the reprocessing of the data presented in the Aspinwall report (2004), but in that investigation the apparatus was operated under unsteady heating conditions and it is unknown whether the data is reliable. The dual controls on the air heater were operated in that study in a manner which caused it to cycle, creating unsteady conditions at all points downstream of Station 2. While T_2 varies from 21 °C to 70 °C, mixture temperatures entering the separator vary only from 52 °C to 57 °C. This could be explained by the fact that air carries very little enthalpy while steam carries very much and thus when the two mix the steam influences the mixture temperature much more than the air. It should be verified experimentally however under steady state conditions. The mass flow rates of water collected vary greatly in the Aspinwall data, as do the mass flow

rates of water which it was possible to collect. The net effect of this variation is hard to understand and could be fleshed out with further research.

The third class of recommendations involves building a new part to the existing apparatus. Many scaled down separators could be constructed and operated in a staged series. The Aspinwall report (2004) did experimentally show and calculations did reinforce that the swirl element could be given a much shorter settling length than it is currently given. Several smaller swirl elements could be fit into the linear space currently being used with moisture being removed between each element. The overall pressure drop an arrangement like this would make is unknown as the pressure drop across the water removal section of the swirl element housing has never been measured.

In current testing a significant amount of saturated air is lost through the water removal tubing. It is unknown precisely how much as the flow rate has never been measured. It is possible that in a staged arrangement that after a few stages are passed there would be little or no moist air left flowing within the housing if the current design is used.

A new swirl element could be created with a steeper vane angle which would impart more rotation to the working fluid. This might create additional pressure drop across the swirl element but would possibly also separate more liquid. Means to recover the swirl velocity should also be considered.

While cooling of the separator body and the pipe running through the separator housing has been explored in this research, no experimentation has been done with cooling the separator housing itself. When the separator is run without cooling water there is approximately a 1.5 °C temperature drop between the air and water mixture entering the housing and the mixture leaving the housing. This is not perfectly adiabatic, but the mixture typically enters the housing around 56 °C and this figure loses only 2.5 % through the separator housing. With the highest rate of cooling supplied in this research the temperature dropped by a totally of 4.5 °C. If the exterior of the separator housing was also cooled it could possibly create a much greater temperature drop and help the separator extract the necessary mass flow rate of water to supply the diesel reformer. If this option is explored it is recommended that the current plastic housing be replaced with something with a higher thermal conductivity. It would be possible to fit a larger pipe coaxially around the inner pipe which houses the swirl element, forming a tube in tube heat exchanger.

Currently the expansion of the humid air stream through the turbine is limited by pressure. The pressure of the stream exiting the turbine is only slightly above atmospheric pressure at 60 mm Hg. The recommended path for future work would install a variable power boiler capable of creating steam at higher pressures than the current boiler is capable of. The high pressure steam which the boiler generated would increase the pressure of the air and water mixture at Station 3, where PEM Fuel Cell exhaust conditions are simulated. Currently the pressure at this station is 172 Kpa gauge (25 psig), but the Amphlett (1993) study shows a range from 138 to 241 Kpa gauge (20-35

psig) as being valid working pressures. If the pressure of the mixture was increased the subsequent expansion through the turbine would create a greater pressure drop and a greater temperature drop. Currently the mixture temperature at Station 3 is 80 °C, which is the upper limit of the operating range prescribed by Amphlett (1993). In order to keep the steam from pushing the actual temperature outside the goal range, the temperature to which air is heated may need to be decreased so that the steam will be forced to heat the air. This path, combined with an investigation of droplet size, will lead to greater mass separation rates through temperature reduction.

No matter what else is done, the crux of the matter is that the humid air stream temperature must be lowered substantially in order to free water from the stream which can then be separated. This could possibly be accomplished by pumping a great deal more water through the current setup, but it would likely be accomplished better by introducing a new heat exchanger or increasing the turbine inlet pressure and allowing the turbine to further drop the stream temperature. Tentative results from reprocessing the data presented by Aspinwall (2004) show separation efficiencies as high as 70%, which is on par with or a little higher than the efficiency of the commercial separator, found to be 65% in that investigation. The axial flow separator design parameters used in the Aspinwall (2004) report have potential to create a very efficient separator, but the current separator is in need of changes in design to increase separation efficiency.

APPENDIX A

CALIBRATIONS AND UNCERTAINTY DATA

A.1 THERMOCOUPLE CALIBRATIONS

Thermocouple	1	2	3	4	5	6	7
Location	Station 1	Station 2	Station 3	Station 4	Station 5	Station 6	Station 7
Intercept	-0.2147	-0.4255	-0.2284	-0.2091	0.0140	-0.3332	-0.1358
Slope	0.9965	1.0022	0.9982	1.0059	0.9959	0.9944	0.9876
SEE	0.1104	0.1387	0.0412	0.0289	0.0764	0.2068	0.2190
R^2	1.0000	1.0000	1.0000	1.0000	1.0000	1.0000	1.0000
k_C	2.2622	2.2622	2.2622	2.2622	2.2622	2.2622	2.2622
U_B	0.25	0.31	0.09	0.07	0.17	0.47	0.50

Thermocouple	8	9	11	12	13	14	15
Location	Station 8	Station 9	Boiler Inlet	Oil	Station 13	Station 14	Station 15
Intercept	-0.0736	-0.1664	-0.0935	-0.1516	-0.4463	-0.2660	-0.2414
Slope	1.0037	1.0038	0.9998	1.0008	0.9978	0.9924	1.0014
SEE	0.0390	0.1118	0.0271	0.0939	0.0237	0.0205	0.0401
R^2	1.0000	1.0000	1.0000	1.0000	1.0000	1.0000	1.0000
k_C	2.2622	2.2622	2.2622	2.2622	2.1315	2.1315	2.2622
U_B	0.088	0.25	0.061	0.21	0.050	0.044	0.091

The above table presents the useful data from the thermocouple calibrations. A linear regression was used for all thermocouples and slope and intercept are presented here. The standard error of estimate and k_c are presented and multiplied together to determine U_B. The variation in k_c is due to the fact that more data points were collected in some calibrations than in others.

A.2 BOILER ROTAMETER CALIBRATION

file: Boiler_rotameter_Cal 9-Jan-04

Summary:

V_dot = 3.97*(Indicated Position) - 35.4

Parameters:

1 lbm = 0.453592 kg

density = 0.998403 kg/L

				start	end	mass	Rotameter	m_dot	m_dot	V_dot	V_dot	V_dot
	time	time	time	mass	mass	in	ind	actual	model	actual	actual	model
	min	sec	frac mins	(lbm)	(lbm)	(lbm)	(mm)	kg/min	kg/min	L/min	mL/min	mL/min
1	3	10.37	3.173	0.420	0.496	0.076	10	0.011	0.004	0.011	10.882	4.317
2	3	7.90	3.132	0.550	0.868	0.318	20	0.046	0.044	0.046	46.133	44.042
3	3	4.56	3.076	0.962	1.558	0.596	30	0.088	0.084	0.088	88.028	83.767
4	3	3.30	3.055	0.460	1.282	0.822	40	0.122	0.123	0.122	122.242	123.493
5	3	5.30	3.088	0.276	1.376	1.100	50	0.162	0.163	0.162	161.819	163.218
6	3	4.59	3.077	0.676	1.994	1.318	60	0.194	0.203	0.195	194.634	202.943
7	3	19.18	3.320	2.456	4.222	1.766	70	0.241	0.242	0.242	241.689	242.669
8	3	8.22	3.137	0.794	2.724	1.930	80	0.279	0.282	0.280	279.514	282.394
9	3	8.90	3.148	3.014	5.226	2.212	90	0.319	0.322	0.319	319.201	322.119
10	3	13.13	3.219	0.796	3.312	2.516	100	0.355	0.361	0.355	355.118	361.845
11	3	13.30	3.222	3.662	6.494	2.832	110	0.399	0.401	0.399	399.367	401.570
12	3	7.18	3.120	0.762	3.804	3.042	120	0.442	0.441	0.443	443.007	441.295
13	3	7.69	3.128	4.278	7.632	3.354	130	0.486	0.480	0.487	487.117	481.021
14	3	3.85	3.064	0.790	4.322	3.532	140	0.523	0.520	0.524	523.683	520.746
15	3	6.25	3.104	5.092	8.942	3.850	150	0.563	0.560	0.563	563.476	560.471

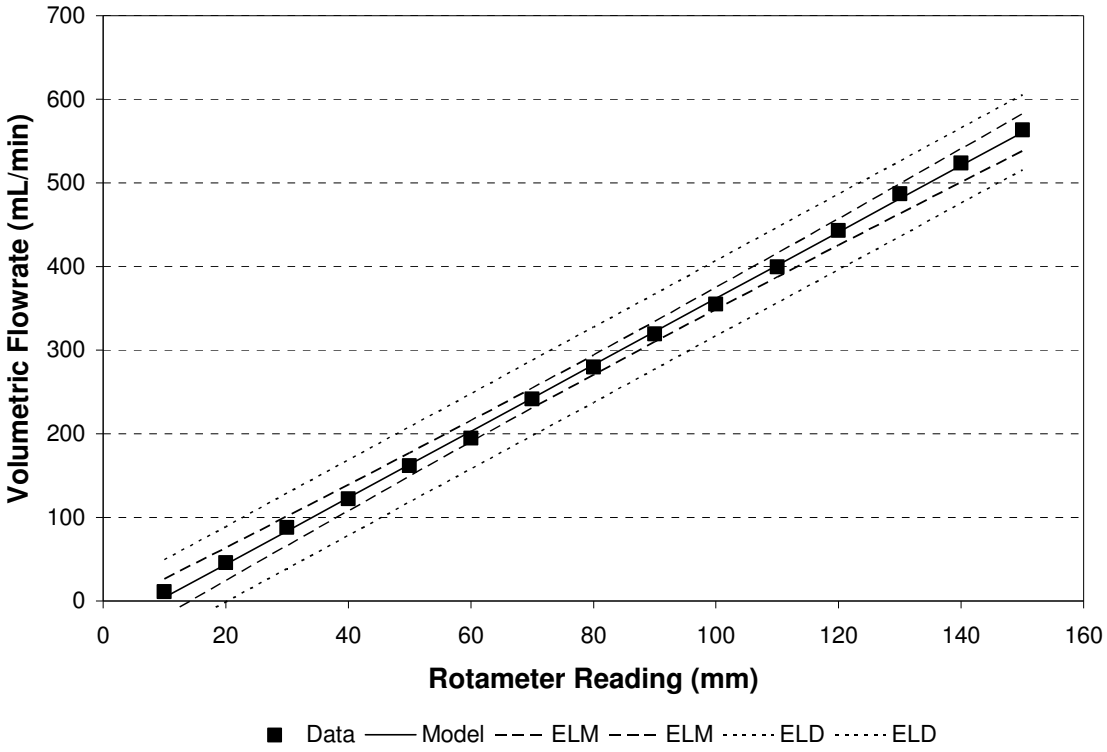

SUMMARY OUTPUT (Position vs Volumetric Flow Rate)

Regression Statistics	
Multiple R	0.999702
R Square	0.999403
Adjusted F	0.999357
Standard E	4.504966
Observatio	15

ANOVA

	df	*SS*	*MS*	*F*	*Significance F*
Regressior	1	441868.3902	441868.3902	21772.58125	2.3948E-22
Residual	13	263.8313302	20.29471771		
Total	14	442132.2216			

	Coefficients	*Standard Error*	*t Stat*	*P-value*	*Lower 95%*	*Upper 95%*	*Lower 95.0%*	*Upper 95.0%*
Intercept	-35.40859	2.447810001	-14.46541546	2.1583E-09	-40.69675961	-30.12041764	-40.69675961	-30.12041764
X Variable	3.972532	0.026922321	147.5553498	2.3948E-22	3.914370307	4.03069456	3.914370307	4.03069456

This boiler inlet rotameter calibration data was taken from Aspinwall (2004),

A.3 DIFFERENTIAL PRESSURE TRANSDUCER CALIBRATION

Differential Pressure Transducer Calibration Data			
Current	Pressure Measured	Pressure Calculated	Model
mA	in H2O	in H2O	in H2O
3.982	0.00	0.00	0.01
4.159	0.07	1.20	1.24
4.480	2.02	3.47	3.46
4.763	3.24	5.57	5.42
4.997	4.07	7.00	7.03
5.210	4.95	8.51	8.51
5.444	5.87	10.10	10.13
5.744	7.10	12.21	12.20
5.968	8.05	13.85	13.75
6.243	9.10	15.65	15.65
6.455	9.95	17.11	17.12
6.709	10.97	18.87	18.87
6.973	12.04	20.71	20.70
7.270	13.24	22.77	22.75
7.509	14.16	24.36	24.41
7.730	15.10	25.97	25.94
7.894	15.75	27.09	27.07
8.174	16.88	29.03	29.01
8.523	18.27	31.42	31.42
8.734	19.10	32.85	32.88
8.885	19.72	33.92	33.92
9.251	21.10	36.29	36.46
9.388	21.72	37.36	37.40
9.704	23.02	39.59	39.59
10.010	24.27	41.74	41.70
10.365	25.68	44.17	44.16
10.699	27.00	46.44	46.47
11.020	28.24	48.57	48.69
11.194	29.02	49.91	49.89
11.466	30.10	51.77	51.77
11.690	31.00	53.32	53.32
11.962	32.08	55.18	55.20
12.237	33.20	57.10	57.11
12.369	33.72	58.00	58.02
12.672	34.95	60.11	60.12
12.933	36.00	61.92	61.92
13.120	36.76	63.23	63.21
13.354	37.70	64.84	64.83
13.619	38.74	66.63	66.66
13.919	39.99	68.78	68.74
14.108	40.76	70.11	70.05
14.415	41.98	72.21	72.17
14.586	42.67	73.39	73.35
14.897	43.90	75.51	75.50
15.080	44.62	76.75	76.77
15.360	45.77	78.72	78.71
15.670	47.00	80.84	80.85
15.815	47.59	81.85	81.85
16.132	48.86	84.04	84.04
16.361	49.80	85.66	85.63

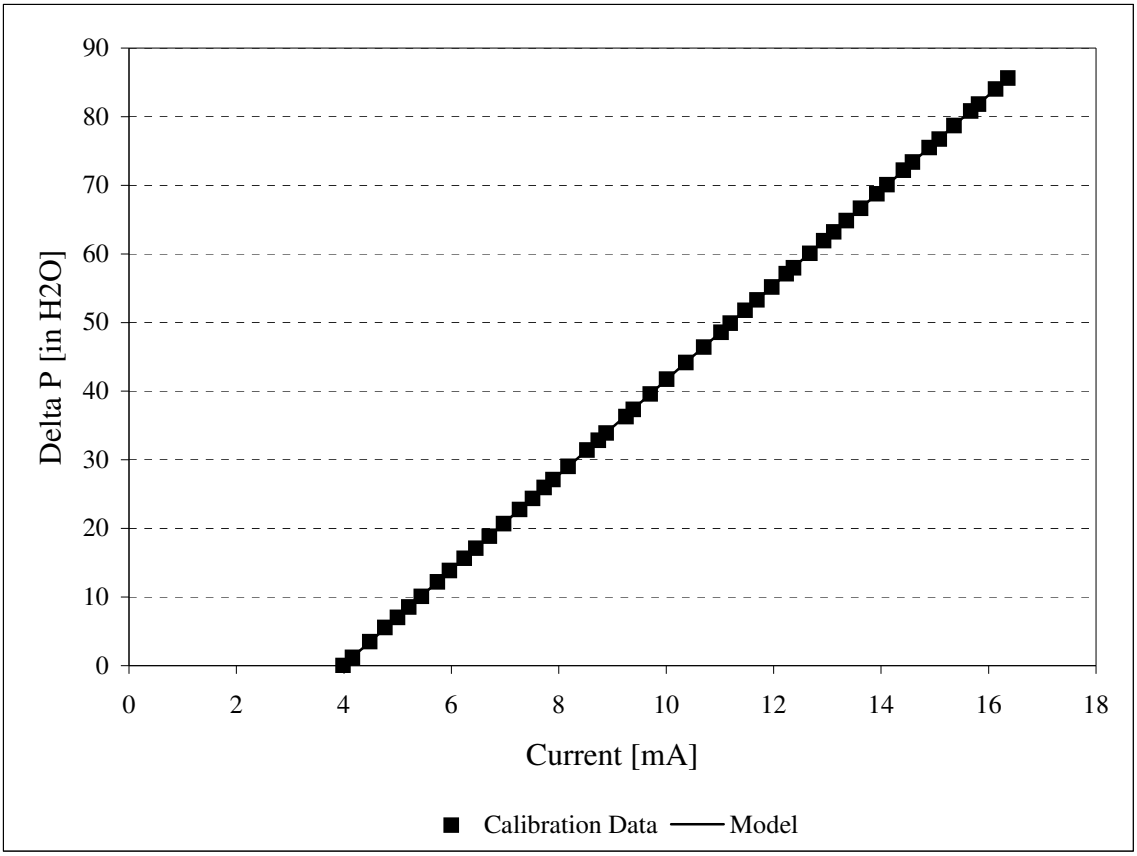

SUMMARY OUTPUT

Regression Statistics	
Multiple R	0.999998411
R Square	0.999996823
Adjusted R Square	0.999996757
Standard Error	0.046283933
Observations	50

ANOVA

	df	*SS*	*MS*	*F*	*Significance F*
Regression	1	32363.60095	32363.60095	15107629.44	1.2826E-133
Residual	48	0.102825718	0.002142202		
Total	49	32363.70378			

	Coefficients	*Standard Error*	*t Stat*	*P-value*	*Lower 95%*	*Upper 95%.ower 95.0%*	*Jpper 95.0%*	
Intercept	-27.52482594	0.019268132	-1428.515566	9.4217E-113	-27.5635671	-27.48608	-27.56357	-27.48608
X Variable 1	6.916032188	0.00177934	3886.853412	1.2826E-133	6.912454588	6.91961	6.912455	6.91961

The differential pressure transducer calibration data was taken from Hull (2002)

A.4 PRECISION UNCERTAINTY IN MEASUREMENTS

A.4.1 Digital Measurements

	T_1	T_2	T_3	T_4	T_5	T_6
	Comp. Air Inlet	Heated Air	Air & Steam Mix	Separator Inlet	Post Separator	Valve Exit
	℃	℃	℃	℃	℃	℃
	21.36129	70.14541	81.14861	56.57929	51.53239	69.03650
	21.45795	70.23059	81.19154	56.63366	51.63099	69.10213
	21.34635	70.15042	81.03981	56.58231	51.61904	69.96325
	21.40514	70.21255	81.10868	56.59841	51.46467	70.72592
	21.44400	70.41299	81.18654	56.70704	51.72660	71.05009
	21.40016	70.37290	81.19753	56.69396	51.50849	71.02920
	21.37226	70.38392	81.14662	56.70643	51.46566	69.98214
	21.42108	70.41198	81.18056	56.75230	51.49853	69.33680
	21.40813	70.40196	81.10170	56.66479	51.55331	70.22377
	21.46792	70.46911	81.15261	56.66178	51.47562	71.16344
Average	21.40843	70.31918	81.14542	56.65800	51.54753	70.16132
Standard Deviation	0.04066	0.12098	0.04972	0.05875	0.08633	0.81706
Number of Points	10	10	10	10	10	10
Coverage Factor	2.26216	2.26216	2.26216	2.26216	2.26216	2.26216
U_A	0.02965	0.08822	0.03625	0.04284	0.06295	0.59582

	T_7	T_8	T_9	WBD	T_{11}	T_{12}
	Boiler Exit	Compressor Inlet	Compressor Exit	At 6	Boiler Inlet	Oil
	℃	℃	℃	Vdc	℃	℃
	159.50240	26.28860	96.58879	11.15214	24.39434	76.36923
	159.50640	26.19224	96.49143	11.69964	24.39834	76.36522
	159.52810	26.38295	96.63698	11.77354	24.39834	76.35722
	159.60420	26.36388	96.67010	12.77810	24.40334	76.38324
	159.60220	26.53251	96.81665	11.54238	24.46733	76.41527
	159.66240	26.37492	96.43823	12.95163	24.46833	76.43128
	159.63970	25.97142	96.74438	11.11046	24.49632	76.48632
	159.67530	26.26551	96.70824	11.30745	24.39734	76.49233
	159.59030	26.36388	96.70021	12.04202	24.35335	76.46130
	159.56370	26.55660	96.79858	11.02588	24.37634	76.48832
Average	159.58747	26.32925	96.65936	11.73832	24.41534	76.42497
Standard Deviation	0.06188	0.16763	0.12387	0.67640	0.04585	0.05455
Number of Points	10	10	10	10	10	10
Coverage Factor	2.26216	2.26216	2.26216	2.26216	2.26216	2.26216
U_A	0.04512	0.12224	0.09033	0.49325	0.03343	0.03978

	T_{13}	T_{14}	T_{15}	%RH	dP7	Pump	RPM
	Cool Water In	Cool Water Out	Turbine Exit	In Comp. Air	Orifice Flow	Wattmeter	Turbine
	℃	℃	℃	%	in. H20	Watts	RPM
	6.33960	10.18620	56.85991	5.83952	27.79557	283.00000	2.67900
	6.32663	10.18223	56.86793	5.75653	27.76573	282.00000	2.67700
	6.36055	10.22490	56.87694	5.84227	27.86231	282.00000	2.67800
	6.36554	10.22589	56.93302	5.83382	27.85411	283.00000	2.67700
	6.39348	10.26063	56.98109	5.87147	27.86694	282.00000	2.67800
	6.37851	10.24574	57.00112	5.69031	27.83878	282.00000	2.67900
	6.38550	10.25170	56.97608	5.76202	27.92726	283.00000	2.67800
	6.40645	10.25765	56.95205	5.79031	27.79709	284.00000	2.67700
	6.39647	10.24680	56.92501	5.79986	27.75281	283.00000	2.67800
	6.43040	10.29536	56.94504	5.93659	27.77356	282.00000	2.67900
Average	6.37831	10.23771	56.93182	5.81227	27.82342	282.60000	2.67800
Standard Deviation	0.03121	0.03436	0.04954	0.06848	0.05541	0.69921	0.00082
Number of Points	10	10	10	10	10	10	10
Coverage Factor	2.26216	2.26216	2.26216	2.26216	2.26216	2.26216	2.26216
U_A	0.02276	0.02505	0.03612	0.04994	0.04041	0.50988	0.00060

These data present the U_A of the digital instrumentation. Each column of data is a set of successive measurements.

A.4.2 Analog Measurements

Measurement	RM-1	RM-9	RM-B	RM-CW	Air Heater Power	Separated Water	Time
Location	Air In Rot.	Comp. Rot.	Boiler Inlet	Cooling Water		Raw	Raw
Units	cfm	cfm	mm	gpm	KW	grams	Min.S
Typical Measurement	7	85	114	0.75	0.59	280	5.1028
U_A	0.05	0.5	0.5	0.125	0.005	0.05	0.04

Measurement	P_1	P_3	dP4	dP5	P_7	P_9	P_{Boiler}	P_{Oil}
Location	Air in P	Air & Steam Mix	Turb. Exit P	dP Element	Steam out P	Comp. Air P	Boiler	Oil
Units	psi	psi	mm Hg	in. H20	psi	psi	psi	psi
Typical Measurement	42	24.75	58	4.2	77.25	9.5	78	14.5
U_A	0.25	0.25	0.5	0.1	0.25	1	0.25	0.5

The uncertainties presented here were determined to be half of the smallest increment the instrument presented. A typical measurement is also presented.

A.5 COOLING WATER ROTAMETER CALIBRATION

water temp (°C)	24
Density of Water (kg/m^3)	997.3

1 lbm =	0.453592	kg	
L/m^3 =	0.001		

Rotameter (gpm)	m_start (lb)	m_end (lb)	dm (lb)	dt (min)	dt (sec)	Total Time (min)	M_dot Actual (kg/min)	M_dot Model (kg/min)	V_dot Actual (L/min)	V_dot Model (L/min)
4	550	650	100	2	56.44	2.94	15.42	15.77	15.47	15.82
4	335	465	130	3	45.63	3.76	15.68	15.77	15.72	15.82
3.5	680	795	115	3	44.25	3.74	13.96	13.73	13.99	13.77
3.5	495	665	170	5	40.75	5.68	13.58	13.73	13.61	13.77
3	180	270	90	3	28.06	3.47	11.77	11.70	11.80	11.73
3	220	315	95	3	35.09	3.58	12.02	11.70	12.05	11.73
2.5	685	770	85	3	50.75	3.85	10.03	9.66	10.05	9.68
2.5	125	200	75	3	28.72	3.48	9.78	9.66	9.81	9.68
2	190	290	100	6	20.06	6.33	7.16	7.62	7.18	7.64
2	395	450	55	3	20.44	3.34	7.47	7.62	7.49	7.64
1.5	470	525	55	4	20.62	4.34	5.74	5.58	5.76	5.60
1.5	645	690	45	3	33.94	3.57	5.72	5.58	5.74	5.60
1.5	305	345	40	3	11.63	3.19	5.68	5.58	5.70	5.60
1	545	575	30	4	26.56	4.44	3.06	3.54	3.07	3.55
1	360	395	35	4	10.35	4.17	3.80	3.54	3.82	3.55
0.5	595	610	15	3	37.43	3.62	1.88	1.51	1.88	1.51
0.5	385	395	10	4	18.03	4.30	1.05	1.51	1.06	1.51

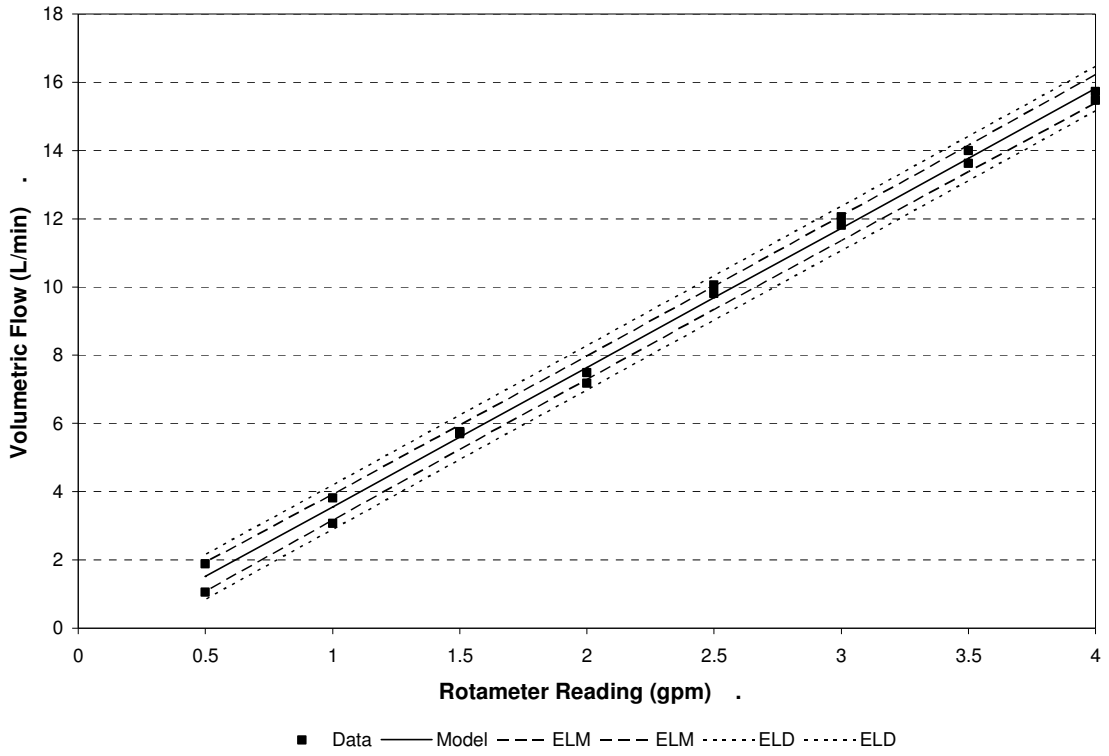

SUMMARY OUTPUT

Regression Statistics	
Multiple R	0.998056122
R Square	0.996116022
Adjusted R Square	0.995857091
Standard Error	0.305762499
Observations	17

ANOVA

	df	*SS*	*MS*	*F*	*Significance F*
Regression	1	359.6606375	359.6606375	3847.020251	1.68648E-19
Residual	15	1.402360583	0.093490706		
Total	16	361.0629981			

	Coefficients	*Standard Error*	*t Stat*	*P-value*	*Lower 95%*	*Upper 95%*	*Lower 95.0%*	*Upper 95.0%*
Intercept	-0.533353719	0.163185553	-3.268388098	0.005184217	-0.881175706	-0.185531733	-0.881175706	-0.185531733
X Variable 1	4.087242192	0.065897378	62.02435208	1.68648E-19	3.946785169	4.227699215	3.946785169	4.227699215

The cooling water rotameter calibration and regression data are presented here. The rotameter was calibrated from 0 Lpm to 15.14 Lpm (4 gpm). The highest flow rate used in the system was 11.35 Lpm (3 gpm).

APPENDIX B

SWIRL ELEMENT CALCULATIONS

B.1 VANE HEIGHT CALCULATIONS

Inputs				
In Pipe Dia (in.)	Model Dia (in.)	Mill Bit Size (in.)	Lip Size (in.) (desired)	Cut Depth (in)
2.000	3.000	0.500	0.063	0.000
2.000	3.000	0.500	0.063	0.000
2.000	3.000	0.500	0.063	0.100
2.000	3.000	0.500	0.063	0.250
2.000	3.000	0.500	0.063	0.150
2.000	3.000	0.500	0.063	0.200
2.000	3.000	0.500	0.063	0.175

Vanes intersect. Therefore, try 15 vanes and a deeper cut to preserve flow area.

2.000	3.000	0.500	0.063	0.250
2.000	3.000	0.500	0.063	0.200

Calculations						
Cent Ang (deg)	T. Height (in.)	Sec Area (in.^2)	T. Area (in.^2)	Sliver	In Pipe A (in.^2)	Vane Area
19.188	1.479	0.377	0.370	0.007	3.142	1.762
19.188	1.479	0.377	0.370	0.007	3.142	1.683
19.188	1.479	0.377	0.370	0.007	3.142	2.483
19.188	1.479	0.377	0.370	0.007	3.142	3.683
19.188	1.479	0.377	0.370	0.007	3.142	2.883
19.188	1.479	0.377	0.370	0.007	3.142	3.283
19.188	1.479	0.377	0.370	0.007	3.142	3.083

19.188	1.479	0.377	0.370	0.007	3.142	3.453
19.188	1.479	0.377	0.370	0.007	3.142	3.078

Results			
Model Perim (in.)	# Vanes	Lip Size (in.) (Actual)	(Pipe - Vane)
9.425	16.755	0.062	1.379
9.425	16.000	0.084	1.459
9.425	16.000	0.084	0.659
9.425	16.000	0.084	-0.541
9.425	16.000	0.084	0.259
9.425	16.000	0.084	-0.141
9.425	16.000	0.084	0.059

9.425	15.000	0.113	-0.311
9.425	15.000	0.113	0.064

APPENDIX C

EES PROGRAM LISTING

```
"System Calculations"
"Revised 3-28-2005"

"Station 1:  Air Supply"
"Station 2: Heated Dry Air"
"Station 3: Mixed Air and Steam (Turbine Inlet)"
"Station 4: Turbine Outlet"
"Station 5: Exhaust to Atmosphere (After Separator)"
"Station 6: Throttled Mixture to RH Probe"
"Station 7: Steam Inlet (before F.O.)"
"Station 8: Compressor Inlet"
"Station 9: Compressor Outlet"

"Inputs Shown at Bottom"
procedure phaseselector(RH_in:RH_out,liqmult)
    if(RH_in<1.0) then
        RH_out=RH_in
        liqmult=0
    else
        RH_out=1.0
        liqmult=1
    ENDif
end

procedure focalc(H_orIFice, T_amb, T_fluid, P_fluid_psig, P_fluid_kPa, P_amb_psia,
K_correction : m_dot_fluid, T_fluid_calc)
    if(H_orifice=0) then
        m_dot_fluid=0
        C=0
    else
        "Geometric characteristics of flow orifice"
        D=0.822                                    "[in] pipe inside diameter"
        d_t=0.315                                  "[in] orifice diameter"
        Beta=d_t/D                                 "ratio of orifice diameter to inside pipe diameter"
        A_D=(pi*D^2/4)*convert(in2,m2)             "[m2] x-sectional area of pipe"
        A_d_t=(pi*d_t^2/4)*convert(in2,m2)         "[m2] area of orifice opening"

        "Ensure phase is superheat"
        "Set fluid temperature to (2 phase temp + 1°C) at measured pressure to ensure
        superheated steam in calculations"
        density_fluid_check=density(STEAM,T=T_fluid,P=P_fluid_kpa)
        if(density_fluid_check>100) then
            T_fluid_calc = temperature(STEAM,P=P_fluid_kPa,X=1) + 1
        else
            T_fluid_calc = T_fluid
        endif

        "Thermophysical properties of steam at station 7"
        density_fluid=density(STEAM,T=T_fluid_calc,P=P_fluid_kpa)
        kvisc_fluid=viscosity(STEAM,T=T_fluid_calc,P=P_fluid_kpa)/density_fluid          "[m2/s]"

        "Thermal Expansion Factor"
        alpha_P=7.2*10^(-6)                "[in/in/F] thermal expansion coefficient of SS pipe"
        alpha_PE=20.3*10^(-6)              "[in/in/F] thermal expansion coefficient of brass orifice"
        T_fluid_calc_F=T_fluid_calc*1.8+32          "[F]"
        T_amb_F = T_amb*1.8+32
```

```
        F_a=1+(2/(1-Beta^4))*(alpha_PE-Beta^4*alpha_P)*(T_fluid_calc_F-T_amb_F)
        "Thermal expansion factor"

        "Fluid Compressibility Factor"
        k=cp(STEAM,T=T_fluid_calc,P=P_fluid_kPa)/cv(STEAM,T=T_fluid_calc,P=P_fluid_kPa)
        "Specific heat ratio of the fluid"
        Y_1=1-(0.41+0.35*Beta^4)*(H_orifice/(27.73*k*(P_fluid_psig+P_amb_psia)))
        "Expansion factor based on upstream pressure"

        "Discharge Coefficient"
        i=0
        j=1
        dP_fluid=H_orifice*convert(inH2O,Pa)          "[Pa]"
        repeat
            i=i+1
            if(i=1) then
                Velocity_fluid[j]=5                   "[m/s]"
            else
                Velocity_fluid[j+1]=(Velocity_fluid[j-1]+9*Velocity_fluid[j])/10
            endif

            Re_D_fluid=(Velocity_fluid[j]*D*convert(in,m)/kvisc_fluid)
            "Reynold's number of fluid"
            lambda=1000/(Re_D_fluid)^0.5
            K_SB=(0.5991+0.0044/D+(0.3155+0.0175/D)*(Beta^4+2*Beta^16))+(0.00052/D-
0.000192+(0.01648-0.00116/D)*(Beta^4+4*Beta^16))*lambda
            C=K_SB*(1-Beta^4)^0.5                     "Empirical Discharge Coefficient"
            V_dot_fluid[j]=C*Y_1*F_a*A_d_t*((2*dP_fluid)/(density_fluid*(1-Beta^4)))^0.5
            "[m3/s]"
            j=j+1
            Velocity_fluid[j]=V_dot_fluid[j-1]/A_D                    "[m/s]"
            error=(Velocity_fluid[j]-Velocity_fluid[j-1])/Velocity_fluid[j]    "convergence criteria"
        until(abs(error)<0.001)
        m_dot_fluid=K_correction*V_dot_fluid[j-1]*density_fluid        "[kg/s]"
    ENDif
end

Procedure boilerpowerflow(H_orIFice, T_in, T_out, P_in, P_out : m_dot_power)
    if(H_orifice=0) then
        m_dot_power=0                                          "[kg/s]"
    else
        Q=207*48*3^0.5*10^(-3)                                 "[kW] 3 phase electric power
        delivered to boiler for 207V line to line and 48 A per leg"
        h_in_boiler=enthalpy(STEAM,T=T_in,P=P_in)              "enthalpy of water into boiler"
        h_out_boiler=enthalpy(STEAM,T=T_out,P=P_out)           "enthalpy of steam out of boiler"
        m_dot_power=Q/(h_out_boiler-h_in_boiler)               "energy equation for boiler,
        gives mass flow rate"
    ENDif
end

procedure
revturbentropy(w_out_2p,s_mix_out_2p,m_dot_liq_2p,S_dot_in,w_in,P_out,m_dot_air:S_dot_out,
m_dot_liq_out,s_mix_out,w_out_s)
    if(m_dot_liq_2p<0.0) then
        m_dot_liq_out=0.0
        w_out_s=w_in
```

```
        S_dot_out=S_dot_in
        s_mix_out=S_dot_out/m_dot_air
    else
        m_dot_liq_out=m_dot_liq_2p
        w_out_s=w_out_2p
        S_dot_out=S_dot_in
        s_mix_out=s_mix_out_2p
    ENDif
end

procedure
revturbwork(P_out,T_out_s,w_out_s,W_dot_turb_s_2p,H_out_s_2p,m_dot_liq_2p,eta_turbine_2p
,H_in,m_dot_air,W_dot_turb:W_dot_turb_s,H_out_s,eta_turbine_s)
    if(m_dot_liq_2p<0.0) then
        h_out_mix_s=enthalpy(AIRH2O,T=T_out_s,P=P_out,w=w_out_s)
        H_out_s=m_dot_air*h_out_mix_s                                    "[kW]"
        W_dot_turb_s=H_in-H_out_s
        eta_turbine_s=W_dot_turb/W_dot_turb_s
    else
        W_dot_turb_s=W_dot_turb_s_2p
        H_out_s=H_out_s_2p
        eta_turbine_s=eta_turbine_2p
    ENDif
end

"Pressure conversions to Absolute kPa"
P_atm_kpa = P_atm*convert(mmHg,kpa)                                  "[kpa]"
P_atm_psi = P_atm*convert(mmHg,psi)                                  "[psi]"
P_kpa[1] = P[1]*convert(psi,kpa)+P_atm_kpa                           "[kpa]"
P_kpa[3] = P[3]*convert(psi,kpa)+P_atm_kpa                           "[kpa]"
P_kpa[4] = dP[4]*convert(inH2O,kpa)+P_atm_kpa                        "[kpa]"
P_kpa[7] = P[7]*convert(psi,kpa)+P_atm_kpa                           "[kpa]"
P_kpa[9] = P[9]*convert(psi,kpa)+P_atm_kpa                           "[kpa]"
P_boiler_kpa = P_boiler*convert(psi,kpa)+P_atm_kpa                   "[kpa]"

"Station 1"
"Air Mass Flow (1 and 9)"
Density_std=density(AIR,T=20,P=101)
T_1_std=294.44                                                       "[K]"
P_1_std=46.7                                                         "[psia]"
P_1_abs=P[1]+P_atm_psi                                               "[psia]"
F_SCFM[1]=RM[1]*((P_1_abs*T_1_std)/(P_1_std*(T[1]+273.15)))^0.5      "mass flow"
Density_1=density(AIR,T=T[1],P=P_kpa[1])
F_cfm_1=(Density_std/Density_1)*F_SCFM[1]                            "[cfm] Vol Flow"
F_m3s_1=F_cfm_1*convert(cfm,m^3/s)                                   "[m3/s] Vol flow"
m_dot[1]=F_m3s_1*Density_1                                           "[kg/s]"

"Water vapor and dry air mass flow rates"
w_1=humrat(AIRH2O,T=T[1],P=P_atm_kpa,R=phi_1_throttled)              "humidity ratio of
throttled air at 1"
phi_1=relhum(AIRH2O,T=T[1],P=P_kPa[1], W=w_1)      "relative humidity of pressurized air at 1"
m_dot_vap_1=m_dot[1]/(1/w_1+1)                     "mass flow rate of water vapor at 1"
m_dot_da=m_dot[1]/(w_1+1)                          "mass flow rate of dry air at 1"

"Station 2"
m_dot_thermal[1]=0.887*Q_measured*4/(T[2]-T[1])
```

```
"Station 3"
"Theoretical T[3] Calculation"
"Vapor and Dry Air Flowrates for Station 3"
{phi_1_throttled=.11}
m_dot_vap_3=m_dot_steam+m_dot_vap_1        "mass flow rate of water vapor at station 3 due
to added steam"
w_3_orifice=m_dot_vap_3/m_dot_da           "humidity ration at 3 using orifice gauge steam
mass flow rate"

"Energy Balance for Mixing"
h_mixture=(m_dot[1]*h_2+m_dot_steam*h_7-Q_dot_23)/m_dot_da          "[kJ/kg_da]
Calculated enthalpy of mix"
h_2=enthalpy(AIRH2O,T=T[2],P=P_kpa[1],w=w_1)                       "[kJ/kg_da]
enthalpy of heated vapor at 2"
h_7=enthalpy(STEAM,T=T_7_calc,P=P_kPa[7])                          "[kJ/kg]
enthalpy of steam at 7, note constant enthalpy boiling into system"
T_theory_3=temperature(AIRH2O,h=h_mixture,P=P_kpa[3],w=w_3_orifice)  "[C] theoretical
temp at 3"
phi_3=relhum(AIRH2O,T=T[3],P=P_kpa[3],w=w_3_orifice)               "Calculated
fractional RH at 3"

"Station 4"
"Turbine Work"
w_3=w_3_orifice                            "the humidity ratio at 3 is defined, can
be switched to humidity ratio defined by wet bulb measurement"
RH_4=relhum(AIRH2O,P=P_kPa[4],T=T[4],W=w_3)   "fractional relative humidity at 4"
call phaseselector(RH_4:phi[4],liqmult)    "function 'phaseselector' determines the
phase at state 4 for the turbine work calculation"
                                           "'phaseselector' returns the relative
humidity at 4 and multiplier for the liquid mass at 4"

"energy"
W_dot_turbine=H_3-H_4                                  "[kW] turbine energy balance"
H_4=m_dot_da*h_4_mix+m_dot_liq_4*h_4_liq               "[kW] extensive enthalpy at 4"
H_3=m_dot_da*h_3_mix                                   "[kW] extensive enthalpy at 3"
h_4_mix=enthalpy(AIRH2O,T=T[4],P=P_kpa[4],w=w_4_mix)   "enthalpy of mixture at 4"
h_4_liq=enthalpy(STEAM,T=T[4],P=P_kpa[4])              "enthalpy of liquid at 4"
h_3_mix=enthalpy(AIRH2O,T=T[3],P=P_kpa[3],w=w_3)       "[kJ/kg_da] enthalpy of mixture
at 3"

"entropy"
S_dot_3=m_dot_da*s_3                                   "[kW/C] extensive entropy at 3"
s_3=entropy(AIRH2O,T=T[3],P=P_kPa[3],w=w_3)            "intensive entropy at 3"

"mass"
w_4_mix=humrat(AIRH2O,T=T[4],P=P_kpa[4],R=phi[4])      "humidity ratio at 4"
m_dot_liq_4=m_dot_da*(w_3-w_4_mix)*liqmult             "[kg/s] mass balance
determines mass flow rate of liquid at 4"
m_dot_water=m_dot_liq_4*convert(kg/s,g/min)            "[g/min]"

"Reversible Turbine"
"First assume 2 phase at station 4 (RH=100%) and calculate the isentropic turbine work with the
following equations"
"The phase is checked in function 'revturbentropy' after EES solves the 2 phase case"
"EES finds T_4_s by using the following 'entropy' and 'mass' groups of equations"
```

```
"entropy"
S_dot_4=S_dot_3                                          "[kW/K] extensive entropy at 4 is
equal to 3 in isentropic case"
S_dot_4=m_dot_da*s_mix_4_s+m_dot_liq_4_s*s_liq_4_s       "[kW/K] statement of extensive
entropy at 4"
s_liq_4_s=entropy(STEAM,T=T_4_s,x=0)                     "[kJ/(kg*K)] entropy of liquid at
4"
s_mix_4_s=entropy(AIRH2O,T=T_4_s,P=P_kPa[4],w=w_4_s)     "[kJ/(kg*K)] entropy of the
air/vapor mixture at 4(isentropic)"

"mass"
w_4_s=humrat(AIRH2O,T=T_4_s,P=P_kPa[4],R=1)              "[kgw/kga] humidity ratio at
4(isentropic)"
m_dot_liq_4_s=m_dot_da*(w_3-w_4_s)                       "[kg/s] mass flow rate of liquid
water at 4(isentropic)"
m_dot_7_correction = 0.98535698                          "Slope from Brent's OFM
Calibration"

"energy"
W_dot_turbine_s=H_3-H_4_s                                "[kW]"
H_4_s=m_dot_da*h_4_mix_s+m_dot_liq_4_s*h_4_liq_s         "[kW] extensive enthalpy at 4
(isentropic)"
h_4_mix_s=enthalpy(AIRH2O,T=T_4_s,P=P_kpa[4],w=w_4_s)    "[kJ/kg]  enthalpy of the
air/vapor mixture at 4(isentropic)"
h_4_liq_s=enthalpy(STEAM,T=T_4_s,x=0)                    "[kJ/kg] enthalpy of the liquid at
4(isentropic)"
eta_turbine_s=W_dot_turbine/W_dot_turbine_s              "dimensionless isentropic
turbine efficiency"

"Now test the phase, if single phase calculate s_mix_4_rev with function 'revturbentropy' then
implicitly calculate T_4_rev with result"
call
revturbentropy(w_4_s,s_mix_4_s,m_dot_liq_4_s,S_dot_3,w_3,P_kPa[4],m_dot_da:S_dot_4_rev,
m_dot_liq_4_rev,s_mix_4_rev,w_4_rev)
s_mix_4_rev=entropy(AIRH2O,T=T_4_rev,P=P_kPa[4],w=w_3)

"The function revturbwork outputs the reversible turbine work for either a 1 or 2 phase state at
station 4"
call
revturbwork(P_kPa[4],T_4_rev,w_4_rev,W_dot_turbine_s,H_4_s,m_dot_liq_4_s,eta_turbine_s,H
_3,m_dot_da,W_dot_turbine:W_dot_turbine_rev,H_4_rev,eta_turbine_rev)

R_P_turbine = P_kpa[3]/P_kpa[4]

"Station 6"
"Wet Bulb Thermometer"
T_db=T[6]                                                "dry bulb temp"
T_wb=T[6]-WBD_6                                          "wet bulb temp from measured wet bulb
depression"
w_6=humrat(AIRH2O,T=T_db,P=P_atm_kPa,B=T_wb)             "humidity ratio at 6"
w_3_wb=w_6                                               "statement of mass conservation,
between 3 and 6"
m_dot_wb_7=(w_3_wb-w_1)*m_dot_da                         "steam mass flow rate calculated using
difference in humidity ratios between 1 and 3"

"Station 7"
```

"Steam Mass Flow"
"Calls function 'focalc' to calculate the steam flow rate using orifice. Returns steam mass flow of 0 if dp[7] is 0"
call focalc(dP[7], T_atm, T[7], P[7], P_kpa[7], P_atm_psi, m_dot_7_correction : m_dot[7], T_7_calc)

"Mass and Energy Losses"
"These equations account for the loss of heat in the heated air line and the loss of condensate in the boiler steam trap"
m_dot_steam=m_dot[7]-m_dot_ST/60000 "[kg/s] Mass flow of steam after steam trap"
Q_dot_23=UA_23*LMTD "[kW] Heat lost to ambient"
LMTD=((T[3]-T_atm)-(T[2]-T_atm))/ln((T[3]-T_atm)/(T[2]-T_atm)) "[C] LMTD for HE with ambient air"
UA_23=0.001328 "[kW/C] experimental UA from 2 to 3"

"Theoretical Steam Mass Flow and Temperature"
Call boilerpowerflow(dP[7], T_boiler_in, T_7_calc, P_boiler_kPa, P_kPa[7] : m_dot_theoretical[7])

"Liquid Water Flowrate to Boiler"
V_dot_boiler_in=(3.9474*RM_boiler-43.5547)*convert(mL/min,m^3/s) "[m3/s] Volumetric flow of water from calibrated rotameter"
density_boiler_in=density(STEAM,T=T_boiler_in,P=P_boiler_kPa) "Density of water entering boiler"
m_dot_boiler_in=V_dot_boiler_in*density_boiler_in "Mass flow of water into boiler"

"Stations 8 and 9"
"Air mass flow rate"
T_9_std=298.00 "[K]"
P_9_std=14.7 "[psia]"
P_9_abs=P[9]+P_atm_psi "[psia]"
F_9_meas_scfm=0.7275*RM[9]+2.3896
F_SCFM[9]=F_9_meas_scfm*((P_9_abs*T_9_std)/(P_9_std*(T[9]+273.15)))^0.5 "mass flow"
Density_9=density(AIR,T=T[9],P=P_kpa[9])
F_cfm_9=(Density_std/Density_9)*F_SCFM[9] "[cfm] vol flow"
F_m3s_9=F_cfm_9*convert(cfm,m^3/s) "[m3/s] vol flow"
m_dot[9]=F_m3s_9*Density_9 "[kg/s]"

"Compressor Work"
h[8]=enthalpy(AIR,T=T[8]) "enthalpy of air (ideal) at 8"
h[9]=enthalpy(AIR,T=T[9]) "enthalpy of air (ideal) at 9"

W_dot_compressor=m_dot[9]*(h[9]-h[8]) "[kW] compressor work"
s[8]=entropy(AIR,T=T[8],P=P_atm_kpa) "entropy at 8"
T_s[9]=temperature(AIR,s=s[8],P=P_kpa[9]) "isentropic temperature at 9"
h_s[9]=enthalpy(AIR,T=T_s[9]) "isentropic enthalpy at 9"
W_dot_compressor_s=m_dot[9]*(h_s[9]-h[8]) "[kW] isentropic compressor work"
Eta_compressor_s=W_dot_compressor_s/W_dot_compressor "isentropic compressor efficiency"

r_p_compressor=p_kpa[9]/P_atm_kpa

"Bearing Work"
UA_oil=10.41 "[W/C] UA of oil reservoir is found experimentally"
W_dot_bearing=(UA_oil*(T_oil-T_atm)-W_dot_pump)/1000 "[kW] work bearing dissipates in oil reservoir"

"Turbocharger System Energy Balance"
Error_work = ((W_dot_turbine - W_dot_bearing - W_dot_compressor) / W_dot_Turbine) * 100
W_dot_balance = W_dot_bearing + W_dot_compressor

"Dummy Variables"
{phi_atm=.45}
T_3_compare=T[3]
P_3_compare=P[3]

"Separation Efficiency"
eta_sep=m_dot_sep/m_dot_water

"wet-bulb accuracy"
dif_OFM_WB=100*(abs(m_dot_steam-m_dot_wb_7))/m_dot_steam

"Inputs"
{T[1]=20.88
T[2]=69.19735
T[3]=80.37699
T[4]=56.06228
T[5]=53.09703
T[6]=68.45977
T[7]=158.8595
T[8]=23.74613
T[9]=93.79233
WBD_6=11.0596
T_boiler_in=25.16521
T_atm=23.4
T_oil=75.37743

P[1]=42
RM[1]=70
P[3]=24.75
dP[4]=31.0
P[7]=77.25
P[9]=9.5
RM[9]=85
P_boiler=78
dP[7]=26.13148
P_atm=738
Q_measured=0.590
phi_1_throttled=0.06330306
W_dot_pump=282
RM_boiler=114
m_dot_sep =34.03
m_dot_ST=5.55}

APPENDIX D

CHARTS TO AID IN REACHING STEADY STATE

D.1 AIR FLOW RATE VS. HEATER POWER AT VARYING EXIT TEMPERATURES

45 °C Air			
RM	F_SCFM	Q input kW	(Q / 4) * Corr. F. kW
6	64.964	0.222	**0.250**
6.25	67.671	0.231	**0.261**
6.5	70.377	0.240	**0.271**
6.75	73.084	0.250	**0.282**
7	75.791	0.259	**0.292**
7.25	78.498	0.268	**0.303**
7.5	81.205	0.277	**0.313**
7.75	83.911	0.287	**0.324**
8	86.618	0.296	**0.334**

50 °C Air			
RM	F_SCFM	Q input kW	(Q / 4) * Corr. F. kW
6	64.964	0.268	**0.303**
6.25	67.671	0.279	**0.315**
6.5	70.377	0.290	**0.328**
6.75	73.084	0.302	**0.341**
7	75.791	0.313	**0.353**
7.25	78.498	0.324	**0.366**
7.5	81.205	0.335	**0.378**
7.75	83.911	0.346	**0.391**
8	86.618	0.357	**0.404**

55 °C Air			
RM	F_SCFM	Q input kW	(Q / 4) * Corr. F. kW
6	64.964	0.314	**0.355**
6.25	67.671	0.327	**0.370**
6.5	70.377	0.340	**0.384**
6.75	73.084	0.354	**0.399**
7	75.791	0.367	**0.414**
7.25	78.498	0.380	**0.429**
7.5	81.205	0.393	**0.444**
7.75	83.911	0.406	**0.458**
8	86.618	0.419	**0.473**

60 °C Air			
RM	F_SCFM	Q input kW	(Q / 4) * Corr. F. kW
6	64.964	0.360	**0.407**
6.25	67.671	0.375	**0.424**
6.5	70.377	0.391	**0.441**
6.75	73.084	0.406	**0.458**
7	75.791	0.421	**0.475**
7.25	78.498	0.436	**0.492**
7.5	81.205	0.451	**0.509**
7.75	83.911	0.466	**0.526**
8	86.618	0.481	**0.543**

65 °C Air			
RM	F_SCFM	Q input kW	(Q / 4) * Corr. F. kW
6	64.964	0.407	**0.459**
6.25	67.671	0.424	**0.478**
6.5	70.377	0.441	**0.497**
6.75	73.084	0.458	**0.517**
7	75.791	0.474	**0.536**
7.25	78.498	0.491	**0.555**
7.5	81.205	0.508	**0.574**
7.75	83.911	0.525	**0.593**
8	86.618	0.542	**0.612**

70 °C Air			
RM	F_SCFM	Q input kW	(Q / 4) * Corr. F. kW
6	64.964	0.453	**0.511**
6.25	67.671	0.472	**0.533**
6.5	70.377	0.491	**0.554**
6.75	73.084	0.510	**0.575**
7	75.791	0.528	**0.597**
7.25	78.498	0.547	**0.618**
7.5	81.205	0.566	**0.639**
7.75	83.911	0.585	**0.661**
8	86.618	0.604	**0.682**

75 °C Air			
RM	F_SCFM	Q input kW	(Q / 4) * Corr. F. kW
6	64.964	0.499	**0.564**
6.25	67.671	0.520	**0.587**
6.5	70.377	0.541	**0.611**
6.75	73.084	0.562	**0.634**
7	75.791	0.582	**0.658**
7.25	78.498	0.603	**0.681**
7.5	81.205	0.624	**0.704**
7.75	83.911	0.645	**0.728**
8	86.618	0.665	**0.751**

80 °C Air			
RM	F_SCFM	Q input kW	(Q / 4) * Corr. F. kW
6	64.964	0.545	**0.616**
6.25	67.671	0.568	**0.641**
6.5	70.377	0.591	**0.667**
6.75	73.084	0.613	**0.693**
7	75.791	0.636	**0.718**
7.25	78.498	0.659	**0.744**
7.5	81.205	0.682	**0.770**
7.75	83.911	0.704	**0.795**
8	86.618	0.727	**0.821**

85 °C Air			
RM	F_SCFM	Q input kW	(Q / 4) * Corr. F. kW
6	64.964	0.592	**0.668**
6.25	67.671	0.616	**0.696**
6.5	70.377	0.641	**0.724**
6.75	73.084	0.665	**0.751**
7	75.791	0.690	**0.779**
7.25	78.498	0.715	**0.807**
7.5	81.205	0.739	**0.835**
7.75	83.911	0.764	**0.863**
8	86.618	0.789	**0.891**

These charts were created to aid in reaching steady state conditions using the autotransformer for control of the power to the air heater. The conditions used to help create these charts are shown on the following page.

Standards		
	English	Metric
T_Std		294.4 K
P_Std	46.7 psig	321.99 kPa
P_Atm	14.7 psia	101.35 kPa
P1	40.00 psia	
P1_Abs	54.70 psia	377.14 kPa
C_p @ 300 K		1.005 kJ/(Kg*K)
Density @ 20° C, P_Atm		1.20 kg/m^3
Density @ 1		4.47 kg/m^3

Q_Actual	0.6 kW
RM_Actual	7
T_in	21 °C
T_out	68 °C
P_in	40 psi
P_in_Abs	54.7 psi
P_in_Abs	377.14 kPa
m_dot_1	0.04325 kg/s
m_dot_thermal_1	0.04883 kg/s
Correction Factor	1.129 %

D.2 BOILER INLET ROTAMETER VS. ORIFICE FLOW METER

RM-B	DP_7	Water Flow	Water Flow	C
mm	in. H2O	m^3/s	m/s	d'less
97	**19.36**	0.001703	4.9742	0.6166
98	**19.82**	0.001723	5.0320	0.6166
99	**20.28**	0.001743	5.0899	0.6166
100	**20.74**	0.001763	5.1477	0.6165
101	**21.21**	0.001782	5.2056	0.6165
102	**21.69**	0.001802	5.2634	0.6165
103	**22.17**	0.001822	5.3213	0.6165
104	**22.66**	0.001842	5.3791	0.6164
105	**23.15**	0.001862	5.4370	0.6164
106	**23.65**	0.001881	5.4949	0.6164
107	**24.15**	0.001901	5.5527	0.6164
108	**24.66**	0.001921	5.6106	0.6163
109	**25.17**	0.001941	5.6684	0.6163
110	**25.69**	0.001961	5.7263	0.6163
111	**26.21**	0.001980	5.7841	0.6163
112	**26.74**	0.002000	5.8420	0.6162
113	**27.28**	0.002020	5.8998	0.6162
114	**27.82**	0.002040	5.9577	0.6162
115	**28.36**	0.002060	6.0156	0.6162
116	**28.91**	0.002080	6.0734	0.6162
117	**29.47**	0.002099	6.1313	0.6161
118	**30.03**	0.002119	6.1891	0.6161
119	**30.59**	0.002139	6.2470	0.6161
120	**31.16**	0.002159	6.3048	0.6161

This chart was created to determine what rotameter values correlate to what orifice flow plate values. The values presented here are not absolute, as they rely on temperature and pressure information and are subject to slight changes. The system was usually run with a RM-B reading of 115 and a DP_7 of 26.

Given Temperatures & Pressures					
T_fluid	T[7]	158.892	℃	318.00578	° F
T_fluid_IN	T[11]	25.7281	℃		
T_amb	T_atm	22.2	℃	71.96	° F
P_fluid_IN	P_fluid_psig	234.422	kPa	34	psi
P_atm_psi	P_amb_psia	738	mmHg	14.27	psia
P[7]	P_fluid_psig			77.25	psig
P_kPa[7]	P_fluid_kPa	631.01	kPa	91.52	psia
dP[7]	H_orIFice			26.19973	in.H2O

Orifice Parameters		
D	0.822	in.
D	0.0208788	m
d_t	0.315	in.
Beta	0.383211679	d'less
A_D	0.000342395	m^2
A_d_t	5.02811E-05	m^2

Thermal Expansion Factor		
alpha_P	0.0000072	in./in./F
alpha_PE	0.0000203	in./in./F
F_a	1.010131541	

Steam Properties		
Density Inlet	996.9	kg/m^3
density_fluid	3.313	kg/m^3
kvisc_fluid	0.000004348	m^2/s
k = (cp)/(cv)	1.384	d'less
Y_1	0.996885427	d'less

	Coefficients
Intercept	-43.55
X Variable 1	3.95

IN	Within Procedure
dP[7]	H_orIFice
T_atm	T_amb
T[7]	T_fluid
P[7]	P_fluid_psig
P_atm_psi	P_amb_psia
P_kPa[7]	P_fluid_kPa
m_dot[7]	m_dot_fluid
C	C

To Use This Sheet:

1. Start the system and get it running at an DP_7 around 26" H2O
2. Enter the proper ambient conditions and orifice flow once near steady state
3. Create a new EES file and enter the routine below
4. Take the EES values and paste them into the Properties Section
5. Make fine adjustment to the rotameter valve to put the system into balance

EES Routine:

```
T_fluid_1 =          158.8921
P_fluid_kpa =          631.01
T_fluid_calc = TEMPERATURE(Steam,P=P_fluid_kPa,X=1) + 1

T_fluid_IN =  25.73
P_fluid_IN =  234.42

density_fluid=density(WATER,T=T_fluid_IN,P=P_fluid_IN)
density_Steam=density(STEAM,T=T_fluid_calc,P=P_fluid_kpa)
kvisc_Steam=viscosity(STEAM,T=T_fluid_calc,P=P_fluid_kpa)/density_steam
k=cp(STEAM,T=T_fluid_calc,P=P_fluid_kPa)/cv(STEAM,T=T_fluid_calc,P=P_fluid_kPa)
```

APPENDIX E

DATA COLLECTION SHEET

Program Version								
Date:							Ambient Conditions	Patm: Tatm:
Item		Desired	Units	1	2	3	4	5
T1 T2	Comp. Air Inlet Heated Air	21 70	°C °C					
T3 T4	Air & Steam Mix Post Turbine	80 55	°C °C					
T5 T6	Post Separator Valve Exit	51 70	°C °C					
T7 T8	Boiler Exit Compressor Inlet	160 25	°C °C					
T9 WBD	Compressor Exit At 6	95 11	°C Vdc					
T11 T12	Boiler Inlet Oil	24 77	°C °C					
T13 T14	Cool Water In Cool Water Out	6 10	°C °C					
T15 %RH	Turbine Exit Temp In Comp. Air	56 6	°C %					
dP7 - in. H20 Boiler in Rot.	Orifice Flow Boiler Inlet	27 115	in. H20					
Boiler P. P7	 Steam out P	77 76.5	psi psi					
P1 Air In Rot.	Air In P RM-1	42 7	psi					
Comp. Rot. P9	RM-9 Comp. Air P	85 9.5	 psi					
Oil P Cool Water Rot.		15	psi gpm					
dP5 P3	dP Element Air & Steam Mix	4 25	in. H20 psi					
dP4 Pump Wattmeter	Turb. Exit P	63 283	mm Hg Watts					
Air Heater Power RPM	 Turbine	0.6 2.669	KW RPM					
Separated Water Separated Water 2	Raw Raw		grams grams					
Time	Raw		min:sec					
Steam Drip			Start Time:		Finish Time:		Weight (g):	
NOTES:								

APPENDIX F

EXPERIMENTAL DATA

		Run #	P1 Air in P psi	P3 Air & Steam Mix psi	P7 Steam out P psi	P9 Comp. Air P psi	P_Boiler psi	P_atm mmHg	dP4 Turb. Exit P in. H20	dP7 Orifice Flow in. H20	%RH *100%	RH_ATM Unmeasured *100%	Air In Rot. RM-1
Day 15	0 GPM	136	41	24.75	77	9.3	77.75	727	33.18	26.51	0.133	0.45	70
w/ Commercial Separator		137	41	24.75	77	9.2	77.75	727	33.18	26.32	0.125	0.45	70
Only Axial Moisture		138	41	24.75	77	9.3	78	727	32.65	26.38	0.131	0.45	70
		139	41	24.75	77.5	9.3	78.5	727	33.18	26.57	0.131	0.45	70
		140	41	24.75	78	9.3	78.75	727	33.18	26.56	0.129	0.45	70
		141	41	24.75	78	9.3	79	727	32.65	26.69	0.125	0.45	70
		142	41	24.75	78.5	9.3	79.25	727	32.65	26.79	0.131	0.45	70
		143	41	24.75	78.5	9.3	79.25	727	32.65	26.87	0.124	0.45	70
		144	41	24.75	78.5	9.3	79	727	33.18	26.64	0.126	0.45	70
		145	41	24.75	78	9.3	78.75	727	33.18	26.79	0.122	0.45	70
Day 15 v.2	0 GPM	136.2	41	24.75	77	9.3	77.75	727	33.18	26.51	0.133	0.45	70
w/ Commercial Separator		137.2	41	24.75	77	9.2	77.75	727	33.18	26.32	0.125	0.45	70
Axial and Commercial Moisture		138.2	41	24.75	77	9.3	78	727	32.65	26.38	0.131	0.45	70
		139.2	41	24.75	77.5	9.3	78.5	727	33.18	26.57	0.131	0.45	70
		140.2	41	24.75	78	9.3	78.75	727	33.18	26.56	0.129	0.45	70
		141.2	41	24.75	78	9.3	79	727	32.65	26.69	0.125	0.45	70
		142.2	41	24.75	78.5	9.3	79.25	727	32.65	26.79	0.131	0.45	70
		143.2	41	24.75	78.5	9.3	79.25	727	32.65	26.87	0.124	0.45	70
		144.2	41	24.75	78.5	9.3	79	727	33.18	26.64	0.126	0.45	70
		145.2	41	24.75	78	9.3	78.75	727	33.18	26.79	0.122	0.45	70
Day 16	0 GPM	146	42	25	79	9.7	79.5	738	31.58	27.00	0.070	0.45	70
Axial Separator		147	42	24.75	77.5	9.6	78.25	738	31.58	26.82	0.069	0.45	70
		148	42	24.75	76.75	9.5	77.5	738	31.04	26.14	0.068	0.45	70
		149	42	24.75	77	9.5	77.75	738	31.04	25.86	0.067	0.45	70
		150	42	24.75	77.5	9.5	78.5	738	31.04	26.25	0.066	0.45	70
	0.5 GPM	151	42	24.75	77.25	9.6	78	738	31.04	26.20	0.067	0.45	70
		152	42	24.75	77	9.5	78	738	31.04	26.22	0.067	0.45	70
		153	42	24.75	77	9.5	78	738	31.04	26.26	0.067	0.45	70
		154	42	24.75	77	9.5	78	738	31.04	26.22	0.066	0.45	70
		155	42	24.75	77	9.5	78	738	31.04	26.37	0.066	0.45	70
	0.75 GPM	156	42	24.75	77.25	9.5	78	738	31.04	26.13	0.063	0.45	70
		157	42	24.75	77.25	9.5	78.25	738	31.04	25.98	0.064	0.45	70
		158	42	25	77.25	9.6	78.25	738	31.04	25.96	0.063	0.45	70
		159	41.75	24.75	77.25	9.6	78	738	31.04	25.93	0.064	0.45	70
		160	41.75	25	77	9.6	78	738	31.04	26.08	0.065	0.45	70
	1 GPM	161	41.5	25	76.75	9.5	77.5	737.5	31.04	26.04	0.064	0.45	70
		162	41.5	25	77.25	9.6	78	737.5	31.04	25.72	0.063	0.45	70
		163	41.5	25	77.5	9.6	78.5	737.5	31.04	25.99	0.064	0.45	70
		164	41.5	25	77.5	9.6	78.5	737.5	31.04	26.10	0.064	0.45	70
		165	41.5	25	77.75	9.6	78.5	737.5	31.04	26.18	0.064	0.45	70
	2 GPM	166	41.5	25	77	9.6	78	737.5	31.04	26.41	0.064	0.45	70
		167	41.5	25	77	9.6	78	737.5	31.04	26.34	0.064	0.45	70
		168	41.5	25	77.25	9.6	78	737.5	31.04	25.68	0.062	0.45	70
		169	41.5	25	77.5	9.6	78.5	737.5	31.04	26.53	0.063	0.45	70
		170	41.5	25	77.25	9.6	78	737.5	31.04	26.41	0.063	0.45	70
	3 GPM	171	41.5	25	77.25	9.6	78	737.5	31.04	26.51	0.063	0.45	70
		172	41.5	25	77.5	9.6	78.5	737.5	31.04	26.42	0.063	0.45	70
		173	41.5	25	77.75	9.6	78.5	737.5	31.04	26.35	0.063	0.45	70
		174	41.5	25	77.75	9.6	78.5	737.5	31.04	26.39	0.064	0.45	70
		175	41.5	25	77.75	9.6	78.75	737.5	31.04	26.31	0.063	0.45	70

Comp. Rot. RM-9	RM Boiler Boiler Inlet	Drip M_dot g/min	Air Heater Power KW	Pump Wattmeter Watts	T12 Oil °C	T_stm °C	T1 Comp. Air Inlet °C	T2 Heated Air °C	T3 Air & Steam Mix °C	T4 - AVG °C	T5 Post Separator °C	T6 Valve Exit °C	T7 Boiler Exit °C
85	116	5.67	0.59	286	74.30	23.2	21.07	70.18	80.85	56.63	55.22	70.18	158.72
85	116	5.67	0.59	285	74.34	23.2	20.98	70.14	80.76	56.57	55.16	69.98	158.67
85	115	5.67	0.595	287	74.37	23.2	21.01	70.31	80.76	56.65	55.35	70.25	158.80
85	114	5.67	0.595	286	74.43	23.2	21.06	70.36	80.84	56.77	55.32	70.97	158.96
85	114	5.67	0.6	287	74.58	23.2	21.05	70.62	81.72	56.66	55.36	71.12	159.07
85	114	5.67	0.6	287	74.64	23.2	21.05	70.63	81.63	56.65	55.40	69.55	159.23
85	115	5.67	0.6	287	74.57	23.2	21.05	70.78	82.07	56.95	55.48	70.47	159.26
85	114	5.67	0.6	287	74.62	23.2	20.98	70.68	82.14	56.95	55.46	69.91	159.26
85	115	5.67	0.6	287	74.63	23.2	21.09	70.79	82.24	57.04	55.56	71.50	159.29
85	116	5.67	0.6	288	74.72	23.2	21.10	70.86	82.23	56.89	55.44	69.71	159.11
85	116	5.67	0.59	286	74.30	23.2	21.07	70.18	80.85	56.63	55.22	70.18	158.72
85	116	5.67	0.59	285	74.34	23.2	20.98	70.14	80.76	56.57	55.16	68.98	158.67
85	115	5.67	0.595	287	74.37	23.2	21.01	70.31	80.76	56.65	55.35	70.25	158.80
85	114	5.67	0.595	286	74.43	23.2	21.06	70.36	80.84	56.77	55.32	70.97	158.96
85	114	5.67	0.6	287	74.58	23.2	21.05	70.62	81.72	56.66	55.36	71.12	159.07
85	114	5.67	0.6	287	74.64	23.2	21.05	70.63	81.63	56.65	55.40	69.55	159.23
85	115	5.67	0.6	287	74.57	23.2	21.05	70.78	82.07	56.95	55.48	70.47	159.26
85	114	5.67	0.6	287	74.62	23.2	20.98	70.68	82.14	56.95	55.46	69.91	159.26
85	115	5.67	0.6	287	74.63	23.2	21.09	70.79	82.24	57.04	55.56	71.50	159.29
85	116	5.67	0.6	288	74.72	23.2	21.10	70.86	82.23	56.89	55.44	69.71	159.11
85	115	6.11	0.6	291	74.63	22.2	20.72	69.70	80.89	56.63	55.32	69.27	158.62
85	115	6.13	0.595	287	74.76	22.2	20.66	69.04	80.48	56.53	55.21	69.89	159.19
85	116	6.16	0.59	287	74.76	22.2	20.74	68.92	80.24	56.32	54.98	68.42	158.67
85	114	6.18	0.595	285	74.68	22.2	20.79	69.09	80.28	56.40	55.06	69.57	158.75
85	115	6.21	0.59	285	74.68	22.2	20.70	69.10	80.48	56.54	55.20	69.75	159.07
85	113	5.55	0.59	284	74.91	22.2	20.78	68.80	80.32	56.14	53.73	69.76	158.89
85	115	5.55	0.59	284	75.08	22.2	20.84	68.95	80.32	56.13	53.64	69.73	158.79
85	115	5.55	0.59	283	75.07	22.2	20.75	69.01	80.34	56.12	53.68	69.15	158.86
85	114	5.55	0.59	283	75.07	22.2	20.78	68.97	80.27	56.09	53.72	68.44	158.85
85	115	5.55	0.59	282	75.10	22.2	20.81	68.89	80.23	56.04	53.73	69.82	158.77
85	114	5.55	0.59	282	75.38	23.4	20.88	69.20	80.38	56.06	53.10	68.46	158.86
85	114	5.55	0.59	282	75.50	23.4	20.84	68.15	80.32	56.06	53.11	69.73	158.97
85	114	5.55	0.59	282	75.47	23.4	20.85	68.14	80.31	56.05	52.99	69.59	159.03
85	114	5.55	0.59	280	75.56	23.4	20.87	69.00	80.38	56.02	52.92	69.91	158.98
85	116	5.55	0.595	281	75.66	23.4	20.89	69.05	80.17	55.97	52.98	69.30	158.84
85	115	5.55	0.595	281	75.74	24.1	20.94	68.83	80.17	55.71	52.37	69.10	158.69
85	114	5.55	0.595	283	74.73	24.1	20.87	68.83	80.20	55.62	52.44	69.51	158.86
85	114	5.55	0.595	283	75.79	24.1	20.91	69.08	80.32	55.89	52.60	69.57	159.00
85	114	5.55	0.595	283	75.86	24.1	20.87	69.06	80.33	55.94	53.65	70.14	159.02
85	114	5.55	0.595	282	75.95	24.1	20.92	69.21	80.42	56.01	52.69	69.09	159.10
85	116	5.55	0.595	282	76.03	24.1	20.98	69.32	80.29	55.83	51.71	70.23	158.79
85	117	5.55	0.595	282	76.10	24.1	21.01	69.34	80.28	55.80	51.73	69.01	158.78
85	115	5.55	0.595	283	75.94	24.1	20.99	69.00	80.31	55.66	51.70	70.18	158.95
85	114	5.55	0.595	281	75.84	24.1	20.99	69.05	80.38	55.66	51.78	70.89	159.00
85	116	5.55	0.595	282	75.84	24.1	20.91	69.18	80.22	55.84	51.75	65.12	158.82
85	115	5.57	0.595	281	76.14	24.3	21.02	69.23	80.37	55.81	51.29	69.68	158.85
85	114	5.57	0.595	281	76.21	24.3	21.09	69.36	80.48	55.96	51.53	70.88	159.01
85	114	5.57	0.595	280	76.25	24.3	21.08	69.35	80.50	55.99	51.52	70.57	159.06
85	114	5.57	0.595	281	76.23	24.3	21.08	69.31	80.50	56.00	51.54	70.13	159.11
85	114	5.57	0.595	280	76.34	24.3	21.08	69.33	80.47	55.99	51.63	70.29	159.13

T9 Compressor Exit °C	WED Station 8 Vdc	T11 Boiler Inlet °C	Separated Water Net g/min
94.54	11.48	25.31	14.69
95.15	11.21	25.12	14.88
94.95	10.94	24.98	14.50
95.53	13.91	25.01	14.49
95.04	13.91	24.84	14.85
94.80	12.25	24.79	15.08
95.62	12.77	24.82	14.89
95.51	11.52	24.58	14.85
95.47	12.47	24.51	14.30
95.20	11.59	24.25	15.07
94.54	11.48	25.31	23.19
95.15	11.21	25.12	23.18
94.95	10.94	24.98	23.01
95.53	13.91	25.01	22.99
95.04	13.91	24.84	23.53
94.80	12.25	24.79	23.59
95.62	12.77	24.82	23.39
95.51	11.52	24.58	23.72
95.47	12.47	24.51	22.80
95.20	11.59	24.25	23.76
93.12	10.81	26.23	14.82
93.10	11.87	25.89	13.72
93.55	10.84	25.81	14.88
93.08	10.55	25.57	14.10
93.27	10.74	25.70	14.88
92.79	12.10	25.73	28.98
93.08	11.31	25.88	29.19
93.44	11.54	25.83	29.13
93.64	10.93	25.81	29.02
93.32	11.63	25.53	28.59
93.78	11.06	25.17	34.03
94.25	10.89	25.00	34.20
94.14	11.98	24.87	33.69
94.58	12.33	24.81	33.81
94.55	11.15	24.57	33.32
94.73	9.41	24.36	35.97
94.71	10.89	24.46	35.87
95.24	11.93	24.46	35.57
95.02	12.34	24.52	35.78
95.39	11.51	24.45	35.20
94.86	11.95	24.16	39.82
95.32	10.98	24.20	39.82
95.06	12.42	24.09	40.02
94.95	11.70	24.31	40.00
95.13	10.19	24.14	39.83
95.34	12.22	24.24	42.34
95.64	10.96	24.33	42.12
95.68	12.87	24.35	42.37
95.89	12.23	24.34	42.10
95.71	12.42	24.41	41.96

		Run #	P1 Air in P psi	P3 Air & Steam Mix psi	P7 Steam out P psi	P9 Comp. Air P psi	P. Boiler psi	P_atm mmHg	dP4 Turb. Exit P in. H2O	dP7 Orifice Flow in. H20	%RH *100%	RH, ATM Unmeasured *100%	Air In Rot. RM-1
Day 13	0 GPM	94	41.5	25	76.5	9.5	77	739.5	33.72	25.82	0.062	0.45	70
Flow Straightener Data		95	41.5	25	76.25	9.5	77	739.5	33.72	25.91	0.061	0.45	70
		96	41.5	25	76.5	9.5	77	739.5	33.72	25.94	0.061	0.45	70
		97	41.5	25	76.75	9.5	77.25	739.5	33.72	26.26	0.064	0.45	70
		98	41.5	25	77	9.5	77.5	739.5	33.72	26.71	0.063	0.45	70
		99	41.5	25	77	9.5	77.75	739.5	33.72	27.13	0.063	0.45	70
		100	41.5	25	77	9.5	77.75	739.5	33.72	27.24	0.063	0.45	70
		101	41.5	25.25	77	9.5	78	739.5	33.72	26.72	0.062	0.45	70
		102	41.5	25.25	77.25	9.5	78	739.5	33.72	26.80	0.062	0.45	70
		103	41.5	25.25	77.25	9.5	78	739.5	33.72	27.50	0.060	0.45	70
	1 GPM	104	41.5	25.25	77.25	9.5	78	739.5	33.72	27.32	0.059	0.45	70
		105	41.5	25.25	77.28	9.5	78	739.5	33.72	27.22	0.058	0.45	70
		106	41.5	25.25	77.25	9.5	78	739.5	33.72	27.34	0.058	0.45	70
		107	41.5	25.25	77.5	9.5	78.25	739.5	33.72	27.34	0.058	0.45	70
		108	41.5	25.25	77.5	9.5	78.25	739.5	33.72	27.38	0.059	0.45	70
		109	41.5	25.25	77.75	9.5	78.5	739.5	33.72	27.52	0.058	0.45	70
		110	41.5	25.25	77.75	9.5	78.5	739.5	33.72	27.58	0.059	0.45	70
	2 GPM	111	41.5	25.25	78	9.5	78.75	739.5	33.72	27.35	0.059	0.45	70
		112	41.5	25.25	78	9.5	78.75	739.5	33.72	27.50	0.059	0.45	70
		113	41.5	25.25	78	9.5	78.75	739.5	33.72	27.46	0.060	0.45	70
		114	41.5	25.25	77.75	9.5	78.5	739.5	33.72	27.34	0.058	0.45	70
		115	41.5	25.25	77	9.5	78	739.5	33.72	27.17	0.058	0.45	70
	3 GPM	116	41.5	25.25	77	9.5	78	739.5	33.72	27.23	0.058	0.45	70
		117	41.5	25.25	77.75	9.5	78.75	739.5	33.72	27.36	0.057	0.45	70
		118	41.5	25.25	78	9.6	79	739.5	33.72	27.52	0.058	0.45	70
		119	41.5	25.25	78.5	9.6	79	739.5	33.72	27.61	0.058	0.45	70
		120	41.5	25.25	78.5	9.6	79.5	739.5	33.72	27.72	0.058	0.45	70
Day 14	0 GPM	121	42	25.5	77.25	9.6	78	741	34.26	27.27	0.065	0.45	70
Flow Straightener Data		122	42	25.5	77.25	9.6	78	741	33.72	27.24	0.071	0.45	70
		123	42	25.75	78	9.6	78.5	741	34.26	27.67	0.069	0.45	70
		124	42	25.75	78	9.6	78.5	741	34.26	27.61	0.069	0.45	70
		125	42	25.5	77.5	9.6	78.25	741	33.72	27.49	0.068	0.45	70
	0.5 GPM	126	42	25.5	76.75	9.6	77.5	741	33.72	27.22	0.064	0.45	70
		127	42	25.5	76.75	9.6	77.5	741	33.72	27.13	0.064	0.45	70
		128	42	25.5	77.25	9.6	78.25	741	33.72	27.31	0.063	0.45	70
		129	42	25.5	77.75	9.6	78.5	741	33.72	27.50	0.062	0.45	70
		130	41.75	25.5	78	9.6	78.5	741	33.72	27.53	0.063	0.45	70
	0.75 GPM	131	42	25.5	78.25	9.6	78.75	740	33.72	27.65	0.063	0.45	70
		132	42	25.75	78	9.6	79	740	33.72	27.61	0.061	0.45	70
		133	41.75	25.75	77.75	9.6	78.5	740	34.26	27.46	0.061	0.45	70
		134	41.75	25.75	77.75	9.6	78.5	740	34.26	27.49	0.061	0.45	70
		135	41.75	25.75	78	9.7	78.75	740	34.26	27.49	0.062	0.45	70

Comp. Rot. RM-9	RM Boiler Boiler Inlet	Drip M_dot g/min	Air Heater Power KW	Pump Wattmeter Watts	T12 Oil °C	T_atm °C	T1 Comp. Air Inlet °C	T2 Heated Air °C	T3 Air & Steam Mix °C	T4 - AVG °C	T5 Post Separator °C	T6 Valve Exit °C	T7 Boiler Exit °C
85	117	6.07	0.59	284	74.78	24	21.50	69.27	80.33	56.31	54.82	69.39	158.73
85	116	6.07	0.59	283	74.85	24	21.52	69.27	80.21	56.22	54.55	69.62	158.55
85	115	6.07	0.59	283	74.98	24	21.54	69.28	80.22	56.27	54.47	68.86	158.61
85	114	6.07	0.59	282	75.04	24	21.41	69.27	80.40	56.36	54.73	68.34	158.72
85	113	6.07	0.59	281	75.09	24	21.44	69.27	80.37	56.41	54.73	69.46	158.81
85	113	6.07	0.59	280	75.14	24	21.42	69.29	80.39	56.43	54.77	69.28	158.85
85	113	6.07	0.59	280	75.10	24	21.42	69.28	80.46	56.42	54.67	69.63	158.83
85	113	6.07	0.59	279	75.14	24	21.32	69.26	80.42	56.42	54.88	69.67	158.87
85	113	6.07	0.59	281	75.14	24	21.35	69.19	80.46	56.39	54.62	69.83	158.97
85	113	6.07	0.59	280	75.23	24	21.34	69.19	80.50	56.46	54.72	68.81	158.92
85	113	5.82	0.59	280	75.20	24.6	21.26	69.10	80.42	56.25	52.40	69.20	158.90
85	113	5.82	0.59	280	75.21	24.6	21.29	69.33	80.52	56.32	52.62	69.75	159.00
85	113	5.82	0.59	280	75.30	24.6	21.33	69.40	80.57	56.36	52.72	69.88	158.98
85	113	5.82	0.595	280	75.39	24.6	21.32	69.38	80.47	56.32	52.64	69.94	159.01
85	113	5.82	0.595	281	75.50	24.6	21.38	69.45	80.59	56.35	52.78	69.61	159.00
85	113	5.82	0.595	281	75.51	24.6	21.40	69.68	80.65	56.48	52.95	69.78	159.12
85	113	5.82	0.595	280	75.59	24.6	21.33	69.70	80.73	56.45	52.71	69.65	159.20
85	113	5.82	0.595	282	75.76	25.8	21.44	69.69	80.72	56.49	51.87	69.70	159.22
85	113	5.82	0.6	282	75.81	25.8	21.49	69.93	80.85	56.55	52.05	70.23	159.28
85	114	5.82	0.6	282	75.94	25.8	21.51	69.99	80.82	56.57	52.07	70.23	159.25
85	117	5.82	0.6	282	75.99	25.8	21.38	69.99	80.72	56.39	51.92	69.46	159.14
85	117	5.82	0.595	282	76.08	25.8	21.26	69.68	80.54	56.21	51.57	70.79	158.84
85	117	5.82	0.6	282	76.03	25.8	21.39	69.70	80.45	56.18	51.29	70.40	158.75
85	114	5.82	0.6	281	76.09	25.8	21.30	69.79	80.68	56.27	51.21	68.89	159.05
85	114	5.82	0.6	283	76.10	25.8	21.41	70.04	80.75	56.46	51.42	70.53	159.25
85	114	5.82	0.6	283	76.21	25.8	21.40	70.08	80.91	56.51	51.40	70.41	159.35
85	114	5.82	0.6	283	76.31	25.8	21.41	70.17	80.99	56.57	51.59	70.66	159.44
85	114	6.13	0.59	284	74.87	22.1	20.61	68.14	80.51	56.23	54.73	68.23	158.99
85	110	6.13	0.59	283	74.62	22.1	20.62	68.18	80.54	56.24	54.79	67.64	158.97
85	109	6.13	0.585	284	74.48	22.1	20.64	68.18	80.76	56.45	54.93	68.44	159.25
85	109	6.13	0.59	285	74.35	22.1	20.65	68.30	80.87	56.52	55.09	68.67	159.34
85	112	6.13	0.59	284	74.29	22.1	20.70	68.30	80.67	56.42	54.90	69.46	159.13
85	115	6.13	0.59	285	74.59	22.1	20.79	68.48	80.40	56.08	53.31	69.41	158.69
85	115	6.13	0.59	285	74.59	22.1	20.82	68.60	80.48	56.16	53.30	70.17	158.76
85	115	6.13	0.595	287	74.56	22.1	20.84	68.99	80.63	56.27	53.43	68.30	158.93
85	114	6.13	0.595	287	74.71	22.1	20.88	69.04	80.76	56.39	53.56	70.51	159.17
85	114	6.13	0.595	285	74.74	22.1	20.85	69.17	80.96	56.51	53.60	69.11	159.23
85	115	6.13	0.595	285	75.18	23.35	20.97	69.50	81.04	56.57	52.91	69.13	159.33
85.5	114	6.13	0.595	285	75.21	23.35	20.90	69.41	80.96	56.48	52.90	70.52	159.36
85	116	6.13	0.595	284	75.36	23.35	20.92	69.09	80.74	56.27	52.57	69.89	159.24
85	116	6.13	0.595	284	75.50	23.35	20.95	69.19	80.80	56.26	52.63	69.84	159.14
85	116	6.13	0.6	286	75.62	23.35	20.97	69.34	80.91	56.37	52.73	70.09	159.23

T9 Compressor Exit °C	WBD Station 6 Vdc	T11 Boiler Inlet °C	Separated Water Net g/min
93.76	11.01	27.85	14.81
94.96	11.57	27.89	14.39
93.93	11.88	27.92	15.94
94.17	10.36	27.95	15.64
94.25	11.96	27.98	15.50
94.16	11.73	27.84	15.58
94.58	11.86	27.73	15.38
94.27	12.04	27.60	16.04
94.64	12.18	27.42	16.28
94.58	8.64	27.25	15.84
94.71	11.29	26.63	40.44
95.02	12.11	26.38	41.59
94.99	11.39	26.14	40.70
94.87	11.44	25.87	40.48
95.30	10.90	25.66	40.26
95.33	12.07	25.46	39.01
95.68	12.57	25.29	38.16
95.97	11.41	25.17	42.99
95.61	12.07	25.06	44.11
95.95	12.34	24.85	43.70
95.91	11.17	24.46	42.33
95.88	13.17	24.34	43.92
95.83	11.26	24.14	46.24
96.23	11.59	24.31	45.80
96.32	12.13	24.28	44.45
96.61	12.70	24.31	44.85
96.33	12.46	24.37	44.83
92.73	9.35	26.17	16.25
93.21	9.78	26.00	16.82
93.35	11.30	25.90	17.23
93.89	11.47	25.76	17.40
93.65	12.21	25.25	16.82
93.09	10.49	24.43	31.33
93.50	12.75	24.26	31.12
93.66	9.70	24.37	29.36
93.43	12.82	24.32	30.54
93.93	11.75	24.31	30.14
93.95	11.42	24.45	34.98
94.63	11.91	24.42	35.21
94.55	12.33	24.27	35.37
94.91	11.57	24.27	35.17
94.94	12.45	24.32	35.14

REFERENCES

Amphlett, et al., "The Operation of a Solid Polymer Fuel Cell: A Parametric Model," Royal Military College of Canada, 1993.

ANSI Z236.1, "American National Standard for Liquid-in-glass Thermometers – General Purpose Laboratory Use", American National Standards Institute, New York., 8 September 1983

ASHRAE Standard, "Standard Methods for Measurement of Moist Air Properties," pp.19-21, American Society of Heating, Refrigeration, and Air Conditioning Engineers, 1982.

ASME Standard MFC-14-2001. Measurement of Fluid Flow Using Small Bore Precision Orifice Meters. American Society of Mechanical Engineers. New York. 2001.

Aspinwall, Jacob Raleigh., "Design of an improved moisture separator in a turbocharger system for fuel cells," Georgia Institute of Technology, Atlanta, Georgia, 2004.

EG&G Technical Services, Inc.; Science Applications International Corporation, "Fuel Cell Handbook", Sixth Edition, U.S. Department of Energy, National Energy Technology Laboratory, 2002.

Hirschenhofer, J.H.; D.B. Stauffer; R.R. Engelman; and M.G. Klett., "Fuel Cell Handbook", Fourth Edition. Parsons Corp. 1998

Hull, Brent, "Fuel Cell Moisture and Energy Recovery," Georgia Institute of Technology, Atlanta, Georgia, 2002

Ladson, Charles L.; Brooks, Cuyler W.; Jr., Hill, Acquilla S.; and Sproles, Darrell W., "Computer Program To Obtain Ordinates for NACA Airfoils", NASA Technical Memorandum 4741, 1996.

McCrometer, "Sales Brochure 24710-10 Rev 1.3/03-05", McCrometer, Helmet, CA, 2005

McTaggert, "Advanced Fuel Cells for Automotive Applications – Development of a Compressor/Expander for Fuel Cells in Automotive Applications," Department of Energy, Arthur D. Little, Inc., 1998.

Nieuwstadt, F. T. M.; Dirkzwager, M., "A Fluid Mechanics Model for an Axial Cyclone Separator," Ind. Eng. Chem. Res.; Vol. 34, No. 10, 3399-3404, 1995

Omega Engineering, Inc, “Omega Product Catalog,”, Stamford, Connecticut, 2005, page G-16

Vaisala, “Vaisala Product Catalog 2005, Ref. B210435en Rev.A,” Helsinki, Finland, 2005.